I would like to acknowledge the Fundação para a Ciência e Tecnologia (FCT, Ministério da Educação e Ciência, Portugal) for the research grant provided (SFRH/BD/72388/2010), within the scope of QREN and POPH – typology 4.1 – co-funded by the European Social Fund.
Acknowledge to FCT Strategic PEst-OE/EQB/LA0023/2013 and exploratory EXPL/AAGTEC/0898/2013 projects.

FCT
Fundação para a Ciência e a Tecnologia
MINISTÉRIO DA EDUCAÇÃO E CIÊNCIA

QUADRO DE REFERÊNCIA ESTRATÉGICO NACIONAL
PORTUGAL 2007.2013

POPH
PROGRAMA OPERACIONAL POTENCIAL HUMANO

UNIÃO EUROPEIA
Fundo Europeu de Desenvolvimento Regional

COMPETE
PROGRAMA OPERACIONAL FACTORES DE COMPETITIVIDADE

Sónia Raquel Alves Fernandes Pereira **Carbon Materials as new generation of new electron shuttles for the anaerobic degradation of environmental xenobiotics** UMinho | 2015

Universidade do Minho
Escola de Engenharia

Sónia Raquel Alves Fernandes Pereira

Carbon Materials as new generation of new electron shuttles for the anaerobic degradation of environmental xenobiotics

julho de 2015

Universidade do Minho
Escola de Engenharia

Sónia Raquel Alves Fernandes Pereira

Carbon Materials as new generation of new electron shuttles for the anaerobic degradation of environmental xenobiotics

Tese de Doutoramento em Engenharia Química e Biológica

Trabalho efetuado sob a orientação da
Doutora Luciana José Ribeiro Pereira
e da
Professora Maria Madalena Santos Alves

julho de 2015

STATEMENT OF INTEGRITY

I hereby declare having conducted my thesis with integrity. I confirm that I have not used plagiarism or any form of falsification of results in the process of the thesis elaboration. I further declare that I have fully acknowledged the Code of Ethical Conduct of the University of Minho.

University of Minho, _____

Name:

Sónia Raquel Alves Fernandes Pereira

Signature:

_____

ACKNOWLEDGMENTS

First of all, I would like to express my deepest gratitude to my supervisors, Doctor Luciana Pereira and Professor Madalena Alves (CEB, University of Minho), for the constant guidance during my research work. Your good supporting advices and friendship have been invaluable on both academic and personal level.

I would like to thank to Doctor Fernando Pereira (FEUP, University of Porto) for the availability, useful discussion and for providing the carbon materials essential for this project, namely for the preparation and characterization of the carbon materials used and studied in this thesis.

To all my colleagues from BRIDGE group, especial to Ana Júlia Cavaleiro, Ângela Abreu, Joana Alves, Andreia Salvador, José Carlos Costa, Rita Castro, Maura Francisca, Marta Casanova, Ana Lu Pereira, Joaquim Alfredo, Carla Magalhães and Patrícia Dias. I would like to thanks for the fantastic working environment, the support and friendship that they have demonstrated all over these years.

I would like to thanks the following friends: Tânia Ferreira, Sónia Matos, Cristiana Castro, Sara Silva Sónia Barbosa, Jorge Padrão, Salomé Duarte, Sérgio Silva and Farhana Massod, for listening, offering me advices, friendship and supporting me through this entire process.

A special thanks to Sara Gonçalves, João Oliveira, Daniela Mesquita and Catarina Oliveira, Ariane Chiareli, I greatly value their friendship and I deeply appreciate their belief in me. Therefore, you all have my eternal gratitude.

Finally and also important, I would like to thank to my sister Li, my parents and Bruno, who always supported and encouraged me in all periods of my life and without their support the accomplishment of this PhD would not be possible.

I dedicate this thesis to my nephews, Francisco and Madalena.

I would like to acknowledge the Fundação para a Ciência e Tecnologia (FCT, Ministério da Educação e Ciência, Portugal) for the research grant provided (SFRH/BD/72388/2010), within the scope of QREN and POPH – typology 4.1 – co-funded by the European Social Fund.

Acknowledge to FCT Strategic PEst-OE/EQB/LA0023/2013 and exploratory EXPL/AAG-TEC/0898/2013 projects.

ABSTRACT

CARBON MATERIALS AS A NEW GENERATION OF ELECTRON SHUTTLES FOR THE ANAEROBIC DEGRADATION OF ENVIRONMENTAL XENOBIOTICS

Residual dyes originated by textile, pharmaceutical, food, chemical and paper industries, are considered xenobiotic compounds and are difficult to remove from the environment, adversely effecting ecosystems. Effluents generated by the textile sector are especially harmful, due to the high quantities of water and chemicals used, in special dyes. The most commonly used class of dyes in fibre textile dyeing and, consequently, the most abundant in textile effluents, are the azo ones. These dyes have one or more functional azo groups (–N=N–) and resist to biodegradation in aerobic conditions. However, under anaerobic conditions the azo linkage can be broken forming aromatic amines, which can be further biodegraded under aerobic conditions. Biological systems combining anaerobic/aerobic bioprocesses are thus suitable strategies for complete mineralization of azo dyes. One problem of this treatment strategy is the relatively slow reduction rate of the azo linkage in the anaerobic phase. The application of redox mediators (RM), as electron shuttles that reduce the activation energy of the reduction reactions, provides an increased decolourisation rate of azo dyes.

In this thesis, the catalytic effect of different carbon materials (CM) is assessed on different azo dyes and nitroanilines (NoA) bioreduction under anaerobic conditions. In a first experiment, commercial activated carbon (AC_0) surface was modified by chemical oxidation with HNO_3 (AC_{HNO3}) and O_2 (AC_{O2}) or thermal treatments under H_2 (AC_{H2}) or N_2 (AC_{N2}). Overall, an increase of the first-order rate constants of chemical reduction of different anionic dyes was obtained in the following order: none < AC_{HNO3} < AC_{O2} < AC_0 < AC_{N2} < AC_{H2}. The catalytic effect of CM was found to be related to their pH of point zero charge (pH_{pzc}) and up to 9-fold reduction rate was obtained with most basic sample AC_{H2}. This is due to the electrostatic attraction of negative anionic dyes and the positive CM at the pH of the reaction, pH 7. Biodecolourisation using granular biomass, in the presence of AC_{H2}, also increased its rate by 2– and 4.5–fold for Mordant Yellow 10 and Reactive Red 2, respectively. Moreover, the redox mediator effect was maintained after three cycles of dye addition. Biological azo dye reduction efficiency was even higher using CM with larger pores, such as nanotubes (CNT) and xerogels (CXA and CXB). This was due to the easier access of the dye molecules to the surface of the CM, due to their larger pores. Acid Orange 10 (AO10) presented higher bioreduction rates using CXB (4.5 ± 0.7 d^{-1}) compared with AC_{H2} (2.1 ± 0.2 d^{-1}). CM were also effective as RM in NoA reduction, contrarily to the obtained with larger azo dyes, where better efficiency was observed using microporous AC_0 and AC_{H2}. The presence of AC_{H2} led to rate increases of 3–fold, 4–fold and 8–fold for *ortho*–, *meta*–, *para*–NoA respectively, as compared with assay in the absence of CM. Moreover, biological reduction of Mordant Yellow 1 led to the formation of *meta*–NoA, which was reduced to *meta*-Phenylenediamine via mediated reaction. Finally, CM were tested in a continuous upflow anaerobic sludge blanket reactor. The AO10 azo dye was totally decolourised with 1.2 g L^{-1} of CM at a 5 h hydraulic retention time, whereas only 20 % of colour removal yield occurred in the absence of CM. The identification of the aromatic amines proved that the colour removal was due to AO10 dye reduction catalyzed by CM. The work developed proved the great potential of very low amounts of CM to improve significantly the reduction rates of different organic compounds.

SUMÁRIO

MATERIAIS DE CARBONO COMO UMA NOVA GERAÇÃO DE TRANSPORTADORES DE ELETRÕES NA DEGRADAÇÃO ANAÉROBIA DE XENOBIÓTICOS AMBIENTAIS

Os corantes existentes nos efluentes industriais dos setores têxtil, farmacêutico, químico, alimentar e da indústria do papel, são considerados compostos xenobióticos e de difícil remoção do meio ambiente, sendo nocivos para o ecossistema. Os efluentes da indústria têxtil são considerados dos mais poluentes não só pela quantidade gerada mas também pela sua composição (corantes). Os corantes azo são os mais usados no tingimento de fibras e consequentemente a classe de corantes mais comuns nos efluentes têxteis. Estes corantes possuem um ou mais grupos azo (–N=N–) e resistem à biodegradação em condições aeróbias. No entanto, em condições anaeróbias, a ligação azo é quebrada formando aminas aromáticas, que posteriormente podem ser biodegradadas sob condições aeróbias. Processos biológicos que combinem as duas etapas, anaeróbia/aeróbia, constituem uma estratégia viável para uma completa mineralização de corantes azo. Contudo, as baixas taxas de redução na fase anaeróbia podem limitar o processo. A aplicação de mediadores redox (MR), como transportadores de eletrões que diminuam a energia de ativação das reações de redução, possibilita o aumento das taxas de descoloração destes corantes.

Esta tese comprova o efeito catalítico dos diferentes materiais de carvão (MC) na bioredução dos diferentes corantes azo e nitroanilinas (NoA). Num primeiro ensaio, a superfície de um Carvão Ativado comercial (CA_0) foi modificada por oxidação química com HNO_3 (CA_{HNO3}) ou O_2 (CA_{O2}) e por tratamentos térmicos com fluxo de H_2 (CA_{H2}) ou de N_2 (CA_{N2}). O aumento da constante de primeira ordem da redução química dos diferentes corantes aniónicos foi conseguido segundo a ordem: sem CA < CA_{HNO3} < CA_{O2}< CA_0< CA_{N2}< CA_{H2}. Conclui-se que o efeito catalítico dos MC está relacionado com o seu pH de carga nula (pH_{pzc}), conseguindo-se atingir uma taxa de redução 9 vezes superior para a amostra mais básica, CA_{H2}. Este resultado explica-se pela atração electroestática dos corantes aniónicos, com carga negativa, e os MC, com carga positiva, ao pH em que a reação foi estudada, pH 7. O CA_{H2} foi também testado na descoloração biológica de corantes resultando num aumento de 2 e 4.5 vezes das taxas de redução para os corantes *Mordant Yellow 10* e *Reactive Red 2*. Constatou-se também que o efeito do MR foi mantido após três ciclos de adição do corante. A eficiência da redução biológica de corantes azo conseguiu ainda ser superior com MC com mesoporos, nomeadamente os nanotubos (NTC) e os xerogeis (XAC and XBC). Tal deve-se ao mais fácil acesso das moléculas dos corantes aos mesoporos dos MC. O corante *Acid Orange 10* (AO10) apresentou uma maior taxa de redução com CXB (4.5 ± 0.7 d^{-1}) em comparação com AC_{H2} (2.1 ± 0.2 d^{-1}). Contrariamente ao efeito conseguido quando utilizados corantes com maior estrutura química, para moléculas menores como é o caso das NoA, melhores resultados foram encontrados com os materiais microporosos (CA_0 e CA_{H2}). A presença de CA_{H2} levou a um aumento das taxas de 3, 4 e 8 vezes para a *orto*–, *meta*– e *para*–NoA respetivamente, comparando com ensaio sem MC. Para além disso, o efeito MR do CA_{H2} foi verificado na redução biológica do corante MY1, e a amina *meta*–NoA foi ainda reduzida a *meta*-fenilenediamina apenas na presença do mediador. Por último, os MC foram testados em reator anaeróbio de manto de biomassa em fluxo ascendente (UASB). Para 1.2 g L^{-1} g de MC e um tempo de retenção hidráulico de 5 h, obteve-se uma descoloração total de AO10, em comparação a apenas 20 % de remoção de cor para um reator sem CM. Através da identificação de aminas aromáticas comprovou-se a redução efectiva do corante AO10, catalisada por MC. O trabalho desenvolvido demonstrou o grande potencial dos MC, a baixas concentrações, para uma melhoria significativa da taxa de redução de compostos xenobióticos.

TABLE OF CONTENTS

1. THESIS SCOPE 1

1.1. CONTEXT 3

1.2. AIMS 5

1.3. THESIS OUTLINE 5

1.4. SCIENTIFIC OUTPUT 7

2. INTRODUCTION 9

2.1. AZO DYES 13

2.1.1. Biodegradation of azo dyes 16

2.1.2. Factors affecting dye biodegradation 19

2.1.3. Bioreactor system for dyed wastewater treatment 22

2.2. REDOX MEDIATORS 24

2.2.1. Activated Carbon 25

2.2.2. Carbon Nanotubes 28

2.2.3. Carbon gels 32

3. THERMAL MODIFICATION OF ACTIVATED CARBON SURFACE CHEMISTRY IMPROVES ITS CAPACITY AS REDOX MEDIATOR FOR AZO DYE REDUCTION 35

3.1. INTRODUCTION 37

3.2. MATERIALS AND METHODS 38

3.2.1. Dyes 38

3.2.2. Preparation of activated carbon samples 38

3.2.3. Textural characterisation of activated carbons 39

3.2.4. Surface chemistry characterisation of activated carbons 40

3.2.5. Chemical dye reduction 41

3.2.6. Biological dye reduction 42

3.2.7. Analytical techniques 42

3.3. RESULTS AND DISCUSSION 43

3.3.1. Textural characterization 43

3.3.2. Surface chemistry characterization 44

3.3.3. Azo dye reduction 46

3.3.4. Effect of AC surface chemical groups on azo dye reduction 49

3.3.5. Biological MY10 reduction 52
3.4. CONCLUSIONS 54

4. CARBON BASED MATERIALS AS NOVEL REDOX MEDIATORS FOR DYE WASTEWATER BIODEGRADATION 57
4.1. INTRODUCTION 59
4.2. MATERIALS AND METHODS 61
4.2.1. Chemicals 61
4.2.2. Preparation and characterization of carbon materials 61
4.2.3. Dye biodegradation 62
4.2.4. Real and model wastewater biodegradation 63
4.2.5. Activity test 64
4.2.6. Analytical techniques 65
4.3. RESULTS AND DISCUSSION 65
4.3.1. Characterisation of carbon materials 65
4.3.2. Kinetics of dye biodegradation 67
4.3.3. Products and mechanism of azo dye reduction 69
4.3.4. Carbon materials as catalysts on dye biodegradation 71
4.3.5. Textile wastewater treatment 74
4.4. CONCLUSIONS 76

5. MICROPOROUS CARBON MATERIALS AS EFFECTIVE ELECTRON SHUTTLES FOR THE ANAEROBIC BIOLOGICAL REDUCTION OF NITROANILINES 77
5.1. INTRODUCTION 79
5.2. MATERIALS AND METHODS 81
5.2.1. Chemicals 81
5.2.2. Preparation and Characterization of Carbon Materials 81
5.2.3. Biological assays 81
5.2.4. Specific methanogenic activity 82
5.2.5. Analytical techniques 83
5.3. DISCUSSION 85
5.3.1. CM as redox mediators on NoA biological reduction 85
5.3.2. MY1 biological reduction 90
5.3.3. AC as electron acceptor 91
5.3.4. Effect of NoA and MY1 and final reduction products on the methanogenic activity 92
5.4. CONCLUSIONS 94

6. AZO DYE REDUCTION IN UASB BIOREACTORS AMENDED WITH CARBON MATERIALS 95
6.1. INTRODUCTION 97
6.2. EXPERIMENTAL 98
6.2.1. Carbon materials and chemicals 98
6.2.2. UASB reactor operation 98
6.2.3. Analysis 100
6.2.4. Microbial analysis 100
6.3. RESULTS 101
6.3.1. Reduction of AO10 in the UASB reactor 101
6.3.2. Products of AO10 decolourisation in the UASB reactor 104
6.3.3. Microbial Communities in UASB reactor treating AO10 105
6.4. CONCLUSIONS 107
7. GENERAL CONCLUSIONS AND FUTURE PERSPECTIVES 109
REFERENCES 113

LIST OF FIGURES

Figure 2.1. Examples of azo dyes' chemical structures. 14

Figure 2.2. Combination of anaerobic/aerobic processes for azo dye biodegradation: reduction of azo dye in the anaerobic process and their correspondent aromatic amines degradation in aerobic process. Illustration adapted from [van der Zee, 2002]. 16

Figure 2.3. Different mechanism for azo dye reduction: direct dye reduction by bacteria (enzymes) or by biogenic reductant (e.g. sulphide) and indirect/mediated reduction of dye by RM. (B) biological step, (C) chemical step. Illustration adapted from [van der Zee *et al.*, 2001]..... 17

Figure 2.4. Different granulometries of AC. Pictures adapted from www.desotec.com (January, 2015). 25

Figure 2.5. AC structure schematic representation (A) and AC pore structure and size (B). Illustration adapted from [Bansal RC, 1988; Henning KD, 2002]. 26

Figure 2.6. Surface groups on AC. Illustration adapted from [Figueiredo *et al.* 1999]. 27

Figure 2.7. Carbon nanotube structures representation (A) and classification (B). Illustration adapted from http://www.nanotechnologies.qc.ca and http://astro.temple.edu/rjohnson/gallery (September, 2011). 29

Figure 3.1. Molecular structure of the azo dyes. 39

Figure 3.2. TPD spectra before and after different treatments: (A) CO_2 evolution and (B) CO evolution. Examples for AC_{HNO3} and AC_{H2}. 45

Figure 3.3. Chemical azo dye decolourisation at pH 5, for the assays with dye alone (Δ), dye and $AC_<$ (▲), dye and Na_2S (□) and dye, Na_2S and AC_0 (■). (A) AO7; (B) RR2; (C) MY10 and (D) DB71.47

Figure 3.4. First order constant rates of dye reduction, calculated at different pH values, in function of the pH_{pzc} of the modified activated carbons. (■) pH 5; (□) pH 7 and (▲) pH 8.7; (A) AO7; (B) RR2; (C) MY10 and (D) DB71. 50

Figure 3.5. Biological MY10 and RR2 dye reduction at pH 7 and with VFAs as substrate. MY10 decolourisation with several AC concentrations using AC_0 (A) and AC_{H2} (B): (▲) without AC; (●) 0.1 $g.L^{-1}$; (■) 0.2 $g.L^{-1}$, (♦) 0.4 $g.L^{-1}$, (x) 0.6 $g.L^{-1}$. RR2 decolourisation with 0.1 g L^{-1} (▲) AC_0 and (■) AC_{H2}, (●) without AC, and with 0.1 $g.L^{-1}$ (Δ) AC_0 and (□) AC_{H2} without biomass. 53

Figure 4.1. Molecular structure of azo days and aromatic amines 60

Figure 4.2. Biodegradation kinetics of MY10 (A) and RR120 (B) at increasing initial dye concentrations. 67

Figure 4.3. Molecular structure of Acid Orange 10 in the hydrazone form. 69

Figure 4.4. HPLC chromatograms of the standards MY10, SA and 5-ASA (A) and of the MY10 biodegradation at (B) 350 nm and (C) 250 nm. 70

Figure 4.5. Mechanism of MY10 biodegradation with formation of the correspondent aromatic amines. 71

Figure 4.6. First order rate curves of AO10 biodegradation: (■) no carbon material; (●) AC_{H2}; (♦) CXA; (▲) CXB; (▼) CNT. Black symbols correspond to the biotic and white symbols to the abiotic assays. 72

Figure 5.1. Molecular structure of the aromatic amines, *o*-, *m*- and *p*-NoA, *m*- and *p*-phe, 5-ASA and the azo dye MY10. 80

Figure 5.2. Biological reduction of *p*-NoA in the presence of AC_0 as monitored by UV-Vis spectroscopy. 85

Figure 5.3. Biological reduction of *m*–NoA in the presence of AC_0 as monitored by HPLC at 350 nm (**A**) and 230 nm (**B**). 86

Figure 5.4. First-order rate curves of *o*–NoA (**A**), *m*–NoA (**B**) and *p*–NoA (**C**) biological reduction. (**x**) no carbon material; (●) AC_0; (▲) AC_{H2}; (♦) AC_{HNO3}; (■) CXA; (⋆) CXB and (▼) CNT. Black symbols correspond to the biotic and white symbols to the abiotic assay. 88

Figure 5.5. HPLC chromatograms of MY1 biological reduction at 230 nm (A) and areas of dye biological reduction, and products formed, within 48 h of reaction (B); (○) 5-ASA; (■)MY1; (Δ) *m*-

Phe; (□) *m*-NoA. Black symbols correspond to the reaction in the absence of AC0 and grey to the reaction in the presence of AC_0 90

Figure 5.6. Photography of magenta complex formed from the reaction of Fe^{2+} (resulted from the reduction by AC_0) with ferrozine (duplicate experiments): (A and B) 0.1 g L^{-1} AC_0 and (D and E) 1.0 g L^{-1} AC_0, previously biologically reduced in the absence and presence of BES, respectively. C and F, are the controls with AC_0 (0.1 and 1.0 g L^{-1}, respectively) incubated in the same conditions of biotic experiments, but without biomass. 91

Figure 6.1. Schematic representation of the UASB reactors. E (effluent out); R (recyclic out); RP (recycling pump); FP (feeding pump); WJ (water jacket). 99

Figure 6.2. Percentage of AO10 decolourisation (A), COD removal and HRT (B) during the experiment for reactor R0 (○), reactor RAC (■) and reactor RCNT (□). 102

Figure 6.3. HPLC results from reactor RAC and R0 phase IV. (A) Chromatogram for 0.5 mmol L^{-1} of aniline at 230 nm; (b) Sample from RAC in phase IV at 230 nm; (c) Sample from R0 in phase IV at 230 nm; (D) Feed sample at 480 nm; (■) AO10 at Rt= 9.6 min; (▲) Aniline at Rt=12.6 min; (●) Aromatic product at Rt=4.3 min. 104

Figure 6.4. DGGE profile of Bacteria in UASB reactor samples. 105

Figure 6.5. Distribution of 16S rRNA genes sequences among *Archaea* (A) and *Bacteria* (B) genera. 106

LIST OF TABLES

Table 1.1. Structure of the thesis 6

Table 2.1. Different classes of the dyes used for specific fibres, main characteristics and degree of fixation on fibres (adapted from [Easton JR, 1995; O'Neill *et al.* 1999]) 15

Table 2.2. Theoretical and experimental properties of CNTs (adapted from Xie *et al.,* 2005) 30

Table 3.1. Textural characterisation of the activated carbon samples 43

Table 3.2. Chemical characterisation of the AC samples 44

Table 3.3. Oxygen-containing surface groups estimated from the TPD spectra deconvolution (± 10 %) 45

Table 3.4. First order rates (d^{-1}) of dye reduction by sulphide, calculated from the reaction at pH 5, 7 and 8.7, in the absence and presence of different AC samples 48

Table 3.5. First order rates (d^{-1}) and degree of biological MY10 reduction in the presence of increasing unmodified (AC_0) and modified (AC_{H2}) activated carbon concentrations 54

Table 4.1. Properties of the prepared carbon material samples 66

Table 4.2. Textural and chemical characterization of prepared carbon materials 66

Table 4.3. Effect of different carbon materials (0.1 g L^{-1}) on the extent (%) and rates (d^{-1}) of dye decolourisation (1 mmol L^{-1})[a] 72

Table 4.4. Decolourisation extent (%) and rates (d^{-1}) of MY10 (1 mmol L^{-1}) during 3 cycles of dye addition 74

Table 4.5. Biodecolourisation extent (%) and rates (d^{-1}) of real and model wastewaters in the absence and presence of CNT (0.1 g L^{-1}) 75

Table 4.6. Biodecolourisation extent (%) and rates (d^{-1}) of Procion dyes (1 mmol L^{-1}) 75

Table 5.1. HPLC retention times (min) of NoA and MY10 at initial incubation time (t0) and after 24 and 48 h biological reaction, in the presence and absence of AC_0, and of the standards *m*-phe, *p*-phe and 5-ASA (expected products of biological reduction)..... 84

Table 5.2. Effect of different CM (0.1 g L^{-1}) on bioreduction extent (%) and rates (d^{-1}) of NoA (1 mmol L^{-1})[a]..... 86

Table 5.3. Potential toxic effect of NoA, MY1 and products of their bioreduction (at concentration of 1 mmol L^{-1} and in the presence of AC_0), on acetoclastic methanogenic bacteria degrading VFA .. 93

Table 6.1. Experimental conditions for the different phases of the UASB bioreactors operation... 99

Table 6.2. Average of decolourisation (%) and COD removal (%) obtained at each phase in UASB reactors operation..... 101

ABBREVIATIONS

A0	Absorbance at $t_{initial}$
At	Absorbance at λ_{max}
ACN	Acetonitrile
AO7	Acid Orange 7
AO10	Acid Orange 10
AC	Activated Carbon
AC_0	Activated Carbon commercial
AC_{HNO3}	Activated Carbon treated by chemical oxidation with HNO_3
AC_{O2}	Activated Carbon treated by chemical oxidation with with O_2
AC_{N2}	Activated Carbon thermal treated with N_2 flow
AC_{H2}	Activated Carbon thermal treated with H_2 flow
5-ASA	5- Aminosalicylic acid
AQDS	Anthraquinone-2,6-disulphonate
AQS	Anthraquinone-2-sulphonate
CNT	Carbon Nanotubes
CX	Carbon Xerogel
COD	Chemical Oxygen Demand
CR	Colour Removal
DB71	Direct Blue 71
HPLC	High Performance Liquid Chromatography
HRT	Hydraulic Retention Time
IC_{50}	Half maximal inhibitory concentration
MY1	Mordant Yellow 1
MY10	Mordant Yellow 10
NoA	Nitroaniline
m-NoA	*meta*-Nitroaniline
o-NoA	*ortho*-Nitroaniline
p-NoA	*para*-Nitroaniline
m-Phe	m-Phenylenediamine
pH_{PZC}	pH from point zero charge

PB	Procion Blue H-ERD
PR	Procion Red H-EXL
PY	Procion Yellow H-EXL
RR2	Reactive Red 2
RR120	Reactive Red 120
RAC	Reactor with Activated Carbon
RCNT	Reactor with Carbon Nanotubes
R0	Reactor Control
SMA	Specific Methanogenic Activity
RB	Remazol Blue RR
RBY	Remazol Brilliant Yellow 3GL
RR	Remazol Yellow RR
Rt	Retention Time
SA	Sulphanilic Acid
λ_{max}	Wavelength of maximum absorbance

CHAPTER 1.
THESIS SCOPE

The motivation behind the research performed in this thesis is revealed. The research aims and the thesis outline are presented as well, including the generated scientific outputs.

CHAPTER 1. THESIS SCOPE

1.1. CONTEXT

Chemical industry is one of the most important industries of the modern world. Due to extensive urbanization, and the consequent industrialization, over 14 million different molecular compounds have been synthesized during the last century [J.C. Charpentier, 2003]. However, these new compounds have originated new sources of pollution often toxic, persistent and difficult to eliminate from the environment. Most of these compounds are xenobiotics and, depending on the chemical properties and quantities, can eventually be incorporated into biological cycles causing several damages in ecosystems [Esteve-Nunez *et al.,* 2001].

Currently, the environmental concern is expressed by more stringent governmental policies imposing lower pollutant discharge limits. These policies are therefore important instruments for ensuring a sustainable future integrating global development with environment preservation. Additionally, are also fundamental to control global warming to reduce environmental pollution (air, soil, rivers and oceans) and consequently, to improve the life quality. Pollution prevention, waste minimization and reuse are being increasingly integrated in the environmental policies. Yet, end of pipe treatment approaches, including severe remediation treatments, are still needed in most of the heavily polluting chemical industries.

Examples of toxic and non-biodegradable organic pollutants are phenols, surfactants, chlorinated compounds, pesticides, aromatic hydrocarbons, among many others [Dojilido R and Best GA, 1993]. Many of these compounds are present in textile industries that generate also high amounts of dyed wastewaters due to the high portion of unfixed dyes to the fibres in the dying process. In addition, high quantities of water are used in the fabric processing [Şen and Demirer, 2003]. The European Community has been aware of this problem, and the European directive 2002/61/EC, that came into force in September 2003, forbids the use of some products, derivatives of a restricted number of azo dyes (most abundant dye class present in textile effluents, presenting 60 – 75 % from total textile dyes [Carliel *et al.,* 1995].

In Portugal, most of the industries of the textile sector are concentrated in the northern region, with almost 60 % located in Vale do Ave region [INE, 2007]. To minimize environmental impacts caused by the discharge of textile effluents, emission limit values were established by the "Decreto-lei N° 236/98 of August 1" and maximum permissible values by "Portaria N° 423/97 of 25 June".

Nowadays, several physical, chemical and biological technologies are available and have been shown to be efficient in treating a variety of complex dyed effluents. However, the selection of the dye removal technique is dependent on several factors such as wastewater characteristics, operation costs (energy and materials) and environmental fate and handling costs of generated waste products [Van der Zee *et al.*, 2002]. Since conventional treatment systems based on chemical or physical methods are expensive and consume high amounts of chemicals and energy, biological treatments present the most versatile dye removal technique [Kandelbauer and Gübitz, 2005]. An anaerobic step followed by an aerobic may represent a significant progress in biological dye decolourisation treatment (Ong *et al.*, 2005). Efficient dye removal takes place during the anaerobic treatment, where the cleavage of the azo linkage takes place resulting in the correspondent aromatic amines formation. During the subsequent aerobic treatment, aromatic amines and other organic compounds are degraded [Van der Zee *et al.,* 2005]. However, some of them are still rather recalcitrant [Tan *et al.,* 2005].

Among the different anaerobic reactors, UASB reactor has been found to be more resistant to xenobiotic and recalcitrant compounds, such as azo dyes and aromatic amines, at sufficient short hydraulic retention times (HRT) [Somari *et al.,* 2008]. However, dye reduction needs longer HRT to achieve high decolourisation extents [Van der Zee *et al.,* 2005].

Redox mediators (RM), compounds which accelerate the electron transfer from a primary electron donor (substrate) to a terminal electron acceptor (dye), can improve the dye reduction rates in one or more orders of magnitude [Van der Zee *et al.,* 2005; Van de Zee and Cervantes, 2009].

Carbon materials (CM), such as activated carbon (AC), have been shown as a feasible redox mediators in dye reduction [Van der Zee *et al.,* 2005; Guo *et al.,* 2007; Mezohegyi *et al.,* 2007, Pereira *et al.,* 2010, 2014] presenting advantages in comparison with soluble mediators (anthraquinone compounds). Advantages of CM include their regeneration and reuse, and the possibility of being retained within the reactors sludge bed. Furthermore, the possibilities of tailoring

CM surface properties determine its performance as catalysts for specific applications, as for dye bioreduction [Rodriguez-Reinoso F, 1998; Pereira *et al.,* 2003; Tsang *et al.,* 2007]. Therefore, the application of RM still represents a challenge to optimize wastewater treatment processes containing xenobiotic compounds.

1.2. AIMS

The aim of this thesis is to obtain insights into the mechanism of reduction reactions catalyzed by different CM, by conducting batch assays and, from the knowledge obtained, to develop an efficient biological process, based on UASB high rate anaerobic bioreactors, for the biological reduction of azo dyes and, possibly of different environmental xenobiotics.

CM, such as AC, carbon nanoporous (carbon nanotubes, CNT) and mesoporous (carbon xerogels, CX), with different surface chemistry, were selectively prepared, characterized and tested at very low concentrations (0.1 g L^{-1}) in pollutants biotransformation, such as azo dyes and aromatic amines (nitroanilines, NoA).

At the later stage, a synthetic wastewater was treated in a high rate UASB reactor amended with CM in order to evaluate the feasibility of the process.

1.3. THESIS OUTLINE

This thesis is organized according to the follow structure (Table 1.1).

The chapters 3 and 4 were adapted from articles Pereira *et al.,* 2010 and Pereira *et al.,* 2014, respectively.

Table 1.1. Structure of the thesis

CHAPTER 1	**Thesis scope** Motivation, aim, thesis outline and scientific output are presented.
CHAPTER 2	**Introduction** The subject and basics concepts about the techniques applied in the framework of dyed wastewater treatment are discussed.
CHAPTER 3	**Thermal modification of activated carbon surface chemistry improves its capacity as redox mediator for azo dye reduction** Study of redox mediating capacity of AC with different chemical superficial groups, by performing batch assays for the reduction of different azo dyes.
CHAPTER 4	**Carbon based materials as novel redox mediators for dyed wastewater biodegradation** The efficiency of the microporous AC as RM was further compared with the mesoporous CNT and CX, in order to access to the effect of CM pore size. Biodegradation of real textile wastewaters was also investigated.
CHAPTER 5	**Microporous carbon materials as effective electron shuttles for the anaerobic biological reduction of nitroanilines** Biological reduction of *ortho*-NoA, *meta*-NoA and *para*-NoA using different CM as RM. Biodegradation of dye Mordant Yellow 1 was also tested, and further biodegradation of the corresponding aromatic amines formed (*m*–NoA and 5–ASA) was evaluated.
CHAPTER 6	**Azo dye reduction in UASB reactor amended with Carbon Materials** Performance of CM as RM on the biological reduction of azo dye in UASB reactor. Different parameters (type, size and concentration of CM) and HRT were studied to optimize the process.
CHAPTER 7	**General Conclusions and Future Perspectives** The most relevant conclusions as well as some future perspectives for further work are presented.

1.4. SCIENTIFIC OUTPUT

PAPERS IN JOURNALS:

Da Motta M, Pereira RA, Alves MM, Pereira L. (2014). UV/TiO_2 photocatalytic reactor for real textile wastewaters treatment. Water Science and Technology 70 (10), 1670–1676. (DOI: 10.2166/wst.2014.428)

Pereira RA, Pereira MFR, Alves MM, Pereira L (2014). Carbon based materials as novel redox mediators for dye wastewater biodegradation. Applied Catalysis B: Environmental 144, 713–720. (DOI: 10.1016/j.apcatb.2013.07.009)

Pereira L, Pereira S, Oliveira C, Apostol L, Gavrilescu M, Pons M.-N, Zahara O, Alves MM (2013) .UV/TiO2 photocatalytic degradation of xanthene dyes. Photochemistry and Photobiology 89 (1), 33–39. (DOI: 10.1111/j.1751-1097.2012.01208.x)

Apostol L, Pereira L, Pereira R, Gavrilescu M, Alves MM (2012). Biological decolorization of xanthene dyes by anaerobic granular biomass. Biodegradation 23 (5), 725–737. (DOI: 10.1007/s10532-012-9548-7)

Apostol L, Pereira L, Pereira R, Alves MM, Gavrilescu M (2011). Effect of ferromagnetic nanoparticle on dyes biodegradation. Bulletin of the Polytechnic Institute of Iasi, Section Chemistry and Chemical Engineering 57 (2), 21–28. (URI: http://hdl.handle.net/1822/27325)

Pereira R, Pereira L, Van der Zee FP, Alves MM. (2010) Fate of aniline and sulfanilic acid in UASB bioreactors under denitrifying conditions. Water Research 45 (1), 191–2 (DOI: 10.1016/j.apcatb.2013.07.009)

Pereira, L, Pereira R, Pereira MFR, Van der Zee FP, Cervantes FJ, Alves MM (2010). Thermal modification of activated carbon surface chemistry improves its capacity as redox mediator for azo dye reduction. Journal of Hazardous Materials, 183(1-3), 931–939, 2010 (DOI: i:10.1016/j.jhazmat.2010.08.005)

ORAL PRESENTATION:

Pereira, L, Pereira RA, Pereira MFR, Alves MM. Anaerobic biotransformation of nitroanilines enhanced by the presence of low amounts of carbon materials. XI Latin American Workshop and Symposium of Anaerobic Digestion. La Habana, Cuba, November 24–27, 2014.

POSTERS IN CONFERENCES:

Pereira RA, Pereira MFR, Alves MM, Pereira L. Improvement of the Upflow Anaerobic Sludge Blanket reactor performance for azo dye reduction by the presence of low amounts of Activated Carbon. CHEMPOR 2014 - Book of Extended Abstracts of the 12th International Chemical and Biological Engineering Conference. No. P-BE46, Porto, Portugal, September 10–12, 10-123-10-125, 2014. ISBN: 978-972-752-170-8

Pereira L, Pereira RA, Pereira, MFR, Alves MM. Carbon based materials: redox mediators for the biodegradation of organic compounds. XIX Encontro Galego-Português de Química. Vigo, Spain, November 13, 22–22, 2013.

Pereira L, Pereira RA, Pereira F, Alves MM. Carbon nanotubes as novel redox mediators for dyed wastewaters biodegradation13th World Congress on Anaerobic Digestion. Santiago de Compostela, Spain, June 25-28, 1–4, 2013.

Pereira L, Pereira RA, Pereira F, Van der Zee FP, Alves M.M. Activated Carbon as a redox mediator: Effect of AC surface chemistry and solution pH on dye reduction. Water Research Conference 2010. No. P051, Lisbon, Portugal, April 11–14, 2010.

Pereira L, Pereira R, Alves MM. Strategies for the bioremediation of azo dyes containing wastewaters. Book of Abstracts of the 2nd Meeting of the Institute for Biotechnology and Bioengineering. Braga, Portugal, October 23–24, 61-61, 2010. ISBN: 978-972-97810-6-3

Pereira R, Pereira L, Pereira F, Van der Zee FP, Alves M.M. Activated carbon as a redox mediator on azo dye reduction: influence of surface chemistry and pH. MicroBiotec09 - Book of Abstracts. Vilamoura, Portugal, November 28–30, 160, 2009. ISBN: 978-972-97810-6-3

CHAPTER 2.
INTRODUCTION

A general introduction of the main research topics involved in this thesis are discussed. First, the environmental impact of xenobiotics such as azo dyes and its biodegradation process are reviewed. Afterwards, the relevant use of carbon materials as redox mediators on dye bioreduction is described, covering the main features and applications of the carbon materials used in this research.

CHAPTER 2. INTRODUCTION

Environmental pollution is one of the major and most urgent problems of the modern world. Xenobiotic compounds enter the environment through anthropogenic activities associated with the industrial activities. In this context, the term xenobiotic has been related to environmental impact, since those compounds are understood as substances foreign to a biological system, which did not exist in nature before their synthesis by humans. It can also cover substances that are present in much higher concentrations than are usually [El-Moneim and Afify, 2010; Puvaneswari *et al.,* 2006]. In other words, those substances exhibited one or more of the following properties: environmental persistence and bioaccumulation, toxicity and potential risks to the human food chain, or endocrine disruption. Their presence in the environment is related with their broad use and improper disposal or other unintentional releases. Consequently, they affect the public health and create several environmental problems, disturbing the water resources, soil fertility, aquatic organisms and ecosystems integrity [Puvaneswari *et al.,* 2006].

Important classes of pollutants with xenobiotic structural features are polycyclic aromatic hydrocarbons (PAHs), halogenated aliphatic, as well as aromatic hydrocarbons, nitroaromatic compounds, azo compounds, s-triazines, organic sulfonic acids and synthetic polymers. [Fetzner S, 1998]. Due to the chemical properties, for instance, the complexity, number and different molecular arrangements of PAHs, or the amphiphilic properties of surfactants, the quantities of xenobiotics released and their metabolic dead-end products, they will be accumulated in the environment or enter into the food chain leading to biomagnifications [Fetzner S, 1998; Mongensen *et al.,* 2003]. During evolution of catabolic enzymes and pathways, microorganisms were not exposed to these structures and have not developed the capability to use them as sources of carbon and energy [Rieger *et al.,* 2002]. In the other hand, xenobiotics are relatively new to the biosphere and microbes have not had enough time to evolve suitable metabolic apparatus to deal with incorporated xenobiotics [Kulkarnier *et al.,* 2007]. Additionally, also compounds that are easily biodegraded can be classified as pollutants due to their continuous release to the environment.

Based on recent advances in pollution control and monitoring technologies, improved analytical capability, lowering the detection limits and the more stringent legislation, concerns on solve the

problem have increased as well as the research for efficient treatment processes before the discharge of pollutants. The conventional physico-chemical methods are costly and often produce undesirable products, which are toxic or just accumulate the compounds (e.g. by adsorption), requiring further treatment steps [Sridevi *et al.,* 2011]. As alternative, many other eco-friendly techniques have been developed namely bioremediation, phytoremediation and application of enzymes [Kandelbauer and Guebitz, 2005; Sinha *et al.*, 2009]. Indeed, the potential of microorganisms and plants to metabolize xenobiotic compounds has been recognized as effective for toxic and hazardous waste removal [Seridevi *et al.,* 2011]. Though, many of those hazardous substances may resist to biodegradation, be only partially biodegraded or just biotransformed. Moreover, the scope and rate of degradation/transformation of xenobiotics is influenced by factors related with the compound to be degraded, such as the chemical structure and concentration, with the microorganism/enzyme/plant involved, as well as with the physicochemical properties of the environment [Grén I, 2012]. Independently of the treatment process applied, the products of partial biodegradation or biotransformation of the xenobiotics may be less harmful as original compound.

Major sources of xenobiotic compounds include [Thakur I, 2008]:

- chemical and pharmaceutical industries;
- pulp and paper bleaching, originating natural and man-made chlorinated organic compounds;
- textile industries, at which different types of dyes and additives in dying processes are applied;
- mining, releasing heavy metals into biogeochemical cycles;
- fossil fuels, which may be accidentally released in large amounts into the ecosystem by oil spills;
- intensive agriculture, that uses massive amounts of fertilizers, pesticides, and herbicides.

Considering both the volume and the composition of wastewater generated, the textile industry is classified as one of the most polluting among all industrial sectors [Houk VS, 1992; Sam and Demirer, 2003]. Therefore, the development of efficient treatments for textile dyeing effluents constitutes an increasingly important research topic [Kumar *et al.,* 2008]. Moreover, as being an important sector of the Portuguese economy, textile industries are undergoing a period of extreme change, which is forcing companies to rethink strategies in order to innovate and gain competitive

advantage. All those reasons have motivated the work developed, and here stated, on novel technologies to improve biological treatment of dyed wastewaters.

2.1. AZO DYES

Important pollutants in textile effluents are mainly recalcitrant organic compounds such as dyes (in range 10 to 200 mg L^{-1}), surfactants, fixers, softeners, chlorinated compounds and salts [Kumar *et al.*, 2008]. It is estimated that up to 800 000 tons/year of dyes are produced globally, and the most employed at industrial scale are the azo dyes (> 50 %) [Qiang *et al.,* 2012]. Azo dyes are aromatic compounds containing azo groups (–N=N–), which are the principal structure element in dye molecule responsible for light absorption (Figure 2.1), and functional groups such as amino (–NH_2), chloride (–Cl), hydroxyl (–OH), methyl (–CH_3), nitro (–NO_2) and sulfonic acid sodium salt (–SO_3Na) [Shaul *et al.,* 1991].

It had been estimated that about 10 to 50 % of overall production is released into the environment, mainly via wastewater, due to the high portion of unfixed dyes to the fibers in dying processes (Table 2.1) [Sam and Demirer, 2003; Qiang *et al.,* 2012]. As an example, the soluble reactive dyes, used in huge quantities, are known to hydrolyze during application without a complete fixation that can be as low as 50 % [Carliel *et al.,* 1998; O'Neill *et al.,* 1999]. Various attractive forces have the potential of binding dyes to fibres. The dominant force depends on the chemical character of the fibre and the chemical groups in the dye molecule. By increasing relative strength of the bond, the types of forces can be: Van der Waals, hydrogen, ionic or covalent [Ingamels *et al.,* 1993; Guaratini and Zanoni, 2000; Rocha G, 2001]. According to the application categories dyes can be classified as seen in Table 2.1.

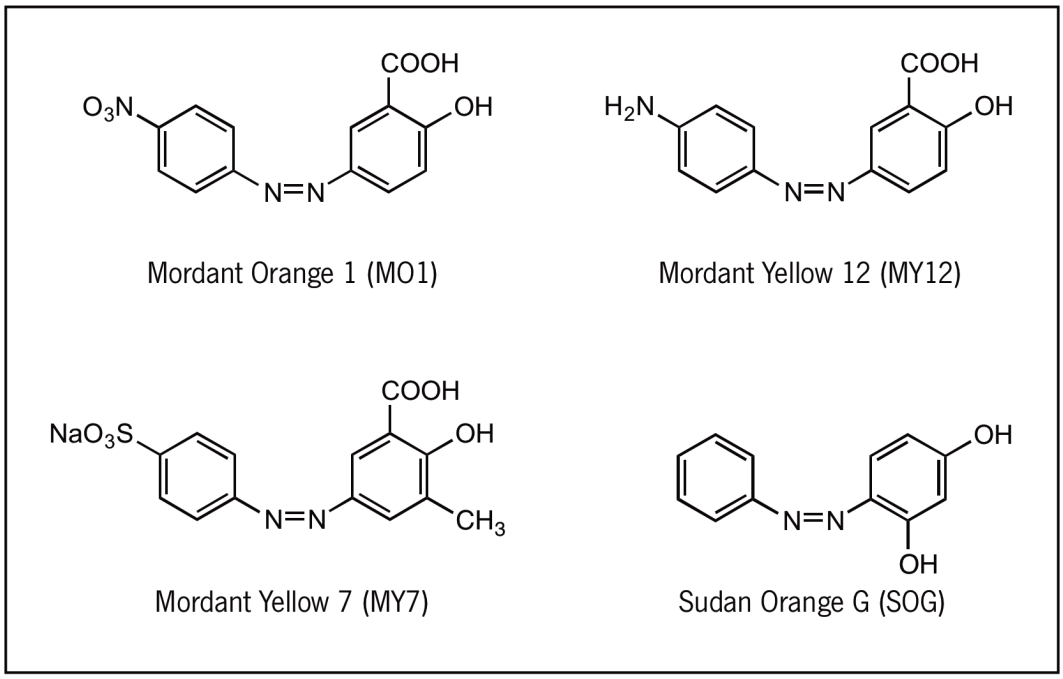

Figure 2.1. Examples of azo dyes' chemical structures.

Textile dyes are visible in water at concentrations as low as 1 mg L^{-1}, leading to a disagreeable aesthetic aspect, and compromising the photosynthesis of algae, reducing the amount of Dissolved Oxygen (DO) and leading to mortality of aquatic species. In addition the end products of dye degradation, aromatic amines, are usually known to be potential carcinogens [O'Neill *et al.*, 1999].

The technical and economic feasibility of each single dye removal technique depends on several factors such as: dye type, wastewater composition, operation costs (energy and materials), environmental fate and handling costs of generated waste products. The use of one individual technique may often not be sufficient to achieve complete decolourisation and, so, combination of different techniques to create an efficient process may be required [Van der Zee, 2002]. Various physical, chemical and biological pre-treatment, main treatment and post treatment techniques can be employed to remove colour from dye containing wastewaters. Physical-chemical techniques include membrane filtration, precipitation, flotation, adsorption, ion change, ion pair extraction, ultrasonic mineralization, electrolysis, advanced oxidation (chlorination, bleaching) and chemical reduction by ozonation, photochemical and Fenton oxidation process [Cooper P., 2003]. The major disadvantage of physical-chemical methods is primarily the high cost, low efficiency, limited

versatility, need for specialized equipment, interference by other wastewater constituents and the handling of the generated waste [Van der Zee and Villaverde, 2005]. Biological processes include bacterial and fungal biosorption and biodegradation in aerobic, anaerobic, anoxic or combined anaerobic/aerobic treatment process. These methods are known to be specific, less energy demanding, effective and environmentally safe, since they result in partial or complete bioconversion of organic pollutants to stable and nontoxic end products [Khan *et al.*, 2011].

Table 2.1. Different classes of the dyes used for specific fibres, main characteristics and degree of fixation on fibres (adapted from [Easton JR, 1995; O'Neill *et al.* 1999])

Dye class	Type of fibre	Characteristics	Fixation (%)
Acid	Polyamide, leather, nylon, wool, silk	Negatively charged when in solution Bind to the cationic NH_3^+ groups present in the fibres	80 – 95
Basic	Acrylic fibres,	Cationic compounds that bind to the acid groups of the fibres	95 – 100
Direct	Cellulose, nylon, cotton, viscose, leather	Large molecules bound by Van der Walls forces to the fibre	75 – 95
Reactive	Cellulose, cotton, wool, nylon	Form covalent bonds with fibres	50 – 90
Disperse	Polyester	Scarcely soluble dye that penetrate the fibre through fibre swelling	90 – 100
Vat	Cellulose fibre, cotton viscose and wool	Insoluble compounds which on reduction give soluble colourless forms (leuco form) with affinity for the fibre	80 – 95
Sulphur	Cellulose fibre, cotton, viscose	Complex polymeric aromatics with heterocyclic S-containing rings	60 – 90

2.1.1. Biodegradation of azo dyes

Biological system with a combining anaerobic/aerobic phase is a logical concept for the removal of azo dyes [Field *et al.,* 1995]. The first step is the anaerobic reduction of azo dyes. Azo dyes accept electrons from different electron donors (such as VFA and flavins azoreductases) resulting in the reductive cleavage of azo linkages and, as a result, the correspondent aromatic amines are formed (Figure 2.2) [Carliell *et al.*, 1995; Razo-Flores *et al.*, 1997; Van der Zee *et al.*, 2000].

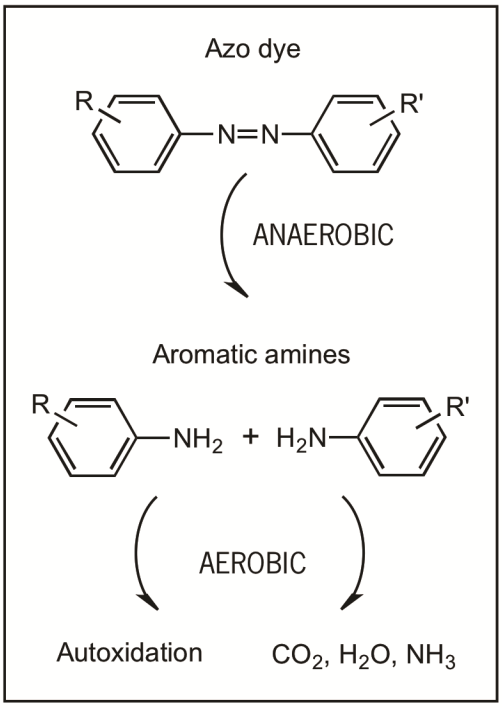

Figure 2.2. Combination of anaerobic/aerobic processes for azo dye biodegradation: reduction of azo dye in the anaerobic process and their correspondent aromatic amines degradation in aerobic process. Illustration adapted from [van der Zee, 2002].

In the aerobic step, occurs the degradation of the aromatic amines. In aerobic conditions the cleavage of the aromatic ring of the aromatic amines leads to the formation of intermediates (e.g. cathecol) for central metabolic pathways [Jothimani *et al.,* 2003]. Other pathway can be by the replacement of other functional groups of the aromatic ring with hydroxyl groups, followed by cleavage by incorporating two oxygen atoms. These reactions are catalysed by hydroxylases and oxygenases [Heider and Fuchs, 1997; Ozer and Demiroz, 2010]. However, this may not apply to all

aromatic amines. It has been demonstrated that particularly sulfonated aromatic amines resisted to biodegradation [Tan *et al.,* 2005], as well as the substituted naphthalene amines [Van der Zee *et al.,* 2005]. Aromatic amines like aniline [Anson and Mackinnon, 1984; Loidl *et al.,* 1990], carboxylated aromatic amines [Stolz *et al.*, 1992; Run *et al.*, 1994], chlorinated aromatic amines [Hwang *et al.*, 1987; Loidl *et al.*, 1990] and (substituted) benzidines [Baird *et al.,* 1977] were found to be degraded under aerobic conditions. Nevertheless, aromatic amines substituted with hydroxyl or carboxyl group, were degraded under methanogenic and sulphate reducing conditions [Razo-Flores *et al.*, 1999; Kalyuzhnyi *et al.,* 2000]. Under denitrifying conditions, 80 % of aniline biodegradation was obtained in an UASB reactor using VFA as carbon source [Pereira *et al.*, 2010]. Its important consider that in the presence of oxygen, some aromatic amines can be subject to autoxidation, which can lead to a high degree of polymerization, oxidative changes in the molecular structure (e.g. deamination), yielding stable, water-soluble, and highly colored compounds [Kudlich *et al.,* 1999].

Several mechanisms have been proposed for the decolourisation of azo dyes under anaerobic conditions such as direct and indirect/mediated dye reduction (Figure 2.3).

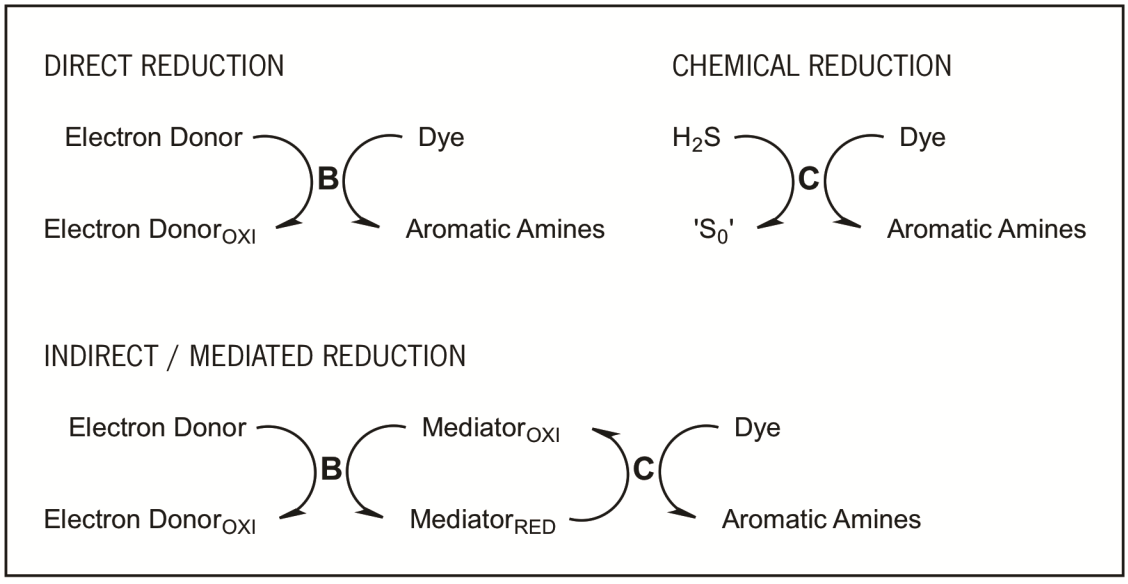

Figure 2.3. Different mechanism for azo dye reduction: direct dye reduction by bacteria (enzymes) or by biogenic reductant (e.g. sulphide) and indirect/mediated reduction of dye by RM. (B) biological step, (C) chemical step. Illustration adapted from [van der Zee *et al.*, 2001].

This reduction may involve different compounds, such as enzymes, RM, chemical reduction by biogenic reductants like sulfide, or a combination of them. Additionally, the location of the reactions can be either intracellular or extracellular [Pandey *et al.,* 2007].

According to direct azo dye biological reduction, specific or non-specific enzymes transfer the reducing equivalents originated from the oxidation of substrate/coenzymes to the azo dyes. Specific enzymes, namely azoredutases, have been found only in aerobic and facultative bacteria showing high specificity to dye structures and have little activity in vivo [Russ *et al.,* 2000; Zimmerman *et al.* 1982, Kulla *et al.,* 1983]. Non-specific enzymes have been isolated from aerobically grown cultures of *Shigella dysenteriae*, Escherichia coli and Bacillus sp. for azo dye reduction [Ghosh *et al.*, 1992; 1993]. Under anaerobic conditions, the reductive cleavage of the azo bond by non-specific cytoplasmic azo reductases has also been studied [Gingell and Watson, 1971; Russ *et al.,* 2000]. The reduced flavins (riboflavin, $FADH_2$, $FMNH_2$) generated by flaving-dependent reductases can transfer electrons to azo dyes. Additionally, other reduced enzyme cofactors as NADH, NADPH, can also act as electron donors for direct azo dye reduction [Stolz A, 2001].

Chemical reductants compounds like dithionite [Davis and Bailey, 1993], zerovalent iron [Nam and Tratnyek, 2000], cysteine, ascorbate or Fe^{2+} [Yoo *et al.*, 2000] may also be involved in direct chemical dye reduction. Sulphide generated via microbial reduction of sulphate in anaerobic conditions, can be able to reduce the azo dyes. Sulphate is a relevant compound and can be present in textile wastewaters due to its use as additive in dyebaths, formed by oxidation of reduced sulphur species, or as a result of neutralization of alkaline dye effluents with sulphuric acid [Yoo *et al.*, 2000; van der Zee, 2002].

Besides from enzyme cofactors, the RM compounds are important stimulants of azo dye bioreduction. The slow rate of reductive anaerobic reactions, due to electron transfer limitations, can be accelerated by adding RM, viewing a more efficient application of anaerobic processes. Indeed, extensive research has been done in order to explore the catalytic effects of different organic molecules with redox mediating properties on the anaerobic chemical and biological transformation of a variety of organic and inorganic compounds. RM are organic molecules that can reversibly be oxidized and reduced, thereby conferring the capacity to serve as an electron carrier in multiple redox reactions [Van der Zee and Cervantes, 2009]. In the presence of RM, the reductive decolourisation of azo dyes occurs in two distinct steps as referred before (Figure 2.3). In the first

step, the RM compound accepts the electrons from the biological substrate oxidation, and in the second, the electrons are chemically transferred to the azo dye (terminal electron acceptor) and consequently the mediator is regenerated [Zhu *et al.,* 2000; Moteleb *et al.,* 2001].

An example of effective RM for azo dye reduction, beyond enzyme cofactors, are quinone compounds such as anthraquinone 2,6-disulfonic acid (AQDS) and anthraquinone-2-sulphonate (AQS), which have been shown to accelerate chemical azo dye reduction by sulphide as well as electrochemical azo dye reduction [Xie *et al.* 2005; Yoo *et al.*, 2000]. In biological systems these compounds were shown to greatly increase the azo dye reduction rates by anaerobic granular sludge in several orders of magnitude [Van der Zee *et al.,* 2003]. Despite these soluble mediators being added at low concentrations (ratio mediator/dye lower than 1), their continuous addition in the systems is necessary, which results in an increase of costs as well as continuous discharge of these recalcitrant compounds [Al-Degs *et al.*, 2008]. To solve this problem, using non-soluble RM seems promising. AC, graphite or alginates beads with immobilized anthraquinones have been shown to act as RM in biological azo dye reduction [Guo *et al.*, 2007; Mezohegyi *et al.*, 2007]. These RM present some advantages compared to the soluble mediators: they can be retained for prolonged time in the bioreactors, can be reused, and do not need to be dosed continually [van der Zee *et al.,* 2003]. In the next section (section 2.2) other CM will be presented as alternative RM improving dye removal efficiency.

2.1.2. Factors affecting dye biodegradation

There are important factors that greatly affect dye removal such as temperature, pH, dye chemical structure, electron donor and acceptor, dye concentration, redox potential and biomass concentration. These parameters must be optimized to grant the maximum dye removal. However, it is noteworthy that dye decolourisation is not influenced by only one factor but a set of factors.

The temperature adequate for dye removal corresponds to the optimum cell culture growth temperature and can vary in the range of 35 °C to 45 °C. The decline in colour removal activity at higher temperatures can be attributed to the denaturation of the azo reductases enzymes or to the loss of cell viability [Chang *et al.*, 2001; Pearce *et al.*, 2003].

Concerning the pH, the neutral condition has been reported as the desired for dye removal, which tend to decrease at strongly acid or alkaline pH values [Pearce *et al.*, 2003]. The growth rate of microorganisms capable of reducing the dyes is significantly affected by pH changing, namely the methanogenic community present in anaerobic bioreactors, which are more efficient at pH 7 [Lee *et al.,* 2009]. However, biological reduction of the azo bonds can result in an increase in the pH due to the formation of aromatic amine metabolites, which are more basic than the original azo compound [Willmott, 1997]. Chang *et al.* (2001) reported that raising the pH value from 5.0 to 7.0 the dye reduction rate increased nearly 2.5–fold, while the rate became insensitive to pH in the range of 7.0 to 9.5.

Other important factor on dye biodegradation is dye chemical structure. Dyes with simple structures and low molecular weights exhibit higher rates of colour removal, contrarily to those with more complex chemical structures with high molecular weight [Sani *et al.,* 1999]. The position and nature of substituent groups in the dye molecule influence the colour removal. Nigam *et al.* (1996) have stated that the groups such as methyl, methoxy, sulpho or nitro groups are more likely to be degraded than hydroxyl or amino group. The substitution of electron withdrawing groups (SO_3H, SO_2NH_2) in the *para* position of the phenyl ring, relative to the azo bond, has been reported to cause an increase in the reduction rate [Sane and Banergee 1999; Pearce *et al.,* 2003]. A similar effect is observed due to the electron density of the –OH, $–NH_2$, $–SO_3Na$ and –COOH groups close to the azo bound, which has a positive effect on dye reduction [Beydille *et al.,* 2000; Chen, 2006; Nigam *et al.,* 2006]. The numbers of azo bonds also influence the dye biodegradation. The author Hu T. (2001) states that biodegradation decreases with the increased of the number of azo bonds in dye molecule.

Many authors suggest that high dye concentrations lead to a decrease on the anaerobic colour removal, associated to the inhibition of metabolic activity. However, it may be due to the blockage of the azoredutases active sites by the dye molecule (with different structures) [Isik and Sponza, 2006; Chang *et al.,* 2001; Saratale *et al.,* 2009; Luangdilok *et al.*, 2000; Rajaguru *et al.*, 2000; Sponza and Isik, 2005]. Furthermore, some active groups (e.g.sulphonic acids groups) on their aromatic rings can inhibit the growth of microorganisms at higher dye concentrations [Chen *et al.,* 2003; Kalyani *et al.,* 2008]. Additionally, microbial activity can be negatively affected due to cell saturation at higher dye concentration in a biosorption process [Ramalho *et al.,* 2004]. Enzymatic

decolourisation studies, demonstrated an optimal dye concentration that gave the highest dye decolourisation rate and a decreasing rate for dye concentrations above the optimal. To improve the decolourisation rate, an adaptation of a microbial community to the dye can promote a natural expression of genes encoding enzymes responsible for its degradation [Ramalho *et al.,* 2004].

Van der Zee and Villaverde (2005) affirm that the presence of an electron donor is a pre-requisite for azo reduction. The requirement amount of electron-donating is 32 mg of COD per mmol of monoazo dye independently of the electron donor type. Different electron donors, such as glucose, acetate, ethanol, VFA, starch, are used for the reduction of different classes of dyes. However, the rate varies with the type of substrate by stimulating specific microorganisms in a mixed culture or affect the enzymatic reaction once different enzymes may be involved in the reaction [Li *et al.,* 1999; Dos Santos *et al.,* 2003].

The presence of an alternative electron acceptor may compete with the azo dye for reducing equivalents. Carlierl *et al.* (1998) investigated on the effect of nitrate and sulphate on the decolourisation of a reactive azo dye, Reactive Red 141. Nitrate was found to delay the decolourisation for a period of time related to the concentration of nitrate initially present in the system. These studies are in accordance with previously published data from batch experiments on azo dye decolourisation revealing that the presence of nitrate [Lourenço *et al.,* 2000; Panswad and Luangdilok, 2000] and also nitrite [Liu *et al.,* 2011] slows down dye decolourisation. On the other hand, sulphate was found to have no discernible effect on the rate of decolourisation. Experiments performed by Van der Zee (2002) demonstrated that sulphate at concentrations up to 60 mM do not obstruct the transfer of electrons to the azo dyes. Probably the redox potential of the reduction of several azo dyes studied was higher than the redox potential of biological sulphate reduction. However, the azo dye reduction and sulphate reduction can proceed simultaneously and in the batch assays, the biogenic sulphide formed contributes to an increase of overall dye reduction. Pereira *et al.,* (2010) also achieved positive results on chemical reduction of different class of azo dye, using sulphide, conducted under anaerobic conditions at different pH values in presence and absence of AC_0. The results demonstrated that AC is the first electron acceptor, being chemically reduced by sulphide and secondly, the electrons from the reduced AC are transferred to the azo dye, the terminal electron acceptor (Chapter 3). Alburquerque *et al.* (2005) tested the effect of ferric iron, which has the ambiguous property of being a competing electron acceptor or a RM on the

decolourisation of the monoazo dye Acid Orange 7 (AO7). The results indicated a positive effect in adding a substoichiometric molar Fe(III)/AO7 ratio of 0.5 on the reactors color removal efficiency, indicating that the role of ferrous iron as electron source for azo dye reduction is more important than the role of ferric iron as competing electron acceptor.

Colour removal is depended on the redox potential of the electron donors and acceptors. It has been reported that anaerobic dye reduction is higher when the redox potential is at its most negative values. Under anaerobic conditions, oxidation–reduction potentials lower than -400 mV are required for high rate of colour removal and also as an effect on the profile of metabolites that are generated during the reduction process [Pearce *et al.,* 2003; Lourenço *et al.,* 2004]. Carliel *et al.* (1995) measured a lower redox potential –500 mV in anaerobic decolourisation of reactive azo dye suggesting that redox potential has a high impact on dye biodegradation.

For the treating textile wastewater, composed of many kinds of dyes, anaerobic azo dye reduction could be readily achieved with different microorganisms [Laszlo *et al.*, 2000]. The use of mixed cultures such as anaerobic granular sludge, which is composed of stable microbial pellets with a high activity, is probably a more logical direction. Indeed, the different microbial consortia present in anaerobic granular sludge can carry out tasks that no individual pure culture can undertake successfully [Pearce *et al.,* 2003]. Furthermore, a positive relation of an increased of biomass concentration with an increased of dye removal has been stated [van der Zee and Villaverde, 2005].

An efficient colour removal biological process should consider the effect of all these factors, nonetheless the nature of the effluent, the location, the climatic conditions and the configuration of the reactor are all of great importance [Pereira and Alves, 2012].

2.1.3. Bioreactor system for dyed wastewater treatment

The biological anaerobic/aerobic systems are the most attractive treatment to be applied for the treatment of wastewaters containing azo dyes [Field *et al.,* 1995]. For this purpose, two different approaches can be used: sequential treatment in separate reactors or an integrated treatment in a single reactor. Concerning the first approach, advanced biological reactors, with different

configurations such as UASB and expanded granular sludge bed (EGSB), have been developed for efficient dyes removal and other compounds of wastewaters [Van der Zee *and* Villaverde 2005]. Relatively to the second approach, many authors have studied dye biodegradation in a temporal separation of anaerobic and aerobic phase in sequential batch reactors (SBR) [Lourenço *et al.,* 2004, 2001; Lovley *et al.,* 1996; Panswad *et al.,* 2001]. For example, Luangdilok *et al.* (2000) reported the biodegradation of reactive dyes in SBR system with 18 h of anoxic/anaerobic phase followed by 5 h of aerobic phase, reaching around 60 % of dyes decolourisation. An overview of the research published on sequential anaerobic-aerobic reactor systems treating azo dye-containing wastewater is presented by Van der Zee and Villaverde (2005), where the distinction made between the different approaches used to obtain a combined anaerobic–aerobic reactor system is outlined.

UASB reactors have been proven as capable of treating several xenobiotics-containing wastewaters. The dense active sludge granules formed, with good setting characteristics and mechanical strength, are the principal feature of the UASB process. Consequently, good COD removal efficiency at high organic loading rates and low HRT can be achieved and the steady-state conditions is rapidly attained [Lettinga G, 1980].

Because the reduction of several azo dyes is a slow process, relatively long HRT are required in anaerobic bioreactors to achieve efficient colour removal. However, this limitation can be overcome by RM [van der Zee and Cervantes 2009].

2.2. REDOX MEDIATORS

Carbon based materials, have excellent properties of specific surface area, surface chemistry and porosity and can be customized for the final applications in several systems such as air and water purification, food, pharmaceutical and chemical industries. Furthermore, its amphoteric character enables to manifest reactivity for many organic and inorganic pollutants. Examples of these CM are the microporous activated carbon (AC), the nanoporous structured materials (carbon nanotubes, CNT) and new mesoporous carbon gels materials (carbon xerogels, CX).

AC was firstly explored in anaerobic bioreactors as a RM on the reduction of azo dyes by Van der Zee *et al.* (2003). The researchers suggest that the quinone groups present in AC surface are the principal electron transferring groups promoting higher decolourisation rates. The effect of AC chemical surface on dye adsorption has also been studied by many authors reporting that quantity and quality of the surface functional groups such as oxygen groups (carboxyl, phenol, carbonyl and lactone groups) associated to the charges of the AC surface determine its performance as catalysts on dye bioreduction [Pereira *et al.,* 2003; Rodriguez-Reinoso F, 1998; Tsang *et al.,* 2007]. Due to their controllable preparation procedure, this material can be tailored to achieve positive modifications in carbon chemical structure groups and be appropriate for specific applications, by proper treatments.

CNT, a member in the carbon family, have been receiving great attention in the scientific community due to their unique relatively large specific surface areas, easily modified surface, and various potential applications [Yao *et al.,* 2010].

Mesoporous CX is also an interesting material, since it possesses high porosity and also a high surface area [Orge *et al.,* 2009] that can also be easily adjusted during the synthesis preparation, as explained further.

The features and principal characteristics of AC, CNT and CX will be briefly discussed in the next section.

2.2.1. Activated Carbon

AC is being prepared from a variety of carbonaceous precursors, including coal, wood, peat, nut shells, industrial and agriculture wastes, by thermal decomposition in a furnace using a controlled atmosphere and heat, and further "activated" either by oxidation with CO_2 or steam, or by treatment with acids, bases or other chemicals. The resulting carbon has a large surface area, which can be higher than 1500 $m^2\ g^{-1}$ [Harris *et al.,* 2008]. Additionally, attempts to form AC materials through organic waste material rich in carbon have been raising attention in the scientific community. In this way, wastes (materials considered as having a big availability and low costs) can be recycled and the produced activated carbon driven to other uses [Tsang *et al.,* 2007].

The most commonly used forms of AC are powders (with a particle size predominantly less than 0.21mm), granules (irregular shaped particles with sizes ranging from 0.2 to 5 mm) and pellets (cylindrical shaped with diameters from 0.8 to 5 mm (Figure 2.4). The choice of granulometry is dependent on the application. As example, in order to have higher available surface area, powder AC is preferred, but to remove materials from a liquid medium, pellets are recommended.

The structure of AC is generally described as a group of randomly cross-linked aromatic sheets and strips, with variable gaps of molecular dimensions between them, corresponding to the pores of the material (Figure 2.5) [Bansal RC, 1988; Henning KD, 2002].

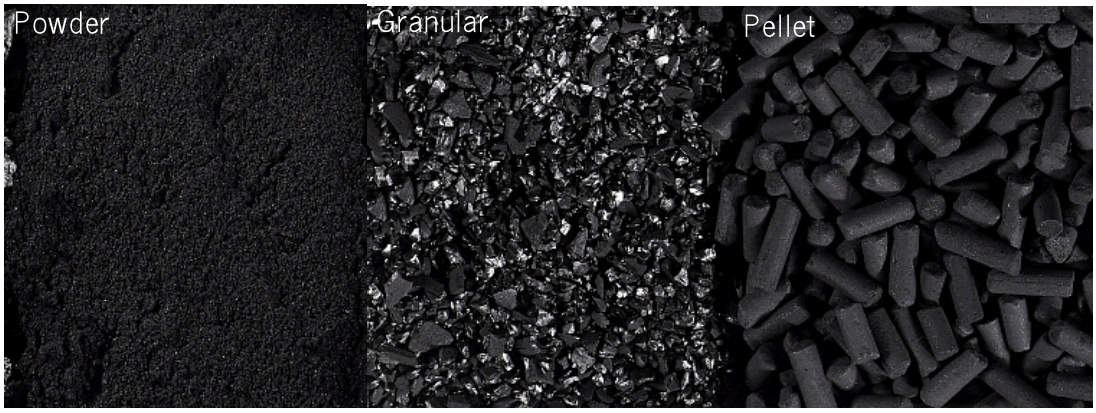

Figure 2.4. Different granulometries of AC. Pictures adapted from www.desotec.com (January, 2015).

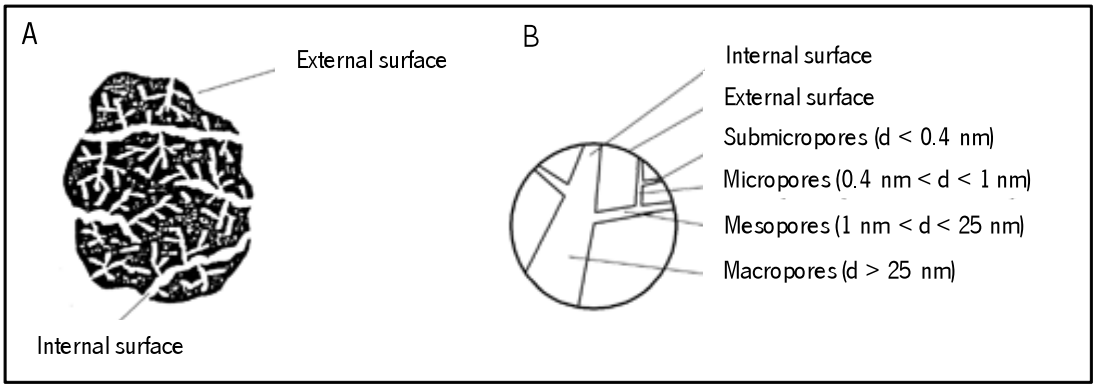

Figure 2.5. AC structure schematic representation (A) and AC pore structure and size (B). Illustration adapted from [Bansal RC, 1988; Henning KD, 2002].

Due to its excellent adsorption properties, AC is widely used in the fields of water and wastewater treatment, gas purification and is largely used in heterogeneous catalysis because it can satisfy most of the required properties (inertness, stability under reaction and regeneration conditions, adequate mechanical properties, high surface area and porosity) [Tsang *et al.,* 2007; Rodríguez-Reinoso F, 1998]. Some publications outline the use of AC as a catalyst in chemical reactions: oxidative dehydrogenation of ethyl benzene [Al-Degs *et al.,* 2008], reduction of NO and N_2O [Muniz *et al.,* 2000; Zhu *et al.,* 2000], reduction of 2,4,6–trinitrotoluene [Moteleb *et al.,* 2001] and decomposition of methane [Moliner *et al.,* 2005].

The production conditions will define the physical and chemical characteristics of the AC obtained, thus it is possible to generate AC with specific features for a specific application [Nieto-Delgado and Rangel-Mendez, 2011].

In Figure 2.6 the most important functional groups in defining the surface chemical properties of AC (that may be present in the starting material or formed in activation step) are represented. Those include oxygen groups such as carboxyl, phenol, carbonyl, quinone and lactone [Bansal RC, 1988].

The nature of the surface functional groups can be modified through physical and chemical treatments, which include liquid phase oxidations with HNO_3 or H_2O_2 and gas phase oxidations with O_2 or N_2O, as well as thermal treatments at high temperatures in different gas environments (N_2, H_2)

to selectively remove some of the functional groups. Additionally, thermal treatments, which remove oxygen groups with acid character, lead to an increase in the basicity of the AC and consequent availability of delocalised π-electrons on the carbon surface [Figueiredo *et al.,* 1999; Pereira *et al.,* 2010; Rodríguez-Reinoso F, 1998].

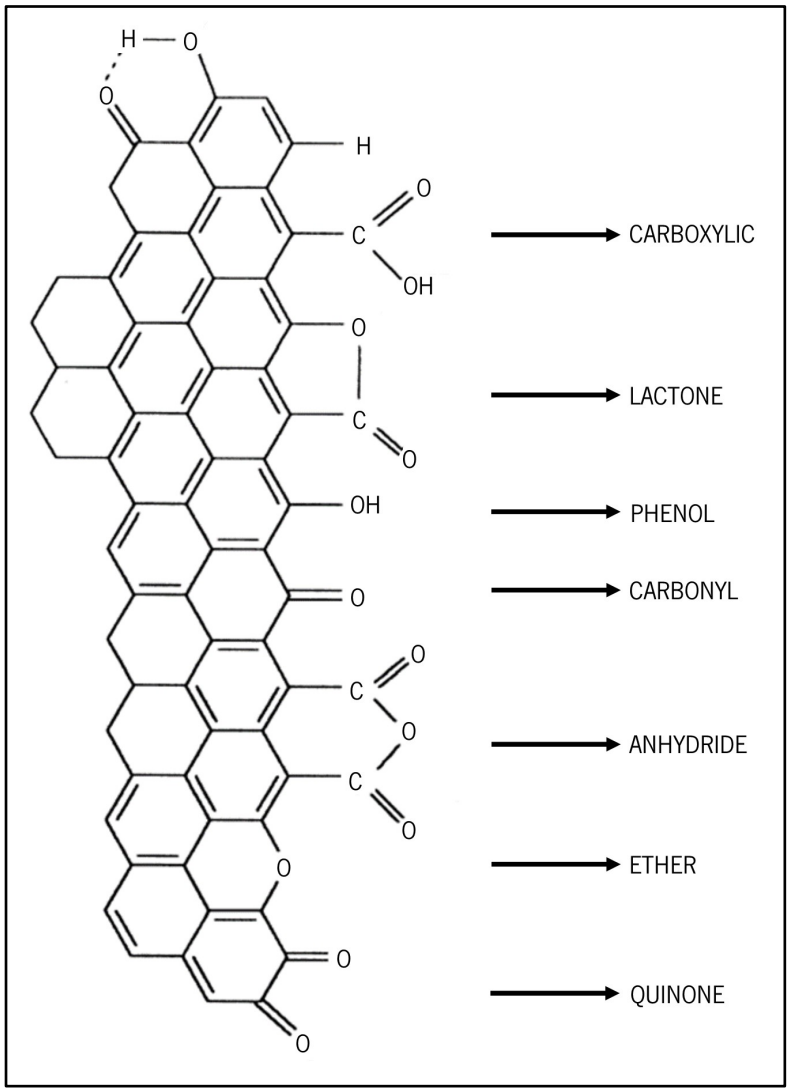

Figure 2.6. Surface groups on AC. Illustration adapted from [Figueiredo *et al.* 1999].

AC samples have amphoteric character and, as a result, their surfaces might be positively or negatively charged depending on the pH of the solution. Carbon surface becomes negatively charged at higher than pH of point zero charge (pH_{pzc}), resulting from the dissociation of surface oxygen

complexes of acid character such as carboxyl and phenolic groups, which are acid sites, and positively charged at pH lower than pH_{pzc} as a result of the existence of electron-rich regions within the graphene layers acting as Lewis basic centers, which accept protons from the aqueous solution [Moreno-Castilla C, 2004].

Dye adsorption on AC has also been proven as an efficient way to remove colour and organic matter from highly coloured effluents [Al-Degs *et al.,* 2008; Pereira *et al.,* 2003]. Its application has been recently extended to in-situ stabilization of marine and fresh-water sediments contaminated by polychlorinated biphenyls (PCBs) and polychlorinated hydrocarbons (PAHs) [Zimmerman *et al.,* 2004; Werner *et al.,* 2005]. The concentrations and bioavailability of aromatic amines were also significantly reduced by adsorption on AC [Faria *et al.,* 2008]. The adsorption capacity of an AC is determined not only by its textural properties but also by the chemical nature of the surface, i.e., the amount and nature of surface functional groups [Pereira *et al.,* 2003]. It is also dependent on the properties of the adsorptive, such as molecular size, polarity, pKa and functional groups. Finally, solution pH, ionic strength and presence of other solutes also influence AC adsorption performance.

The effect of AC chemical surface on dye adsorption has been studied by many authors [Faria *et al.,* 2008; Pereira *et al.,* 2003; Tsang *et al.,* 2007]. The redox mediating capacity of AC samples with different chemical superficial groups will be discussed in chapter 3.

2.2.2. Carbon Nanotubes

A Carbon nanotube is a tube-shaped material, having a diameter ranging from < 1 up to 50 nm and it was first reported by Lijima in 1991. CNT include single-wall (SWCNTs) and multi-wall (MWCNTs), depending on the number of layer comprising them, and can be thought of as cylindrical hollow micro-crystals of graphite (Figure 2.7 A). Based on the direction of hexagons, nanotubes can be classified as zigzag, armchair or chiral (Figure 2.7 B).

A considerable amount of techniques have been developed to produce nanotubes [Kumar and Ando, 2007]. The most widespread methods of CNTs synthesis include arc discharge, laser vaporization and chemical vapour deposition (CVD).

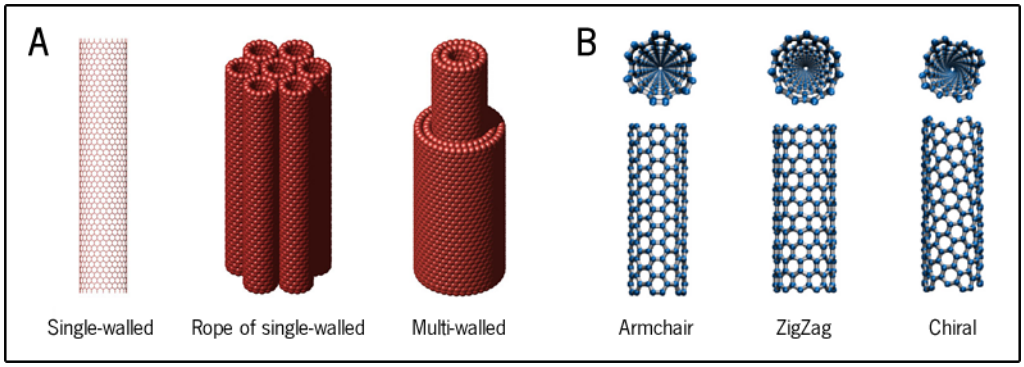

Figure 2.7. Carbon nanotube structures representation (A) and classification (B). Illustration adapted from http://www.nanotechnologies.qc.ca and http://astro.temple.edu/rjohnson/gallery (September, 2011).

Arc-discharge method, in which the first CNTs were discovered, employs evaporation of graphite electrodes in electric arcs that involve very high temperatures (around 4000 °C) [Lijima S., 1991]. Although arc-grown CNT are well crystallized, they are highly impure. Laser-vaporization technique employs evaporation of high-purity graphite target by high-power lasers in conjunction with high-temperature furnaces [Thess *et al.,* 1996]. Despite laser-grown CNTs being of high purity, their production yield is very low and the production process is not energetically efficient. CVD, incorporating catalyst-assisted thermal decomposition of hydrocarbons (purified petroleum products as methane, ethylene, acetylene, benzene, xylene) is the most used method of producing CNTs. This is a low-cost and scalable technique for mass production of CNTs, in comparison to the other techniques previously described. Studies made by Kumar and Andol (2007) produced high-purity CNTs using an environmental-friendly hydrocarbon: camphor, a botanical hydrocarbon [Kumar and Ando, 2007].

The unique physical, chemical and electronic properties of CNTs (Table 2.2) are exploited by their mutable hybridization states and structure sensitivity to alterations in synthesis conditions, which promote the interest in the innovation of new technologies and applications [Xie *et al.,* 2005].

Table 2.2. Theoretical and experimental properties of CNTs (adapted from Xie *et al.,* 2005)

Properties	SWCNTs	MWCNTs
Specific Gravity	0.8 g cm^{-3}	1.8 g cm^{-3}
Elastic Modulus	~ 1 TPa	~ 0.3 – 1 TPa
Strength	50 – 500 GPa	10 – 60 GPa
Resistivity	5 – 50 Ωcm	5 – 50 Ωcm
Thermal conductivity	3000 W m^{-1} K^{-1}	3000 W m^{-1} K^{-1}
Thermal Stability	> 700 °C (in air) 2800 °C (in vacuum)	> 700 °C (in air) 2800 °C (in vacuum)
Specific Surface area	~ 400 – 900 m^2 g^{-1}	~ 200 – 400 m^2 g^{-1}

Carbon nanotube technology can be used for a wide range of new and current applications such as: conductive plastics, structural composite materials, flat-panel displays, gas storage, antifouling paint, micro- and nano-electronics, technical textiles, ultra-capacitors, atomic force microscope (AFM) tips, batteries with improved lifetime, biosensors for harmful gases and extra strong fibers. The technology behind CNT production has also the potential to make important advancements in water security and protection of biothreat agents. CNTs are relatively new adsorbents for trace pollutants from wastewater and they have been characterized as efficient adsorbents with a capacity that exceeds the AC [Long *et al.,* 2001]. Considerable attention has focused on adsorption of contaminants such as Zn^{2+} [Lu and Yang, 2001], Cd^{2+} [Li *et al.,* 2003], Pb^{2+} [Kabashi *et al.,* 2009], Cu^{2+} [Wu C-H, 2007], Cr^{6+} [Di *et al.,* 2006], fluoride [Li *et al.,* 2003b], dioxin [Long *et al.,* 2001], arsenate [Peng *et al.*, 2005], trihalomethanes [Lu *et al.*, 2005] and 1,2-dichlorobenzene [Peng *et al.*, 2003] to CNT. These compounds are non-degradable, highly toxic, carcinogenic, and can result in accumulative poisoning, cancer and nervous system damage. Similarly, CNTs are ideal sorbents for the removal of dyes from textile wastewater [Yau *et al.*, 2010]. As example, batch adsorption experiments were carried out by Shahryari *et al.* (2010) for the removal of Methylene Blue as a basic dye from aqueous solutions using CNT. The effects of major variables that influence the efficiency of

the process such as, initial dye concentration, temperature, CNT concentration and pH, were investigated. Experimental results have shown that, the amount of dye adsorption increased with increasing the initial concentration of the dye, CNT dosage and temperature. The dye removal (10 mg L^{-1}) using 400 mg L^{-1} of CNTs was more than 90 %. The adsorption efficiency of CNTs for the reactive dye Procion Red MX-5B at various pH values (6.5 and 10) and temperatures (280 to 320 K) was examined by Chung-Hsin Wu (2007b). The adsorption capacity was highest when 0.25 g L^{-1} of CNT was added. Positive enthalpy (ΔH°) and entropy (ΔS°) values indicated that the adsorption of Procion Red MX-5B (20 mg L^{-1}) onto CNT was endothermic, which result was supported by the increasing dye adsorption with temperature. The values of enthalpy, free energy of adsorption (ΔG°) and activation energy (E_a) suggested that the reactive dye adsorption onto CNT was a physisorption process and was spontaneous [Wu C-H, 2007; Kuo *et al.,* 2008]. Apart from adsorption properties, recent filtration studies using CNT have also revealed the capability of CNT nanofilters to remove pathogenic microorganisms such as protozoa, bacteria and viruses in wastewater treatment, with microorganisms being retained on the surface of CNT based on a depth-filtration mechanism [Mostafavi *et al.,* 2009]. Li *et al.* (2008) observed strong antimicrobial properties of CNT. This behavior allows CNT to replace chemical disinfectants as a new effective strategy to control microbial pathogens avoiding the formation of harmful disinfection byproducts (DBPs) such as trihalomethanes, haloacetic acids or aldehydes [Li *et al.,* 2008]. Highly purified CNTs exhibit strong antimicrobial activity toward Gram positive and Gram-negative bacteria, as well as bacterial spores. The activities inflicted by the antimicrobial property can be attributed to impairment of pathogen cellular function by destruction of major constituents (e.g. cell wall) interference with the pathogen cellular metabolic processes and inhibition of pathogen growth by blockage of the synthesis of key cellular constituents (e.g. DNA, coenzymes and cell wall proteins) [Ong *et al.,* 2010]. Direct contact of E. coli cell with SWCNTs leads to severe membrane damage and subsequent cell inactivation [Kang *et al.,* 2007]. Some studies have also proposed CNT as scaffolding for antimicrobial agents like Ag nanoparticles [Morones *et al.,* 2005] and antimicrobial lysozyme [Nepal *et al.,* 2008] due to their excellent mechanical properties. In many applications, in scientific or technological fields, it is necessary to tailor the chemical nature of the CNT wall in order to take advantage of their properties. For example, for biological applications of nanotubes as substrates for proteins, the noncovalent attachment of a pyrene derivative to the nanotube has been reported to immobilize enzymes on the surface of the nanotube [Chen *et al.,* 2001]. Using CNT as a reinforcing component in polymer

composites requires the ability to tailor the nature of nanotubes walls in order to control the interfacial interactions between the nanotubes and the polymer chains. These interactions govern the load-transfer efficiency from the polymer to the nanotubes and hence the reinforcement efficiency. Two main approaches are considered for the surface modification of CNTs [Eitan *et al.,* 2003]: one is noncovalent attachment of molecules, while the second is covalent attachment of functional groups to the walls of the nanotubes. Noncovalent attachment is based mainly on Van der Waals forces and is controlled by thermodynamic criteria. The advantage of noncovalent attachment is that the perfect structure of the nanotube is not altered, thus its mechanical properties do not change. The main potential disadvantage of noncovalent attachment is that the forces between the wrapping molecule and the nanotube might be weak, thus as a filler in a composite the efficiency of the load transfer might be low. The covalent attachment of functional groups to the surface of nanotubes can improve the efficiency of load transfer. However, it must be noted that these functional groups might introduce defects on the walls of the perfect structure of the nanotubes. These defects will lower the strength of the reinforcing component. Therefore, there will be a trade-off between the strength of the interface and the strength of the nanotube filler. Studies have been done to chemically modify single and MWCNTs [Ong *et al.,* 2010]. Lui *et al.* (2006) reported on a simple, nondestructive method to noncovalently modify MWNTs with a graft polymer synthesized polystyrene-g-(glycidyl methacrylate-co-styrene) (PS-g-(GMA-co-St)). The noncovalent modification strategy is based on the affinity of the PS main chains to the surface of pristine MWNTs (p-MWNTs) and the modified MWNTs can be solubilised in a wide variety of polar and nonpolar organic solvents at the same time.

2.2.3. Carbon gels

Several works were recent dedicated to the preparation of synthetic porous CM, with special attention to the control of the textural properties, affirming to be the key for an efficient (electro) catalytic and adsorption processes [Zimmerman *et al.,* 2004].

Carbon gels are porous materials that are highly sensitive to the conditions at which they are synthesized. They are very easy to tailor in terms of shape, porous texture and surface chemistry.

They can be obtained by different procedures but the preparation basically consists of three steps: (*i*) gel synthesis, involving the formation of a three-dimensional polymer in a solvent (gelation), followed by a curing period, (*ii*) gel drying, where the solvent is removed to obtain an organic gel, and finally (*iii*) pyrolysis under an inert atmosphere to form the porous carbon material, i.e. the so-called carbon gel [Lufrano *et al.,* 2011]. There are three types of carbon gels, depending on the synthesis method: carbon aerogels (CA), carbon cryogels (CC) and carbon xerogels CX. Their synthesis method only differs in the way of drying. An aerogel, in general, is produced when the solvent contained within the voids of a gelatinous structure is exchanged with an alternative solvent, such as liquid CO_2, that can be removed supercritically in the absence of a vapour-liquid interface and thus without any interfacial tension. Ideally, this supercritical drying process leaves the gel structure unchanged with no shrinkage of the internal voids or pores [Zanto *et al.,* 2002]. In contrast, a CX is produced when the solvent is removed by conventional methods such as evaporation under normal, nonsupercritical conditions [Pekala RW, 1989]. CC can be synthesized by an inverse emulsion polymerization of resorcinol with formaldehyde, followed by freeze-drying and pyrolysis in an inert atmosphere [Yamamoto *et al.,* 2002].

Carbon gels are composed of interconnected near-spherical nodules, the size of which depends on the precursor solution composition, the pH being a key variable. An experiment executed by Job *et al.* (2005) synthesized several CX with different pore texture (i.e. pore size and pore volume) modifying the pH of the precursor solution. By changing the pH of the resorcinol-formaldehyde solution (RF), one can modify the size of the nodules and thus the size of the pores after drying and pyrolysis. So, according to these results, the pore size was adjusted between 25 and 300 nm. RF aqueous gels are among the most studied systems.

Most of the published works on RF gels agree that the synthesis and drying processes are the steps that define the size and volume of the mesopores and macropores in the final carbon gels and that the development of the micropores takes place during the subsequent pyrolysis step [Kand *et al.,* 2008]. The meso or macro porosity formed during the synthesis is barely altered during thermal stabilization (i.e. the pyrolysis step). The microporosity created during the pyrolysis can be increased through an activation process. RF carbon gels usually have surfaces of around 600 to 700 $m^2\ g^{-1}$, whereas AC surfaces can exceed 2000 $m^2\ g^{-1}$. To overcome this limitation, carbon gels can be chemically activated for specific applications where high surface areas are required.

Lufrano *et al.* (2011) prepared a CX that was chemically activated with 75 wt % orthophosphoric acid using an activating agent/carbon gel mass ratio of 3:1. The results showed an increased up to 3–fold of BET specific surface (S_{BET}) of activated carbon gel compared to not activated carbon gels: S_{BET} of 2360 m^2 g^1 and 650 m^2 g^1, respectively. Some researches on adsorption of dyes onto carbon gels are already published [Cooper *et al.,* 1999; Wu *et al.,* 2004]. As example, the study followed by Wu *et al.* (2005), a mesoporous xerogel modified by direct incorporation of functional groups (propyl group) was used for studying the adsorption kinetics and thermodynamics of an organic dye (Brilliant Blue FCF), under various experimental conditions. The equilibrium adsorption amount increases with the increase in initial dye concentration, temperature, solution acidity, and ionic strength. The thermodynamic analysis indicates that the adsorption is spontaneous and endothermic. Electrostatic attraction and hydrophobic interaction are suggested to be the dominant interactions between dye and the xerogels surface.

CHAPTER 3.

THERMAL MODIFICATION OF ACTIVATED CARBON SURFACE CHEMISTRY IMPROVES ITS CAPACITY AS REDOX MEDIATOR FOR AZO DYE REDUCTION

The surface chemistry of a commercial activated carbon (AC_0) was selectively modified by chemical oxidation with HNO_3 (AC_{HNO3}) or O_2 (AC_{O2}), and thermal treatments under H_2 (AC_{H2}) or N_2 (AC_{N2}) flow. The effect of modified AC on anaerobic chemical reduction of four dyes (acid orange 7, reactive red 2, mordant yellow 10 and direct blue 71) was assayed with sulphide at different pH values 5, 7 and 9. Batch experiments with low amounts of AC (0.1 g L^{-1}) showed a 9–fold increase of the reduction rate, comparing with assays without AC. Optimal rates were obtained at pH 5 except for MY10 (higher at pH 7). In general, rates increased with increasing pH_{pzc}, following the trend $AC_{HNO3} < AC_{O2} < AC_0 < AC_{N2} < AC_{H2}$. The highest reduction rate was obtained for MY10 with AC_{H2} at pH 7. In a biological system using granular biomass, AC_{H2} showed a 2– and a 4.5–fold increase in the decolourisation rates of MY10 and RR2, respectively. In this biological system, the reduction rate was independent of AC concentration in the tested range of 0.1–0.6 g L^{-1}.

CHAPTER 3.
THERMAL MODIFICATION OF ACTIVATED CARBON SURFACE CHEMISTRY IMPROVES ITS CAPACITY AS REDOX MEDIATOR FOR AZO DYE REDUCTION

3.1. INTRODUCTION

Azo dyes are commonly reduced under anaerobic conditions, although the rate of the reaction may be rather low, especially for dyes with high polarity or complicated structure. This poses a serious problem for the application the treatment of dying wastewater, because long HRT is necessary to reach a satisfactory extent of dye reduction [Van der Zee *et al.,* 2001]. Moreover, addition of RM has also been proved to significantly accelerate the rate of azo dye reduction by favouring electron transfer from primary electron donor (co-substrate) to terminal electron acceptor (azo dye). Using these RM, higher reductive efficiency can be achieved in anaerobic bioreactors, operated at HRT realistic for wastewater treatment practice [Dos Santos *et al.,* 2004; Cervantes *et al.,* 2001; Van der Zee and Cervantes, 2009]. AC has been shown as a feasible RM and presenting advantages in comparison with soluble ones (e.g. AQDS, AQS) [Mezohegyi *et al.,* 2007; Van der Zee *et al.,* 2003]. Furthermore, its amphoteric character enables to manifest reactivity for many organic and inorganic pollutants. Adsorption on AC has also been proven to be efficient in removing colour and organic matter from highly coloured effluents and as a catalyst in chemical reactions [Al-Degs *et al.,* 2008; Faria *et al.,* 2005; Malik *et al.,* 2004; Moliner *et al.*, 2005; Moteleb *et al.,* 2001; Muniz *et al.,* 2000; Pereira *et al.,* 2003; Zhu *et al.,* 2000]. Other advantage of AC is that it can be modified physically and chemically, in order to optimize its performance. The effect of AC chemical surface on dye adsorption was previously studied [Al-Degs *et al.,* 2000;Pereira *et al.,* 2003; Tsang *et al.,* 2007], and very recently Mezohegyi *et al.* (2010) found that decolourisation rates, in upflow stirred packed-bed reactors, were significantly influenced by the textural properties of AC and moderately affected by its surface chemistry. However, these authors performed experiments in reactors with working volumes of 2 mL and 500 g of AC per L, which is too far from potential applicability.

In the present work, the redox mediating capacity of AC samples with different chemical superficial groups was explored in batch assays for the reduction of four azo dyes (acid, direct, mordant and

reactive), at different pH values. Since sulphate is a common pollutant present in textile wastewater being biologically reduced to sulphide, during anaerobic treatment and sulphide has been reported to be an azo dye reducing agent [Cervantes *et al.,* 2007; Van der Zee *et al.,* 2001], sulphide was initially elected as chemical reducing agent. This choice was also based on its suitability to limit the system variability. AC samples were obtained by chemical/thermal treatments of a commercial AC. Biological assays were performed in the best conditions obtained by the chemical dye reduction studies. AC was mixed with anaerobic granular sludge at final concentrations in the range of 0.1–0.6 g L^{-1}.

3.2. MATERIALS AND METHODS

3.2.1. Dyes

Reactive Red 2 (RR2, dye content 40 %), Acid Orange 7 (AO7, dye content 85 %), Mordant Yellow 10 (MY10, dye content 85 %) and Direct Blue 71 (DB71, dye content 50 %), were selected as azo dye model compounds. The chemical structures of the dyes are illustrated in Figure 3.1. Dyes were purchased from Sigma and used without additional purification. Stock solutions of 14 mmol L^{-1} were prepared in deionised water. RR2 was hydrolysed under alkaline conditions (pH 12 adjusted with 1 mol L^{-1} NaOH) by boiling the solution for 1h; after that period, solution was cooled down, pH was settled to 7 with 1 mol L^{-1} HCl and final volume adjusted with deionised water.

3.2.2. Preparation of activated carbon samples

A Norit ROX 0.8 activated carbon (pellets of 0.8 mm diameter and 5 mm length) was used as supplied by Norit as a starting material (sample AC_0). In order to prepare AC with different chemical composition on the surface, maintaining the original textural properties as much as possible, different treatments were performed according to those previously described by Pereira and co-

workers (2003), as following: i) chemical oxidation of AC_0 with 6 mol L^{-1} of HNO_3 at boiling temperature for 3 h (sample AC_{HNO3}) and ii) starting from AC_{HNO3}, 1 h of thermal treatment under N_2 flow at 900 °C (sample AC_{N2}) or H_2 flow at 700 °C (sample AC_{H2}). Gas oxidation of AC_0 with 5 % O_2 at 425 °C for 6 h was made in order to prepare the sample AC_{O2}; in this case, some burning of the sample occurred (12.5 %) which will result in alteration of the textural properties [Cervantes *et al.*, 2007].

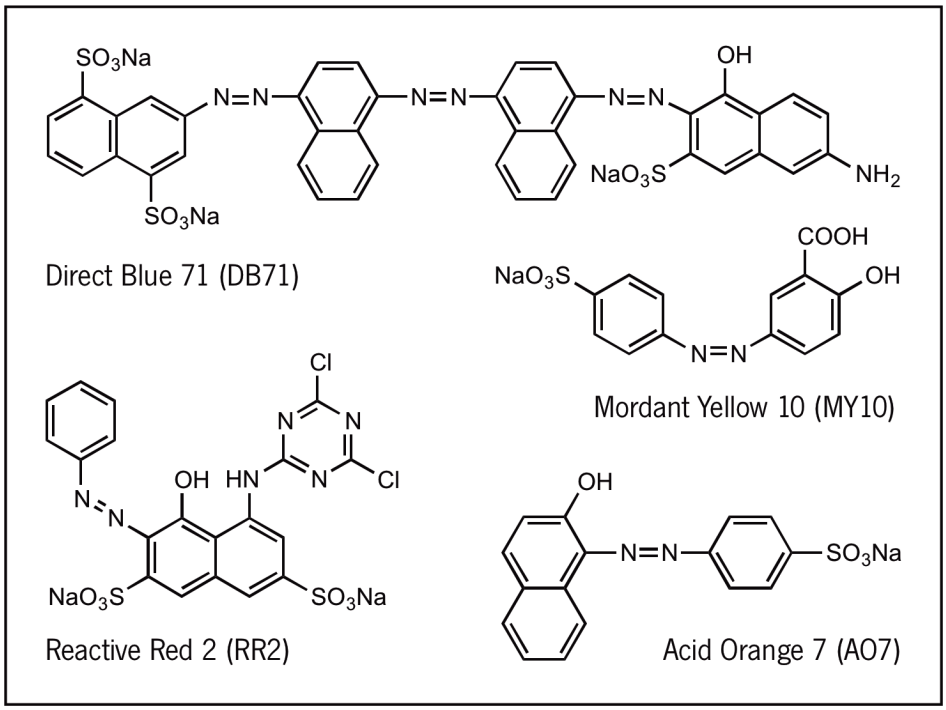

Figure 3.1. Molecular structure of the azo dyes.

3.2.3. Textural characterisation of activated carbons

The textural characterisation of the materials was based on N_2 adsorption isotherms, determined at 77 K with a Coulter Omnisorp 100 CX apparatus. The BET surface area (S_{BET}) was calculated using the BET equation. The micropore volume (W_{micro}) and mesopore surface area (S_{meso}) were calculated by the t-method, using the standard isotherms for carbon materials proposed by Rodriguez-Reinoso *et al.* (1987). The adsorption data were also analysed with the Dubinin equation. In all cases, a type IV

deviation was noted [Linares-Solango *et al.,* 1987]. Two microporous structures were taken into account, and the corresponding volumes, W_{01} (smaller pores) and W_{02} (larger pores), were calculated [Linares-Solango *et al.,* 1987]. The Stoeckli equation [Stoeckli *et al.,* 1989] was used to estimate the average micropore width of the smaller pores (L_1), using a value of 0.34 for the affinity coefficient of nitrogen.

3.2.4. Surface chemistry characterisation of activated carbons

Activated carbon samples have amphoteric behaviour and in general the more acidic samples are the less basic ones. Acidity and basicity is related with the chemical groups at the AC surface; the surface chemistry of AC samples was characterized by the estimation of material acidity and basicity, the pH of point zero charge (pH_{pzc}) and CO/CO_2 release by temperature-programmed desorption (TPD) as described by Figueiredo *et al.* (1999). Briefly:

i) The CO_2 spectrum was decomposed into three contributions, corresponding to carboxylic acids (low temperatures), carboxylic anhydrides (intermediate temperatures) and lactones (high temperatures).
ii) The carboxylic anhydrides decompose by releasing one CO and one CO_2 molecule. Thus, a peak of the same shape and equal magnitude to that found on the CO_2 spectrum was included in CO spectrum. This peak was pre-defined from the deconvolution of the CO_2 spectrum.
iii) In addition to the carboxylic anhydrides, the CO spectrum includes contributions from phenols (intermediate temperatures) and carbonyl/quinones (high temperatures).

The pH_{pzc} is a critical value for determining quantitatively the net charge (positive or negative) carried on the AC surface as a function of the solution pH. Its determination was carried out as follows: 50 cm^3 of 0.01 mol L^{-1} NaCl solution was placed in a closed Erlenmeyer flask. The pH was adjusted to a value between 2 and 12 with the solutions 0.1 mol L^{-1} HCl or 0.1 mol L^{-1} NaOH. Then, 0.15 g of each AC sample was added and the final pH measured after 48 h under agitation at room temperature. The pH_{pzc} is the point where the curve pH_{final} *vs* pH_{inital} crosses the line $pH_{initial} = pH_{final}$.

3.2.5. Chemical dye reduction

Batch experiments were conducted in order to evaluate the capacity of the synthesized AC samples as a redox mediator on the reduction of different azo dyes by sulphide. Buffered solutions at different pH values, 20 mmol L^{-1} of sodium acetate for pH 5.0 and 6 mmol L^{-1} sodium bicarbonate for pH 7.0 and 8.7, were prepared. AC pellets were crushed to obtain particles with different size. A preliminary screening showed that the size of AC particles significantly affects their role as a redox mediator for dye reduction by sulphide. An increase of the rate of decolourisation was obtained with decreasing the AC size. Therefore, all the experiments were conducted with AC particles with a diameter less than 0.315 mm. The flasks, containing different samples of activated carbon (0.1 g L^{-1}) and buffer, were sealed with butyl rubber stoppers and flushed for 5 min with oxygen-free N_2 gas for pH 5.0 and 8.7 and with N_2:CO_2 (80:20 %) for pH 7.0. After flushing, sulphide was added with a syringe from a partially neutralised stock solution (0.1 mol L^{-1} Na_2S) to obtain an initial total sulphide concentration of 1 mmol L^{-1} for azo and 2 mmol L^{-1} for trisazo dyes. According to the stoichiometry of dye reduction by sulphide, 2 moles of sulphide are required per mole of azo dye when sulphide is oxidised to elemental sulphur [Van der Zee *et al.,* 2003]. Controls without sulphide were incorporated to correct for dye adsorption, as well as to verify the stability of the dyes. The vials were pre-incubated (over night) in a 37 °C rotary shaker at 135 min^{-1}. After that time, 0.3 mmol L^{-1} of dye was added with a syringe (1 mL) to the reaction solution, from a concentrated stock (14 mmol L^{-1}). All the experiments were prepared in triplicate. First order reduction rate constants were calculated in OriginPro 6.1 software, applying the follow equation 1:

$$C_t = C_0 + C_i\, e^{-kt} \qquad \text{(Equation 1)}$$

Where C_t is the concentration at time t; C_0, the offset; C_i, the concentration at time initial time, k, the first-order rate constant (d^{-1}) and t, is the accumulated time of the experiment.

Colour removal (CR) was calculated according to equation 2:

$$CR\ (\%) = 100 \times (A_0 - A_t) / A_0 \qquad \text{(Equation 2)}$$

Where A_0 is the absorbance at λ_{max} of the dye at the beginning of incubation and A_t, the absorbance at λ_{max} at a selected time.

3.2.6. Biological dye reduction

Biological assays using anaerobic granular biomass (1 gVS L^{-1}) were performed in batch. The best conditions from the chemical dye reduction were reproduced: sodium bicarbonate solution at pH 7 containing 0.3 mmol L^{-1} of MY10 and 0.1 g L^{-1} of AC_{H2}. As controls, assays without AC and with AC_0 were also run. Co-substrates are required as an electron source for the reduction; different carbon sources were tested (2 g L^{-1}): glucose, lactose, and VFA (acetic, propionic and butyric acid, 1:10:10). As macronutrients, 2.8 g L^{-1} NH_4Cl, 2.5 g L^{-1} KH_2PO_4, 1.0 g L^{-1} $MgSO_4.7H_2O$ and 0.06 g L^{-1} CaCl, were added. All the assays were performed in triplicate. The effect of AC concentration was evaluated by testing increasing amounts of untreated (AC_0) and treated AC (AC_{H2}) ranging from 0.1 to 0.6 g L^{-1}.

3.2.7. Analytical techniques

Colour decrease was monitored spectrophotometrically in a 96-well plate reader (ELISA BIO-TEK, Izasa). At select intervals, samples were withdrawn (300 μL), centrifuged at 1500 min^{-1} rotation for 10 min to remove the AC and diluted, with the same buffer as of the reaction, due to the high absorbance of the dye, even at low concentrations. The visible spectra (300–900 nm) were recorded and dye concentration calculated at λ_{max}. Molar extinction coefficients were calculated for each dye at λ_{max}: ε_{480nm}= 9.60 L mol^{-1} cm^{-1} for AO7; ε_{540nm}= 28.64 L mol^{-1} cm^{-1} for RR2; ε_{350nm}= 15.52 L mol^{-1} cm^{-1} for MY10 and ε_{590nm}= 7672 L mol^{-1} cm^{-1} for DB71. No changes were observed in the visible spectra with the pH of the solution.

3.3. RESULTS AND DISCUSSION

3.3.1. Textural characterization

A set of modified AC samples was prepared by different methods in order to obtain materials with different surface chemical groups (acidic and basic) but maintaining their textural properties. The results of textural characterization resulting from the N_2 equilibrium adsorption isotherms at 77 K are presented in Table 3.1. No major changes were observed in the textural properties of AC for the liquid phase oxidations and thermal treatments, as expected. However, a slight decrease occurred in the surface area and pore volume for the oxidation with HNO_3. These changes may result from the collapse of some of the pore walls caused from the drastic conditions of the treatment. On the other hand, sample prepared by O_2 oxidation presents an increase of the micropore volume and average micropore width. This effect is directly related with the burn-off (BO) degree [Cervantes *et al.,* 2007]. Consequently, an additional contribution of the textural properties of AC on its behaviour as a catalyst on dye reduction may be expected for the last material. For the other AC samples, the behaviour may be attributed mainly to differences on the chemical surface properties produced by different treatments.

Table 3.1. Textural characterisation of the activated carbon samples

Sample	S_{BET} ($m^2\ g^{-1}$) (± 10)	W_{micro} ($cm^3\ g^{-1}$) (± 0.005)	S_{meso} ($m^2\ g^{-1}$) (± 5)	W_{01} ($m^2\ g^{-1}$) (± 0.005)	W_{02} ($cm^3\ g^{-1}$) (± 0.005)	L_1 (nm) (± 0.1)
AC_0	1032	0.382	138	0.350	0.038	1.0
AC_{HNO3}	893	0.346	102	0.309	0.032	1.0
AC_{O2}	1281	0.497	149	0.450	0.045	1.2
AC_{N2}	947	0.359	90.5	0.340	0.023	1.1
AC_{H2}	987	0.377	129	0.334	0.039	1.1

3.3.2. Surface chemistry characterization

Table 3.2 summarizes the results obtained from the chemical characterization of AC samples used in this study. Surface oxygen groups on carbon materials decompose upon heating, releasing CO and/or CO_2 at different temperatures. According to this, it is possible to identify and estimate the amount of oxygenated groups on a given carbon by TPD experiments.

Table 3.2. Chemical characterisation of the AC samples

Sample	CO^a (µmol g^{-1}) (± 20)	CO_2^a (µmol g^{-1}) (± 20)	Basicity (meq HCL g^{-1}) (± 0.005)	Acidity (meq NaOH g^{-1}) (± 0.005)	pH_{pzc} (± 0.2)
AC_0	814	243	0.457	0.370	8.4
AC_{HNO3}	2402	1103	-0.065	1.720	2.7
AC_{O2}	4105	239	n.d.	n.d.	4.5
AC_{N2}	890	120	0.547	0.432	9.2
AC_{H2}	590	59	0.640	0.086	10.8

n.d. not defined; a – amounts of CO and CO_2 released, obtained by integration of the areas under TDP spectra

Table 3.3 shows the amount of each type of oxygen-containing surface groups estimated from the deconvolution of the TPD spectra (Figure 3.2) following the method previously proposed in references [Cervantes *et al.,* 2007; Stoeckli *et al.,* 1989].

The highest amount of carboxylic groups was generated by the oxidation with HNO_3, which presents a value almost 7 times higher than those generated with other treatments. Although to a lesser degree, this sample also presents the highest amount of anhydrides and lactones groups. These acidic groups are responsible for the high acidity and the lower pH_{pzc} value obtained. In fact, the basicity and acidity of the samples are related with the chemical groups at the surface, thus complementing the results obtained from TPD experiments.

Table 3.3. Oxygen-containing surface groups estimated from the TPD spectra deconvolution (± 10 %)

Sample	Carboxylic acids (μmol g^{-1})	Anhydrides (μmol g^{-1})	Lactones (μmol g^{-1})	Phenols (μmol g^{-1})	Carbonyl/quinones (μmol g^{-1})
AC_0	110	79	54	428	307
AC_{HNO3}	723	222	158	948	1232
AC_{O2}	0	90	149	1321	2694
AC_{N2}	67	15	38	307	568
AC_{H2}	48	0	11	249	341

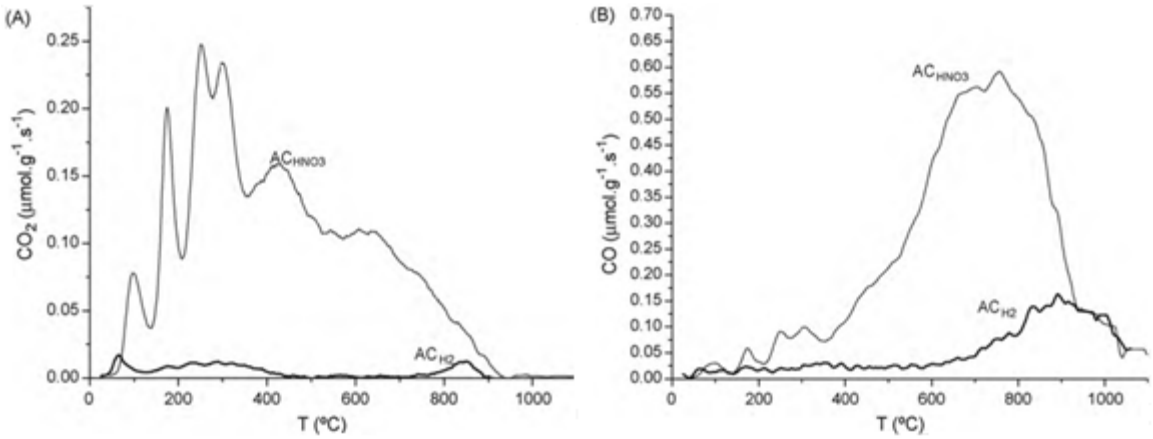

Figure 3.2. TPD spectra before and after different treatments: (A) CO_2 evolution and (B) CO evolution. Examples for AC_{HNO3} and AC_{H2}.

Higher CO_2 release was obtained for more acidic samples, AC_{HNO3} (pH_{pzc} of 2.7) and AC_{O2} (pH_{pzc} of 4.5), which indicates that liquid and gas oxidation produce samples with a higher amount of surface oxygen-containing groups. The gas oxidation treatment (AC_{O2}) was the most effective to introduce phenols and carbonyl/quinone groups, being almost the double when compared with the nitric acid treatment. Thermal treatments at high temperature produce materials with low amount of oxygen-containing groups and high basicity, resulting mainly from the ketonic groups remaining on the surface, from the low amount of acidic groups, and from the delocalised π-electrons of the carbon basal planes. These electrons are responsible for the high basicity of the thermal treated samples. The acidic oxygen-surface groups have a withdrawal character fixing those π-electrons [Menendez *et*

al., 1996]. Comparing the two thermal treatments, with H_2 more basic materials are generated (pH_{pzc} of 10.8), since a stabilization of the reactive sites by C–H bonds occurs [Pereira *et al.,* 2003; Menendez *et al.,* 1996] and also an enhanced effect of the π-electron system. N_2 treatments leave unsaturated carbon atoms that are very reactive for subsequent oxygen adsorption, forming again some of the removed groups upon ambient air exposure. The pH_{pzc} of this sample is 9.2.

3.3.3. Azo dye reduction

Chemical azo dye reduction using sulphide was conducted under anaerobic conditions at pH values of 5.0, 7.0 and 8.7, both in presence and absence of AC_0 (Table 3.4). Different classes of dyes, acid (AO7), reactive (RR2), mordant (MY10) and direct (DB71), were tested.

Decolourisation was followed spectrophotometricaly and a decrease in the intensity of the maximum absorption band was observed for all the dyes, indicating the cleavage of the aromatic azo groups (data not shown), generally related to the formation of lower molecular weight aromatic amines that may be more susceptive to degradation under biological aerobic conditions. The spectra of DB71 shifted from 590 to 550 nm and the solution changed from blue to light violet colour. All the reactions followed a first order kinetic model (Figure 3.3, example for pH= 5) and the apparent rate constants and degrees of colour removal were calculated from the initial slope of the concentration *vs* time data (Table 3.4). Undoubtedly, the pH of dye solution played an important role in the dye reduction. In the assays without AC, only DB71 was reduced in the three tested pH, but the rate was circa 3–fold higher at pH 5 (4.4 ± 0.6 d^{-1}).

The mordant dye was decolourised only at pH 5 and 7, (1.1 ± 0.1) d^{-1} and (1.4 ± 0.1) d^{-1}, respectively. AO7 and RR2 were the most resistant to the reduction by sulphide; very low rates were obtained: (0.2 ± 0.1) d^{-1} at pH 7, for AO7 and (0.9 ± 0.1) d^{-1} at pH 5, for RR2.

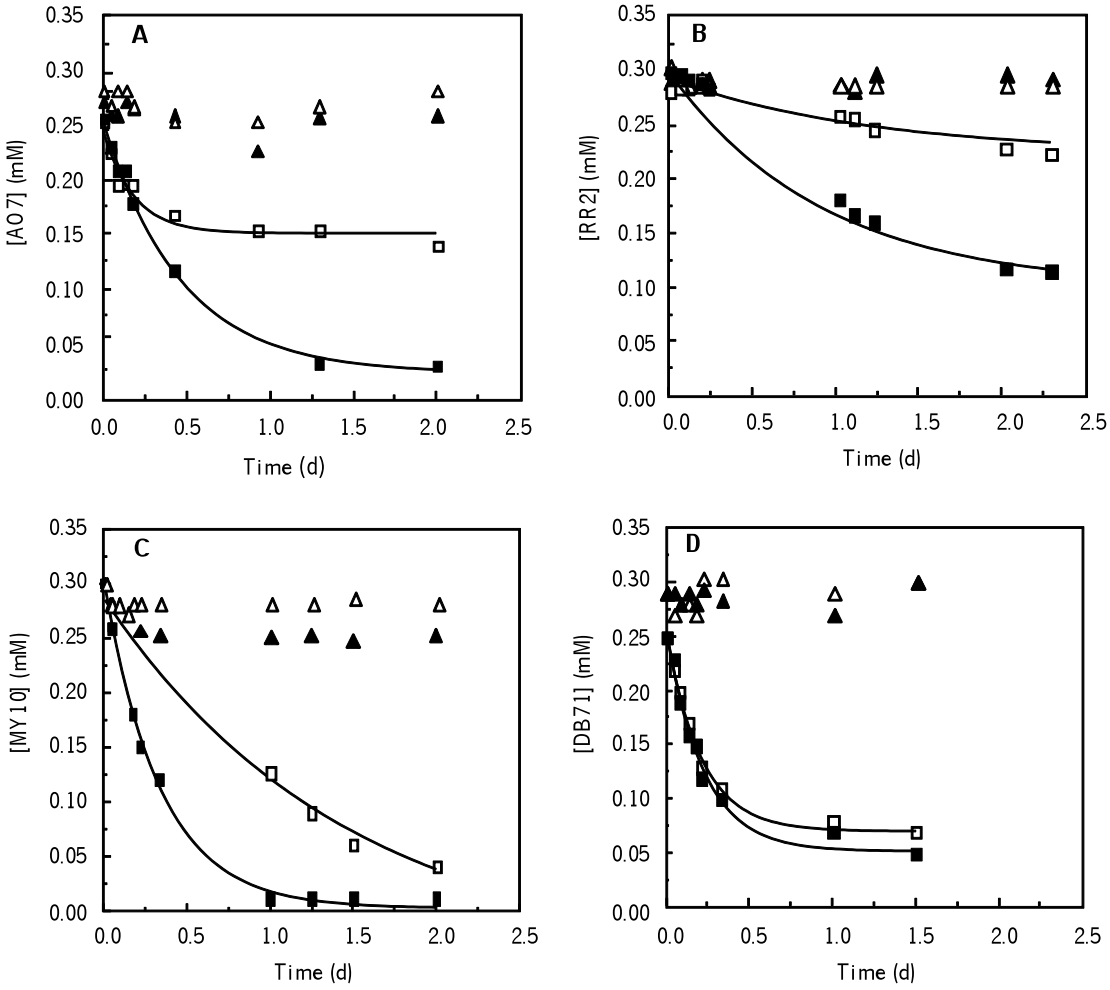

Figure 3.3. Chemical azo dye decolourisation at pH 5, for the assays with dye alone (Δ), dye and AC_c (▲), dye and Na_2S (□) and dye, Na_2S and AC_0 (■). (A) AO7; (B) RR2; (C) MY10 and (D) DB71.

The presence of AC in the reaction solution leads to an improvement of the reduction rates up to 5–fold for AO7, 4–fold for MY10 and 3–fold for DB71. Moreover, the presence of AC turned the decolourisation of all dyes possible in the three pH tested, with better results under acidic conditions, except for MY10, which was faster decolourised at pH 7 (Table 3.4). Contrary to the other dyes, for which worse values were calculated under alkaline conditions, no bigger differences were obtained for DB71 in the presence of AC0 at pH 7 (2.8 ± 0.4 d^{-1}) and 8.7 (3.2 ± 0.3 d^{-1}).

Table 3.4. First order rates (d^{-1}) of dye reduction by sulphide, calculated from the reaction at pH 5, 7 and 8.7, in the absence and presence of different AC samples

Dye	pH	No AC	AC_{HNO3}	AC_{O2}	AC_{0}	AC_{N2}	AC_{H2}
	5.0	0	2.2 ± 0.1	2.4 ± 0.2	2.6 ± 0.6	3.0 ± 0.3	3.4 ± 0.3
AO7	7.0	0.2 ± 0.1	0.7 ± 0.1	0.6 ± 0.1	0.5 ± 0.1	0.8 ± 0.1	1.2 ± 0.1
	8.7	0	0.1 ± 0.1	0.2 ± 0.1	0.3 ± 0.1	1.1 ± 0.2	1.4 ± 0.2
	5.0	0.9 ± 0.1	1.3 ± 0.1	1.2 ± 0.1	1.2 ± 0.1	1.3 ± 0.1	1.2 ± 0.1
RR2	7.0	0	0.9 ± 0.1	1.1 ± 0.1	1.2 ± 0.1	1.2 ± 0.1	1.3 ± 0.1
	8.7	0	0.7 ± 0.1	0.9 ± 0.1	0.2 ± 0.1	0.9 ± 0.1	1.0 ± 0.1
	5.0	1.1 ± 0.1	1.9 ± 0.3	3.8 ± 0.2	2.9 ± 0.2	4.3 ± 0.6	4.2 ± 0.4
MY10	7.0	1.4 ± 0.1	2.8 ± 0.2	6.2 ± 1.1	5.9 ± 0.1	7.4 ± 0.7	12.1 ± 1.3
	8.7	0	2.3 ± 0.3	2.5 ± 0.7	0.9 ± 0.1	2.9 ± 0.1	4.0 ± 0.8
	5.0	4.4 ± 0.6	4.9 ± 0.2	4.6 ± 0.1	4.9 ± 0.2	5.1 ± 0.2	5.6 ± 0.3
DB71	7.0	1.7 ± 0.3	1.6 ± 0.2	1.6 ± 0.1	2.8 ± 0.4	2.9 ± 0.6	3.0 ± 0.1
	8.7	1.4 ± 0.1	3.3 ± 0.1	3.6 ± 0.1	3.2 ± 0.3	3.7 ± 0.2	4.8 ± 0.3

Activated carbon samples have amphoteric character and, as a result, their surfaces might be positively or negatively charged depending on the pH of the solution. Carbon surface becomes positively charged at pH < pH_{pzc} and negatively at pH > pH_{pzc} because the four tested dyes are anionic, adsorption and the transfer of electrons is more favourable when the carbon surface is positively charged. Negatively charged surface sites on the activated carbon might cause the electrostatic repulsion of the anionic dyes. Therefore, the worst performance at pH 8.7 is expected considering the pH_{pzc} of AC_{0} of 8.4. Similarly, considering the pH_{pzc} of all the samples, higher rates at pH 5 than 7 and 8.7 would be expected with samples AC_{HNO3} and AC_{O2}, but not the bigger differences obtained with AC_{N2} and AC_{H2}; however, decolourisation varies also with other parameters such as the molecular structure, pKa and potential redox of the dye, and those have also a dependence on the

solution pH. Under optimum conditions, MY10 was almost completely decolourised; the degrees of decolourisation for the other dyes were lower, 80 % for DB71 and 60 % for AO7 and RR2. Colour removal due to adsorption on activated carbon occurs only for the smaller dyes and at low extent: ~25 % for AO7 and 15 % for MY10. Bigger molecules are more difficult to adsorb due to diffusion limitations. These data suggest that the major role of AC was to enhance the chemical reduction of dye, rather than dye adsorption; the low adsorption degrees are also explained by the little concentration of the catalyst in the solution and the high solubility of the used dyes. AC is the first electron acceptor, being chemically reduced by sulphide and secondly, the electrons from the reduced AC are transferred to the azo dye, the terminal electron acceptor. In previous experiments, chemical reduction of AO7 could also be accelerated by low amounts of AC [Van der Zee *et al.,* 2003]; with 0.5 mmol L^{-1} of sulphide, AO7 removal of 80 % was obtained within 5 days in the presence of AC and only 40 % within 2 weeks in the absence. The amount of AC used was the same as in this study, resulting in similar AO7 adsorption, 22 %. In experiments with higher AC concentration, the same reduction results were obtained, but the degree of adsorption increased. In the same study, it was demonstrated that the reduction of RR2 in a lab-scale bioreactor was largely enhanced by AC [Van der Zee *et al.,* 2003].

3.3.4. Effect of AC surface chemical groups on azo dye reduction

Activated carbon treatments are known to produce significant changes in carbon surface chemistry and these, in turn, can have dramatic effects on the behaviour as adsorbent [Faria *et al.,* 2005, 2008; Pereira *et al.,* 2003] and as catalyst [Moliner *et al.,* 2005; Moteleb *et al.,* 2001; Muniz *et al.*, 2000; Pereira *et al.,* 1999; Zhu *et al.,* 2000]. We investigated the influence of AC surface chemical groups on its behaviour as a RM for dye reduction by sulphide. As pointed before, dye reduction is also dependent on the pH of the solution; thus the reaction was carried out at different pH values, in batch assays. The first order rates are given in Table 3.4. A dependence of dye reduction on the type of AC can be observed, with higher rates for the reaction solutions containing the most basic activated carbons (AC_{N2} and AC_{H2}). These AC are characterized by a high content of electron rich sites on their basal planes (electrons π) and by a low concentration of electron withdrawing groups. The π–electrons are responsible for the better performance as redox mediators, due to the high

attainability by the dye. Mezohegyi *et al.* (2010) have also postulated that delocalised π-electrons seemed to play a role in the catalytic reduction in the absence of surface oxygen.

In general, rates increased with increasing the pH_{pzc}, following the trend $AC_{HNO3} < AC_{O2} < AC_{0} < AC_{N2} < AC_{H2}$ (Figure 3.4). This behaviour was less pronounced for RR2 reduction, with similar rates at all the conditions.

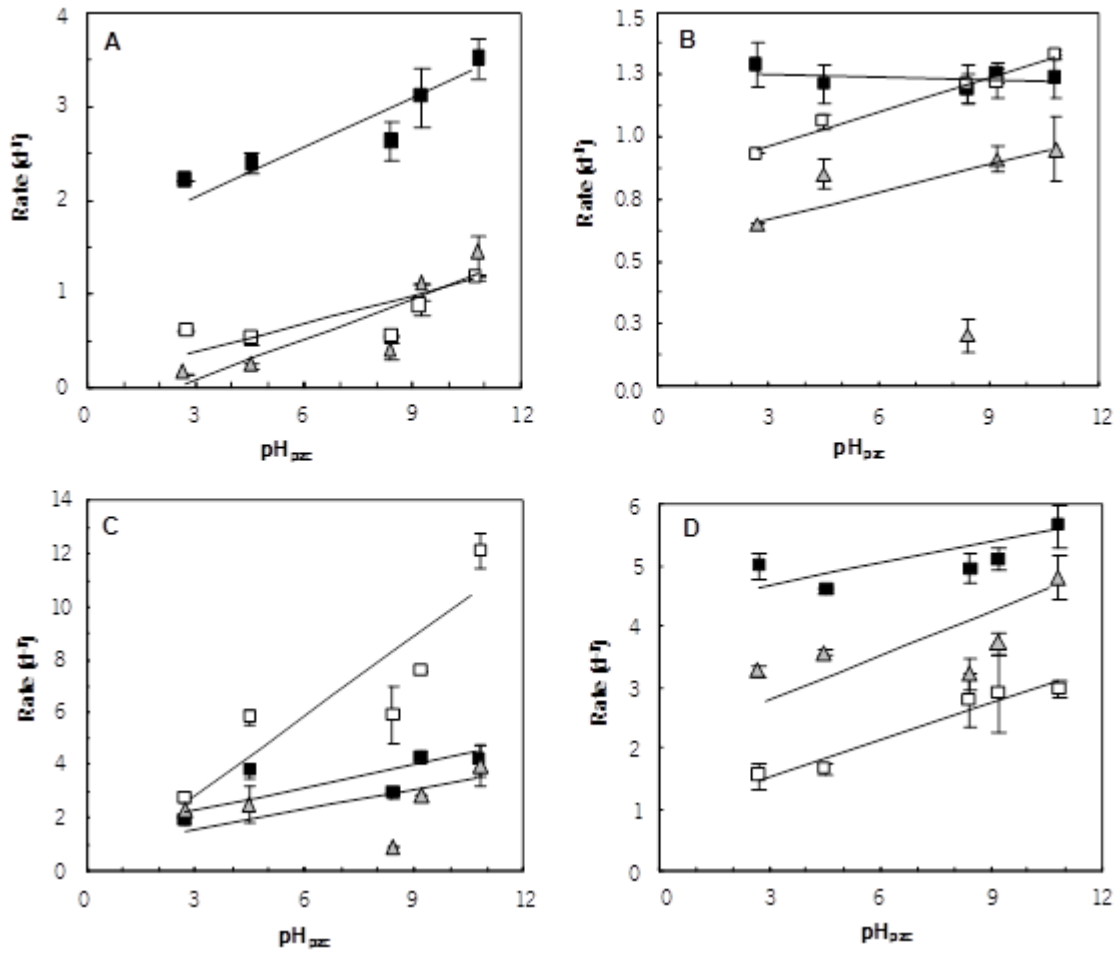

Figure 3.4. First order constant rates of dye reduction, calculated at different pH values, in function of the pH_{pzc} of the modified activated carbons. (■) pH 5; (□) pH 7 and (▲) pH 8.7; (A) AO7; (B) RR2; (C) MY10 and (D) DB71.

Other deviations are the values for RR2 and MY10 reductions with AC_{0} at pH 8.7, lower than the calculated with AC_{HNO3} and AC_{O2}. According to the previous sequence, MY10 reduction at pH 5 and 7

with AC_{O2} is also higher than the expected; those results may be a consequence of the textural properties alteration due to the burn-of when treating this AC sample. The higher content of quinone groups present in AC_{HNO3} and AC_{O2} compared to AC_{N2}, AC_{H2} and the original AC would have promoted a higher decolourisation rates for the azo dyes studied considering that quinone groups have been proposed as the main electron-transferring groups in AC [Van der Zee *et al.,* 2003]. Nevertheless, the larger amount of oxygen-containing groups prevailing on the surface of AC_{HNO3} and AC_{O2}, compared to the other AC samples, also promotes a higher repulsion between the azo dyes and the surface of the these AC, which seems to be the main factor affecting the overall kinetics of the decolourisation process. As with AC_0, the adsorption obtained with modified AC samples was also low (maximal of 30 % for AO7 and 18 % for MY10 with AC_{H2}). The low adsorption obtained is expected due to the small AC concentration used. Therefore, the total dye removal in the chemical assays is mostly due to their reduction. It is worth to mention that high AC concentration limits the process application, due to excessive costs. In their experiments, Mezohegyi *et al.* (2010) have used 5000 times' higher AC concentration than in our work. The effect of pH was also evident on the rates of dye reduction. Except for MY10, which was better degraded at neutral pH, higher rates were obtained at pH 5 with all type of activated carbons. Reactive dye reduction was less influenced by the type of AC and pH, since similar rates were obtained at all the conditions (~1 d^{-1}), apart from the strange low value with AC_0 at pH 8.7 (0.2 d^{-1}). Comparing the four studied dyes, at the optimal conditions, better decolourisation was achieved in order of: MY10 > DB71 > AO7 > RR2. In fact, MY10 was completely reduced within 1 day, at a rate of (12 ± 1.3) d^{-1} with AC_{H2}, being 2–fold, 4–fold and 9–fold higher than the obtained for the dyes DB71, AO7 and RR2, respectively. Its reduction was the largest improved by the presence of AC, with an increase of 9–fold as compared with the assay without AC. Decolourisation rates are also related with the electron density around the azo bond. Electro withdrawing groups such as –OH and $–NH_2$ decrease the electron density around the azo bond and facilitate its reduction. A similar effect in a simple reduction of the azo bond is observed for dyes carrying groups such as $–SO_3Na$, and –COOH [Chen H, 2006]. The NH group, on the other hand, is known to demote it [Shen *et al.,* 2001]. MY10 and DB71 are richer in those first groups and RR2 have the secondary amine on is structure. Triazyl groups, also present in RR2, were found to give low dye reduction rates [Van der Zee *et al.,* 2001; Cervantes *et al.,* 2007], explained by the reducing equivalents required for the reductive dechlorination, which may compete with the azo

chromophore. Redox mediators are not only involved in the transfer of reducing equivalents, but also in minimizing the steric hindrance of the dye molecule [dos Santos *et al.,* 2004].

3.3.5. Biological MY10 reduction

The possibility of using AC as mediator in a biological system was investigated by conducting batch experiments with granular biomass and using MY10 and RR2 as model compounds Different substrates were tested in the biological MY10 reduction, in the absence and presence of AC, and 4–fold higher rates were obtained with VFAs (data not shown). Our findings are in agreement with previous studies that investigated the role of various electron donors on the reduction of dyes, concluding that the rates vary with the type of substrate by stimulating specific microorganisms in a mixed culture [dos Santos *et al.,* 2003; Van der Zee *et al.,* 2001, 2009]. Figure 3.5A shows the results of biological MY10 reduction, with VFAs as substrate, in the absence and presence of unmodified (AC_0) and modified (AC_{H2}) activated carbon. Contrarily to the obtained chemically, MY10 reduction rates in the absence and presence of AC0 were the same, (10.2 ± 1.4) d^{-1} (Figure 3.5 B; Table 3.5). However, with the thermal treated AC (AC_{H2}) the decolourisation rate duplicated (19.4 ± 0.2 d^{-1}). This result shows that, as observed in the chemical assays, AC surface chemistry plays a role in the biological dye decolourisation and that thermal modification of AC improves its capacity as RM. Additionally, different AC amounts were tested and it was found that increasing concentrations from 0.1g L^{-1} to 0.6 g L^{-1} lead to an increase of the dye adsorption (from 10 % to 65 % not shown) but the reduction rates were similar with untreated and treated AC (Figure 3.5 A and B; Table 3.5). This finding is of great importance once AC is costly and therefore the use of low amounts is an advantage for biological processes application. Furthermore, as a RM, AC is cycled from its oxidized and reduced states and thus should be very effecting at low concentrations. With RR2 previously found as a more recalcitrant one, untreated AC could increase 3–fold the rate of decolourisation (Figure 3.5 C). Once more, thermal treated AC reveals to be more effective, increasing 4.5–fold the dye reduction rate.

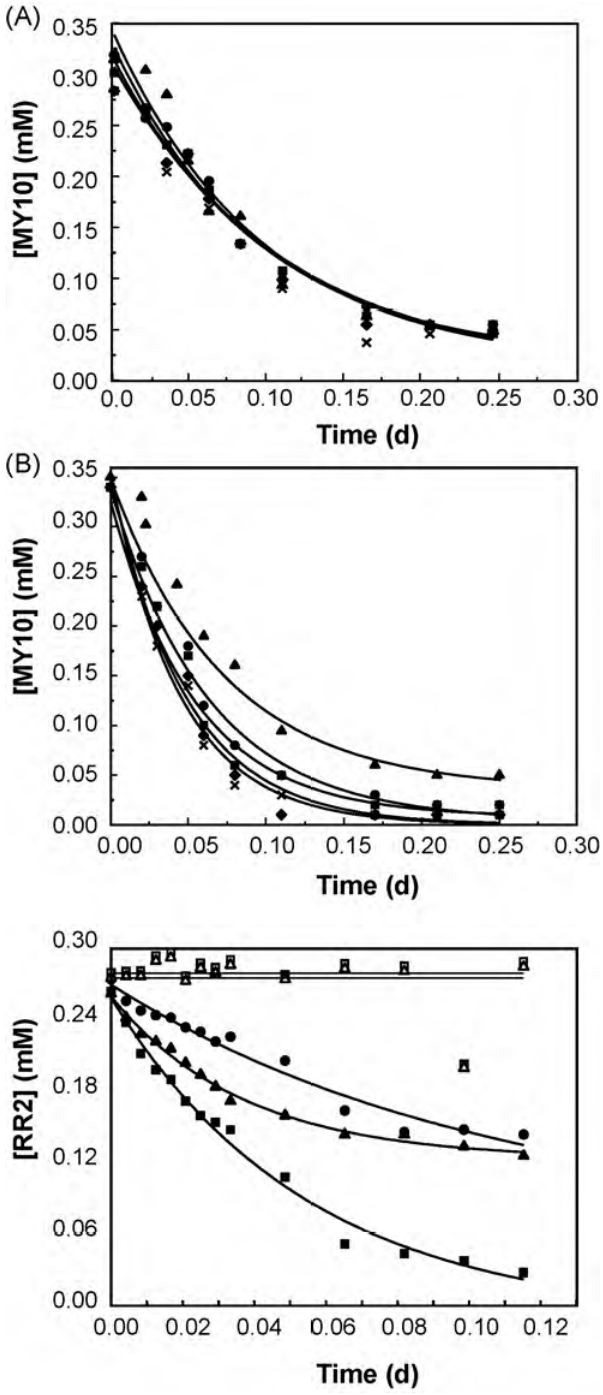

Figure 3.5. Biological MY10 and RR2 dye reduction at pH 7 and with VFAs as substrate. MY10 decolourisation with several AC concentrations using AC_0 (A) and AC_{H2} (B): (▲) without AC; (●) 0.1 $g.L^{-1}$; (■) 0.2 $g.L^{-1}$, (♦) 0.4 $g.L^{-1}$, (x) 0.6 $g.L^{-1}$. RR2 decolourisation with 0.1 g L^{-1} (▲) AC_0 and (■) AC_{H2}, (●) without AC, and with 0.1 $g.L^{-1}$ (Δ) AC_0 and (□) AC_{H2} without biomass.

Table 3.5. First order rates (d^{-1}) and degree of biological MY10 reduction in the presence of increasing unmodified (AC_0) and modified (AC_{H2}) activated carbon concentrations

AC sample	[AC] (g L^{-1})	Rate (d^{-1})	Decolourisation (%)
No AC	0	10.2 ± 1.7	87 ± 1
AC_0	0. 1	10.2 ± 1.4	86 ± 1
	0.2	9.9 ± 0.5	85 ± 1
	0.4	9.8 ± 2.2	83 ± 2
	0.6	11.3 ± 1.2	78 ± 1
AC_{H2}	0. 1	19.4 ± 0.2	87 ± 1
	0.2	18.7 ± 1.3	90 ± 1
	0.4	23.6 ± 3.8	88 ± 0
	0.6	19.6 ± 1.5	89 ± 1

3.4. CONCLUSIONS

The results obtained in the present work demonstrate the catalytic effect, on azo dyes reduction rates, of activated carbon with different surface chemistry, obtained by chemical or thermal treatments. Dye reduction rates increased up to 9–fold using an AC concentration of 0.1 g L^{-1}, as compared with an assay not amended with AC. Amongst the four dyes tested, MY10, AO7, RR2 and DB71, better results were obtained at pH 5, except for MY10, with higher rates determined at pH 7. AC performance as a catalyst was, in this case, improved by surface modification, applying thermal treatments. In order to be an effective redox mediator for anionic dyes, the carbon should have a high pH_{pzc}. This means that at pH lower than pH_{pzc}, the carbon will be positively charged, favouring electrostatic attraction between the carbon and the anionic dyes tested. Reduction rates increased with the activated carbon basicity as following: $AC_{HNO3} < AC_{O2} < AC_0 < AC_{N2} < AC_{H2}$. Dye reduction rates

in the presence of AC also varied among the different dyes. Higher rates were obtained in order of: MY10 > DB71 > AO7 > RR2. Dye reduction by sulphide in the absence of AC was very limited, since only DB71 was reduced at the three pH tested and MY10 at pH 5 and 7. AO7 and RR2 were more resistant to chemical reduction. We have also demonstrated that surface modified AC_{H2} could duplicate MY10 decolourisation rate in a biological assay, which was independent of the AC concentration in the tested range of 0.1–0.6 g L^{-1}. As AC can be retained in a reactor for prolonged time, it is an attractive alternative to soluble redox mediators in a biological reactor system. The low amount of AC used in this work and the positive results demonstrated for chemical and biological catalysis constitutes a significant breakthrough in the field of redox mediated processes which will certainly open new perspectives for wastewater treatment processes of several xenobiotics.

CHAPTER 4.

CARBON BASED MATERIALS AS NOVEL REDOX MEDIATORS FOR DYED WASTEWATER BIODEGRADATION

Residual dyes present in textile wastewaters constitutes a severe environmental problem. To manage this problem, biological treatment systems consist a promising technology. The application of this technology to residual dyes treatment involves the slow process of electron transfer in anaerobic sludge reductive transformations. To accelerate the process, redox mediators can be used such as activated carbon (AC). Microporous thermal treated AC (AC_{H2}) and mesoporous carbons (the CXA and CXB xerogels and carbon nanotubes, CNT) were tested on azo dye and textile wastewater biodegradation. With these carbon materials, around 85 % of MY10 and 70 % of RR120 colour removal was obtained. For MY10 and RR120, the reduction rates increased in the order: control < AC_{H2} < CXA < CXB < CNT. No biodegradation of AO10 occurred in the absence of carbon materials. On the other hand, 98 % of AO10 color removal was achieved with CXB and CNT. CNT had also a mediator effect in the biological treatment of real textile wastewaters.

CHAPTER 4.
CARBON BASED MATERIALS AS NOVEL REDOX MEDIATORS FOR DYED WASTEWATER BIODEGRADATION

4.1. INTRODUCTION

Textile industry faces an environmental problem related to the incomplete dye fixation onto textile fibres, during the aqueous dyeing process, and needs to implement innovative and sustainable effluent treatment processes to remove colour. Biological treatments are the most viable treatment systems and the efficiency of dye removal could be further enhanced by the use of RM (e.g. insoluble AC). In Chapter 3, it is demonstrated the role of surface chemistry of activated carbon in the performance as catalysis of chemical and biological reduction of dyes. However, activated carbons are generally microporous, with low macropore or mesopore volumes, which can induce diffusion limitations during the catalytic and adsorptive processes. The use of CX and CNT as catalysts for organic pollutants degradation has been demonstrated before [Gonçalves *et al.,* 2010; Orge *et al.,* 2012]. These new mesoporous materials may present technological advantages as new shape catalyst mainly for large molecules (*e.g.* azo dyes) degradation. CX has excellent properties, such as high specific surface area, porosity and conductivity and controllable average pore size, which can be customized for the final applications.

In the present study, the mesoporous materials, CX and CNT, were studied for the first time as RM on anaerobic dye reduction and compared with the microporous thermal modified activated carbon, AC_{H2}. Three azo dyes from different classes (mordant, reactive and acid) were tested: Mordant Yellow 10 (MY10), Reactive Red 120 (RR120) and Acid Orange 10 (AO10). Biodegradation of real textile wastewaters was also investigated. The chemical structures of dyes and aromatic amines used are illustrated in Figure 4.1.

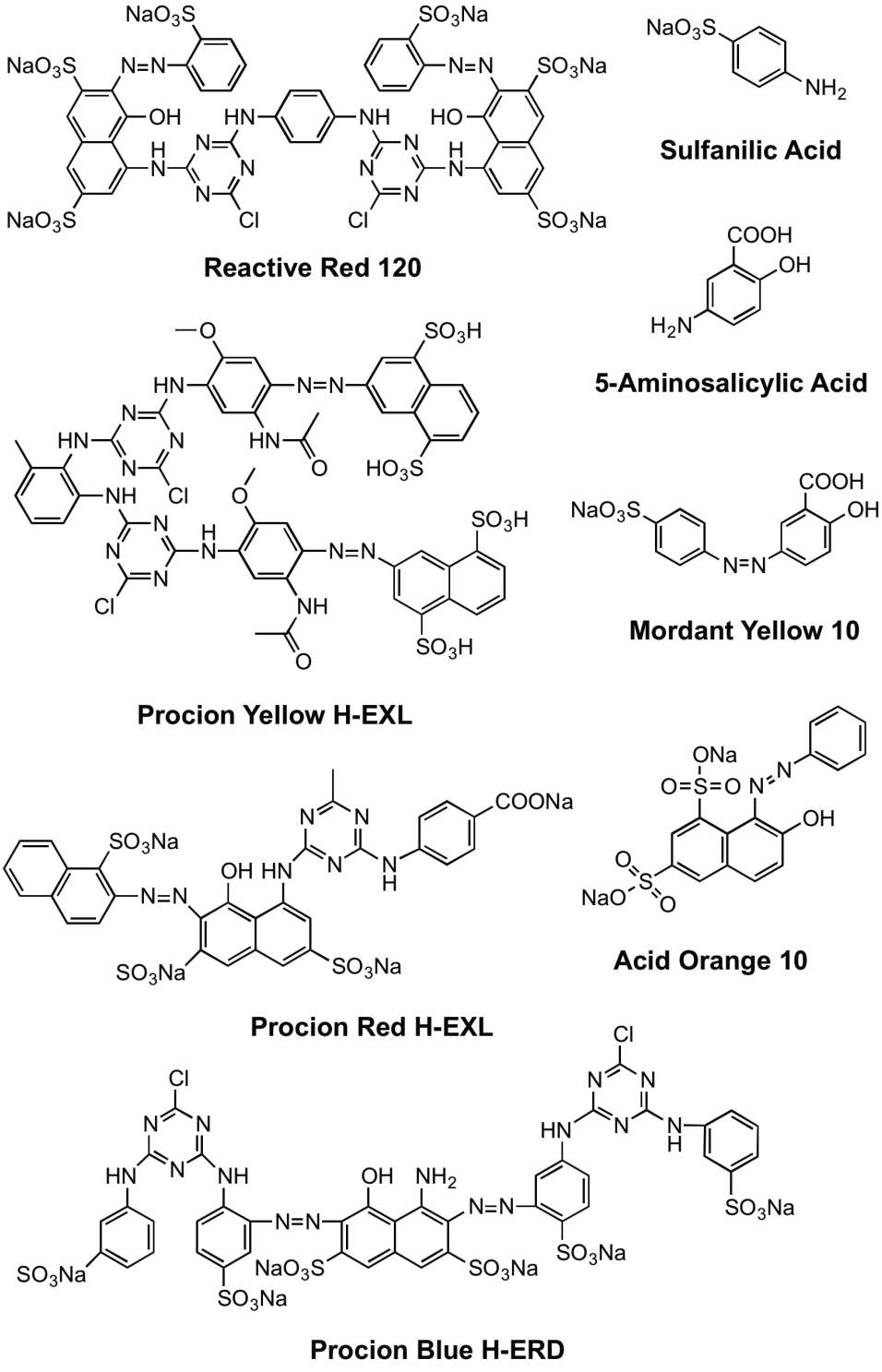

Figure 4.1. Molecular structure of azo days and aromatic amines

4.2. MATERIALS AND METHODS

4.2.1. Chemicals

MY10 (dye content 85 %), RR120 (dye content 50 %) and AO10 (dye content 90 %) were purchased from Sigma and used without additional purification. Stock solutions of 15 mmol L^{-1} were prepared in deionised water. Aromatic amines were also purchased from Sigma at the highest analytic grade purity commercially available. The chemicals used to prepare the macronutrients solution were purchase from Sigma or Fluka at highest analytic grade purity commercially available. The solvents acetonitrile and acetic acid for HPLC analysis were purchased from Panreac.

4.2.2. Preparation and characterization of carbon materials

Different sets of catalysts were prepared: AC_{H2}, CX and CNT. To prepare the sample AC_{H2}, a commercial Norit ROX0.8 activated carbon (AC), which is an extruded acid washed activated carbon, with cylindrical pellets of 0.8 mm diameter and 5 mm length, was firstly chemical oxidised with 6 mol L^{-1} of HNO_3 at boiling temperature for 3 h, followed by thermal treatment under H_2 flow at 700 °C for 1 h [Pereira *et al.,* 2010]. The synthesis of the CX consisted in the polycondensation of resorcinol (99 %, Aldrich) with formaldehyde (37 %, Aldrich) at an initially controlled pH [Orge *et al.,* 2012]. Samples were synthesised by the sol–gel process at pH 6.25 (CXA) and 5.45 (CXB) in order to obtain materials with different textural properties. After setting the pH of the sol–gel process with NaOH solutions, polymerisation was carried out at 85 °C during 3 days. Then, the gel was ground and dried in an oven during 4 days (first day at 60 °C, second day at 80 °C, third day at 100 °C and fourth day at 120 °C). After that, the material was carbonised under nitrogen flow at 800 °C, using the following temperature program: from room temperature to 150 °C (hold 2 h), than to 400 °C (hold 1 h), further to 600 °C (hold 1 h) and to 800 °C (hold 6 h), in all steps at increments of 2 °C min^{-1}. Materials were finally cooled down to room temperature. The textural characterisation of the materials was based on

the corresponding N_2 equilibrium adsorption/desorption isotherms, determined at –196 °C with a Quantachrome Instruments NOVA 4200e apparatus [Orge *et al.,* 2012]. BET surface areas (S_{BET}), mesoporous surface areas ($S_{\neq \mu pores}$), micropore volumes ($V_{\mu pores}$) and average mesopore diameters were obtained by the Barret, Joyner and Halenda (BJH) method. The morphology and the semiquantitative elemental analysis of the catalysts were attained by scanning electron microscopy (SEM) and energy dispersive X-ray spectroscopy (EDS), respectively, in a JEOL JSM 35C/Noran Voyager system. XRD spectra were recorded on a Philips X'Pert MPD diffractometer (Cu Kα= 0.15406 nm). A commercial MWCNT sample (Nanocyl 3100) was also tested. According to the supplier, it has an average diameter of 9.5 nm, an average length of 1.5 m and carbon purity higher than 95 %. Tessonnier *et al.* (2009) characterised this material as having an average inner and outer diameters of 4 and 10 nm, respectively. In the same work, it was observed that Nanocyl 3100 contains growth catalyst impurities, mainly Fe and Co (0.19 % and 0.07 %, respectively), sulphur (0.14 %), which is probably due to the purification process, and traces of Al (0.03 %).

4.2.3. Dye biodegradation

Biological dye decolourisation assays were conducted in 70 mL serum bottles, sealed with a butyl rubber stopper, containing 25 mL of medium. The primary electron donating substrate of the medium was composed of 2 g L^{-1} chemical oxygen demand (COD) of a NaOH-neutralised VFA mixture, containing acetate, propionate and butyrate in a COD based ratio of 1:10:10. Basal nutrients were also added: NH_4Cl (2.8 g L^{-1}), $CaCl_2$ (0.06 g L^{-1}), KH_2PO_4 (2.5 g L^{-1}), $MgSO_4.7H_2O$ (1 g L^{-1}). Medium was buffered at a pH of 7.3 ± 0.2 with $NaHCO_3$ (2.5 g L^{-1}). Non-adapted anaerobic granular sludge was in the medium at a concentration of (2.5 ± 0.5) g L^{-1} volatile suspended solids (VSS). The kinetic of azo dye decolourisation was conducted at dye concentrations in the range 0.15 and 4.0 mmol L^{-1}. The effect of the different carbon materials (AC_{H2}, CXA, CXB, CNT) on dye decolourisation was tested with dye concentration of 1 mmol L^{-1}. The amount of carbon materials used, 0.1 g L^{-1}, is in accordance with previous work, in which AC concentrations from 0.1 g L^{-1} to 0.6 g L^{-1} were tested and lead to an increase of the dye adsorption (from less than 10 % to 65 %), but the decolourisation rates were similar. These

results are important once activated carbon is costly and therefore the use of low amounts is an advantage for the application of the biological process. Furthermore, as a redox mediator, AC is cycled from its oxidised and reduced states and thus should be very effective at low concentrations. Sludge was incubated overnight at 37 °C, in a rotary shaker, with rotation at 120 min^{-1}. After the pre-incubation period, dye and VFA (2 gCOD L^{-1}) were added with a syringe from the stock solution to the desired concentration. Controls without carbon material and without biomass were also conducted. All experiments were prepared in triplicate. In order to evaluate the reutilisation of carbon materials and the efficiency of the process, three cycles, of 24 h, of dye addition, were carried out without carbon material regeneration. VFAs were also added at the beginning of each cycle.

4.2.4. Real and model wastewater biodegradation

Two real effluents were collect from a textile company "Valintece Tecelagem de Malhas, SA" (Fafe, Portugal) after the dying process. The effluent A, contained three reactive azo dyes, namely Procion Blue HEXL (PB), Procion Yellow HEXL (PY) and Procion Red HEXL (PR) and the effluent B, contained three other reactive dyes, Remazol Yellow RR (RY), Remazol Brilliant Yellow 3GL (RBY) and Remazol Blue RR (RB). The structures of the dyes, except for RY and RB, are illustrated in Figure 4.1. The dyes used in the textile company are all from DyeStar. The industrial water contained also 20 g L^{-1} of sodium chloride and 6 g L^{-1} of sodium carbonate. The pH was 7.86, for effluent A and 10.11, for effluent B. Except for pH, which was corrected with NaOH to 7, real wastewaters were treated as supplied by the textile company. The initial absorbance at the λ_{max} (510 nm, for effluent A and 420 nm, for B) was 0.5 and 0.15, respectively. A model wastewater was prepared by mixing the Procion dyes (obtained from the textile company) at equally concentration, 0.1 g L^{-1}, with final absorbance at 510 nm of 1. The pH of the solution was 7. The effect of salts was also evaluated by preparing a model wastewater containing also 20 g L^{-1} of sodium chloride and 6 g L^{-1} of sodium carbonate. Batch assays were prepared as described in Section 4.2.3, but containing real or model wastewater instead of the dye solutions. The effect of carbon materials was also investigated at concentration of 0.1 g L^{-1}. Controls without CM were also performed.

4.2.5. Activity test

Specific methanogenic activity (SMA) tests were performed in serum bottles of 25 mL, containing 12.5 mL of buffer solution: 3.05 g L^{-1} sodium bicarbonate and 1 g L^{-1} of Resazurin. Vials were supplemented with 0.4 g anaerobic granular sludge, which corresponds to (2.1 ± 0.2) g of volatile suspended solids (VSS) per litre, and the headspace was flushed with a mixture of N_2:CO_2 (80:20, v:v). The final pH was 7.2 ± 0.2. Following the addition of 0.125 mol L^{-1} Na_2S, under strict anaerobic conditions, the flasks were incubated overnight at 37 °C at 120 min^{-1} rotation. After that period, the substrate (3 mmol L^{-1} of ethanol) and the dye solution to be tested were added and the flasks were maintained at 37 °C and a rotation at 120 min^{-1} over the entire assay. The pressure was measured every 60 min by using a hand-held pressure transducer, able of measuring a pressure variation of ± 2 atm (0–202.6 kPa) with a minimum detectable variation of 0.005 bar, corresponding to 0.05 mL of biogas in a 10 mL headspace. The assay was finished when the pressure remained stable. Methane content of the biogas was measured by gas chromatography using a Chrompack Haysep Q (80–100 mesh) column (Chrompack, Les Ulis, France), with N_2 as carrier gas at 30 cm^3 min^{-1} and a flame ionisation detector. Temperatures of the injection port, column, and flame-ionisation detector were 120 °C, 40 °C and 130 °C, respectively. The values of methane production were corrected for the standard temperature and pressure conditions (STP). In order to determine the activities, the values of pressure (calibrated as an analogical signal in mV) were plotted as a function of time and the initial slopes of the methane were calculated. SMA values were determined dividing the initial slope by the VSS content of each vial at the end of the experiment and were expressed in mL CH4 $gVSS^{-1}$ d^{-1}. Background methane production due to the residual substrate was subtracted. Test included series containing increasing dye concentration, in the range of 0.0625–4 mmol L^{-1}, to evaluate the effect of the dyes on the biomass activity. The effect of the carbon materials, at concentration of 0.1 g L^{-1}, on the methanogenic activity was also tested, in the presence and absence of 1 mmol L^{-1} dye. Two controls were made in the same conditions, one containing only ethanol (no dye) and the other without any substrate or dye (blank assay). All batch experiments were performed in triplicate. The effect of dye was evaluated by comparing with the control containing only ethanol.

4.2.6. Analytical techniques

Colour decrease was monitored spectrophotometrically in a 96-well plate reader (ELISA BIO-TEK, Izasa). At select intervals, samples were withdrawn (300 μL), centrifuged with rotation at 5000 min^{-1} for10 min to remove the biomass and/or CM, and diluted to obtain less than one absorbance unit. Dilutions were made with ascorbic acid solution in order to avoid products autoxidation. The visible spectra (300–900 nm) were recorded and the dye concentration was calculated at λ_{max}. Molar extinction coefficients were calculated for each dye at λ_{max}: ε_{350nm}= 15.52 L $mmol^{-1}$ cm^{-1} for MY10; ε_{510nm}= 28.59 L $mmol^{-1}$ cm^{-1} for RR120; ε_{480nm}= 24.59 L $mmol^{-1}$ cm^{-1} for AO10 and ε_{510nm}= 22.65 L $mmol^{-1}$ cm^{-1} for the model wastewater.

The first-order reduction rate constants were calculated applying the equation 1 and colour removal (CR) was calculated according to equation 2 in Chapter 3 (section 3.2.5).

HPLC analyses were performed in a HPLC (JASCOAS-2057 Plus) equipped with a diode array detector. A C18 reverse phase Nucleodur MNC18 column (250 mm x 9 mm x 4.0 mm, 5 μmol L^{-1} particle size and pore of 100 °A from Machenerey-Nagel, Switzerland) was used. Mobile phase was composed of two solvents: A (1 % of acetic acid solution, pH 3.5) and B (acetonitrile, ACN). Compounds were eluted at a flow rate of 0.5 mL min^{-1} and at room temperature, with isocratic condition of 0 % of ACN over 10 min, followed of an increased from 0–80 % ACN, during 20 min, and remaining in this conditions more 6 min. Compounds elution was monitored at λ_{max} of dyes and at λ_{max} of the standards (250 nm for SA and 300 nm for 5-ASA).

4.3. RESULTS AND DISCUSSION

4.3.1. Characterisation of carbon materials

The selected properties of the prepared materials are presented in Tables 4.1 and 4.2.

Table 4.1. Properties of the prepared carbon material samples

Sample	S_{BET} (m^2 g^{-1})	S_{meso} (m^2 g^{-1})	V_{micro} (cm^3 g^{-1})	dBJH [a] (nm)
AC_{H2}	987	129	0.377	-
CXA	540	168	0.192	3.2
CXB	566	233	0.165	24.4
CNT	331	331	0	-

[a] Average mesopore diameter obtained by the Barret,Joyner and Halenda (BJH) method applied to the desorption isotherm.

Table 4.2. Textural and chemical characterization of prepared carbon materials

Sample	CO_2 [a] (μmol g^{-1})	CO [a] (μmol g^{-1})	CO/CO_2 [b]
AC_{H2}	59	590	10
CNT	25	478	19

[a] Amounts of CO and CO_2 released, obtained by integration of the areas under TPD spectra.
[b] Mass percentage of oxygen on the surface, obtained from TPD data assuming that all the surface oxygen is released as CO and/or CO_2.

The characterisation of the thermal modified AC sample, AC_{H2}, was previously described in Chapter 3 (section 3.2.2.). Thermal treatments at high temperature produce materials with low amount of oxygen containing surface groups and high basicity, resulting mainly from some ketonic groups remaining on the surface, from the low amount of acidic groups, and from the delocalised π-electrons of the carbon basal planes. These electrons are responsible for the high basicity of the AC_{H2} sample. Compared with the other CM prepared, this sample is characterised by the presence of micropores and by the higher surface area. Characterisation of the mesoporous materials tested, carbon xerogels and carbon nanotubes, was previous reported [Gonçalves *et al.,* 2010; Orge *et al.,* 2012]. The main differences among the carbon xerogels (CX) prepared at different initial pHs are in the average mesopore diameter. The carbon xerogel

prepared at pH 5.45, CXB, has the largest mesopore size (d_{BJH}= 24.4 and 3.2 nm for CXB and CXA, respectively). Contrary to the carbon xerogel samples that have cylindrical pores, the mesoporosity of the CNT sample results from the free space in the CNT bundles, with a pore size distribution between 10 and 24 nm [Orge *et al.,* 2010]. This type of pore structure facilitates the access of large molecules to the carbon surface. CNT sample presents lower oxygen-containing surface groups, especially CO releasing groups.

4.3.2. Kinetics of dye biodegradation

Different classes of dyes, acid (AO10), mordant (MY10) and reactive (RR120), were tested for anaerobic colour removal. As monitored by spectrophotometry, a decrease in the intensity of the maximum absorption band was observed for MY10 and RR120 (data not shown). Maximum colour removals were obtained after 3 h for MY10 and 9 h for RR120, being (83 ± 1) % and (67 ± 3) %, respectively. No further colour decrease was detected in 24 h of monitoring. The acid dye, AO10, was not biodegraded. The kinetics of MY10 and RR120 biodegradation were studied at different initial dye concentrations (range from 0.15 to 4 mmol L^{-1}). Similar behaviour was observed for both dyes, with first-order rates increasing with dye concentration up to 1 mmol L^{-1} for MY10, and 1.5 mmol L^{-1} for RR120, and inhibition at higher concentrations (Figure 4.2).

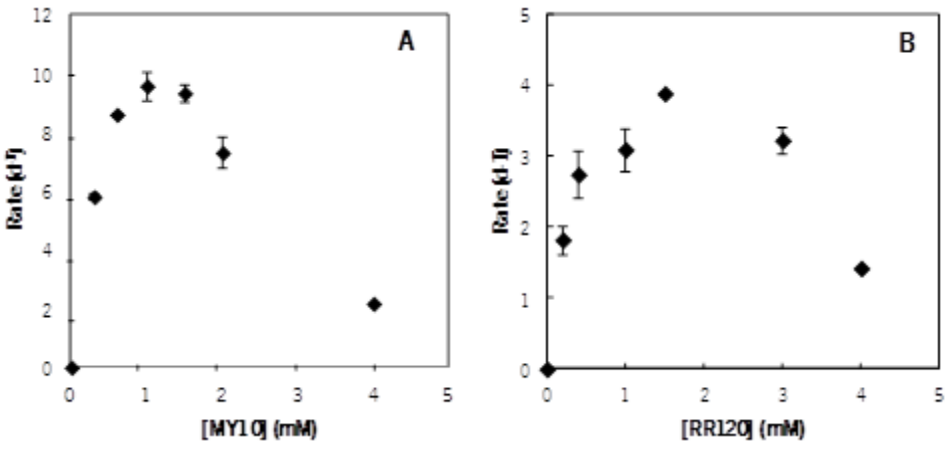

Figure 4.2. Biodegradation kinetics of MY10 (A) and RR120 (B) at increasing initial dye concentrations.

In an anaerobic process, dyes are used as final electron acceptor compounds and the cosubstrate as electron donors, at higher dye concentrations bacteria can use also dyes as co-substrate and a competition between both substrates may result in kinetics inhibition [Isik *et al.,* 2004, 2006].

Other possibility may be the toxicity exerted by the dyes when used at high levels and also of the formed products [Isik *et al.,* 2006]. This possibility is corroborated by the results of activity tests for MY10. An increase of inhibition was also detected with the increase of dye concentration (data not shown). The activity decreased from 1.4 g COD-CH4 $gVSS^{-1}$ d^{-1}, with 1 mmol L^{-1} (366 mg L^{-1}) of dye, to 0.94 gCOD-CH4 $gVSS^{-1}$ d^{-1}, with 4 mmol L^{-1} (1465 mg L^{-1}) of dye, corresponding to a decrease of 39 % on biomass activity. In the case of RR120, the activity was not affected by the dye in the range of the tested concentrations. This may be due to the fact that this dye has a bigger structure, being less accessible to the cells. On the other hand, in the presence of AO10, around 70 % of methanogenic activity was obtained with all the dye concentrations tested in the range 0.0625 mmol L^{-1} (28.3 mg L^{-1}) to 4 mmol L^{-1} (1809.5 mg L^{-1}). Anaerobic batch toxicity assays usually do not reveal severe inhibition of methanogenesis at azo dye concentrations below 100 mg L^{-1}, however, at high dye concentrations, decrease of the activity has been reported in some of the reactor studies [Van der Zee *et al.,* 2005]. It is worth to mention that in dye house effluents, dyes are usually present at concentrations of 10–250 mg L^{-1}, depending on the dyes and processes used [O'Neill *et al.,* 1999]. Similarly to the extent of decolourisation, also the rates of reaction have varied among the dyes. The maximal rate obtained was almost 2.5–fold higher for the monoazo MY10, (9.50 ± 0.49) d^{-1}, than for the diazo RR120, (3.88 ± 0.02) d^{-1}, which has a more complex structure. Dyes with simple structures and low molecular weights are reported to exhibit higher rates of colour removal [Sani *et al.,* 1999]. Colour removal can also be related, in some cases, to the number of azo bonds in the dye molecule [Hu *et al.,* 2001]. Reduction rates are also influenced by changes in electron density in the region of the azo group. The substitution of electron withdrawing groups ($–SO_3H$, $–SO_2NH_2$) in the *p*– position of the phenyl ring, relative to the azo bond, has been reported to cause an increase in the reduction rate [Pereira *et al.,* 2010; Pearce *et al.,* 2006], which is the case of MY10. Electron withdrawing groups such as –OH and $–NH_2$ decrease the electron density around the azo bond and facilitate its reduction [Nigam *et al.,* 1996]. Hydrogen bonding, in addition to the electron density in the region of the azo bond, has a significant effect

on the rate of reduction [Beydilli *et al.,* 2000]. The position and the nature of the substituents on the dye molecule influence the azo-hydrazone tautomerism of hydroxyazo compounds [Hsueh *et al.,* 2009; Ozen *et al.,* 2007]. The hydroxy proton of phenylazo-naphthol derivatives is labile and can bond with a nitrogen atom of the azo group, causing a rapidly formed tautomeric equilibrium between the azo and hydrozone forms (i.e. –N=N–, N–NH; Figure 4.3 is an example for AO10).

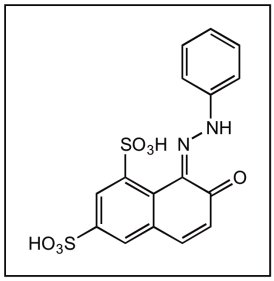

Figure 4.3. Molecular structure of Acid Orange 10 in the hydrazone form.

Some authors have observed a decreased of reduction rate with substrates that were stabilised in the hydrazone form [Ramalho *et al.,* 2004; Zimmerman *et al.,* 1982]. This may contribute for the non-biodegradability of AO10. It is worth to note that factors as for example, substituents groups, potential redox or pKa of substrates, which are also related to the chemical structure, are also known to play an important role in determining the reaction rates [Chen H, 2006].

4.3.3. Products and mechanism of azo dye reduction

Under anaerobic conditions, colour removal is associated with the cleavage of the azo bound, with formation of the correspondent aromatic amines [Brás *et al.,* 2005; Mendes *et al.,* 2011; Pereira *et al.,* 2009; Ramalho *et al.,* 2002]. In an attempt to prove that the colour removal is due to the reduction of the dye molecules to the correspondent aromatic amines, the final products of the biodecolourisation of MY10 were identified by HPLC. The absorbance decreased over time and 2 new peaks at Rt 6.9 and 8.3 min were formed (Figure 4.4 A and B).

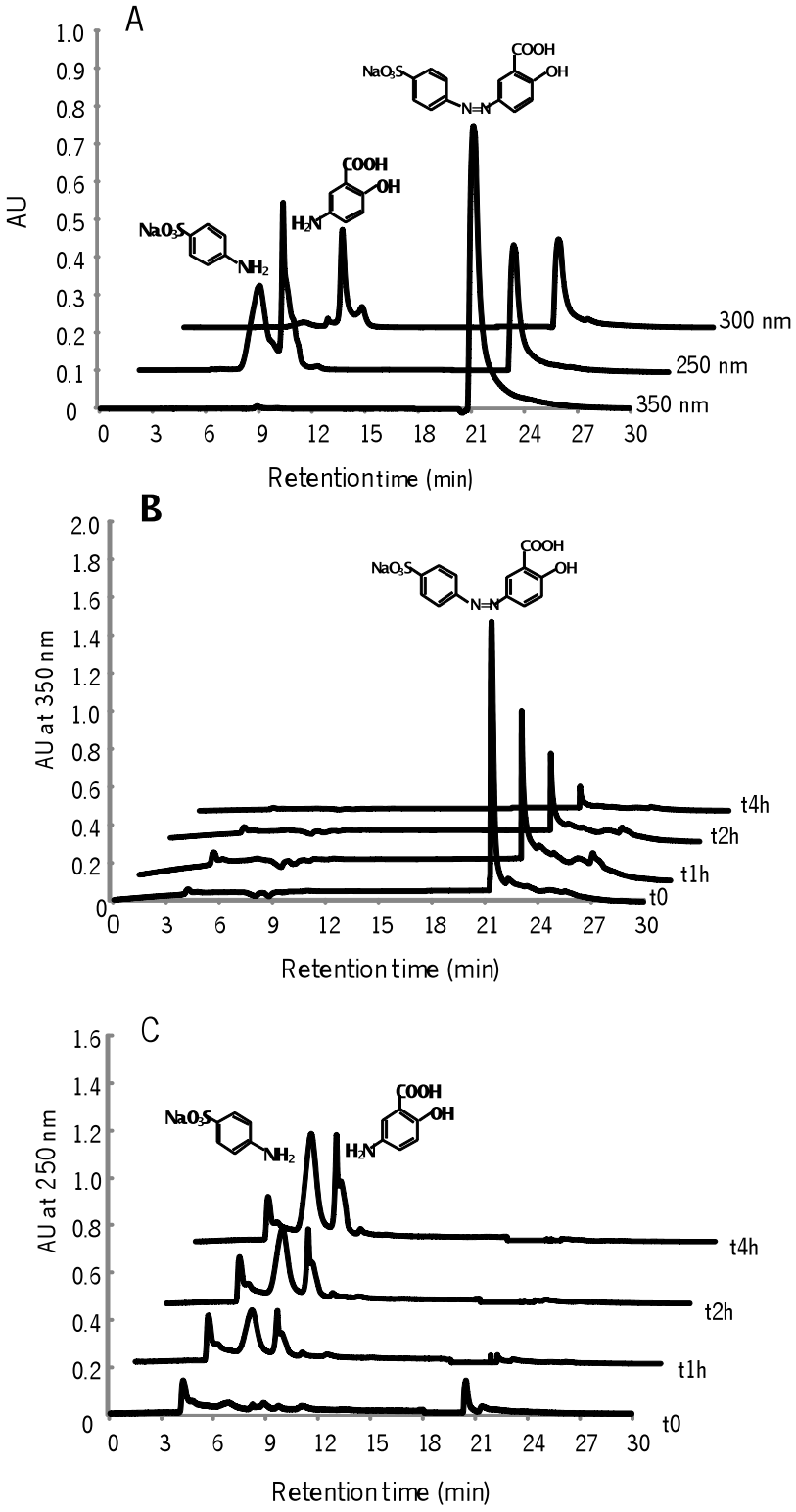

Figure 4.4. HPLC chromatograms of the standards MY10, SA and 5-ASA (A) and of the MY10 biodegradation at (B) 350 nm and (C) 250 nm.

The products were identified by comparison with authentic standards as sulfanilic acid (SA) and 5– aminosalicylic acid (5–ASA), respectively (Figure 4.4). According to these results, the mechanism of biodegradation by reduction of azo dye was confirmed (Figure 4.5). The increase of absorbance of the peaks corresponding to the aromatic amines indicates that they are not degraded, but accumulate under anaerobic conditions. These results are in accordance to Brás *et al.* (2005), who have also identified by HPLC the aromatic amine sulfanilic acid from the biodegradation of Acid Orange 7 meaning that SA was not mineralised under anaerobic conditions, in the test conditions. Studies on the biodegradation of SA and 5–ASA by Tan *et al.* (1999) showed that 5–ASA and SA could only be degraded if an inoculum from aerobic enrichment cultures was added to the batch experiments.

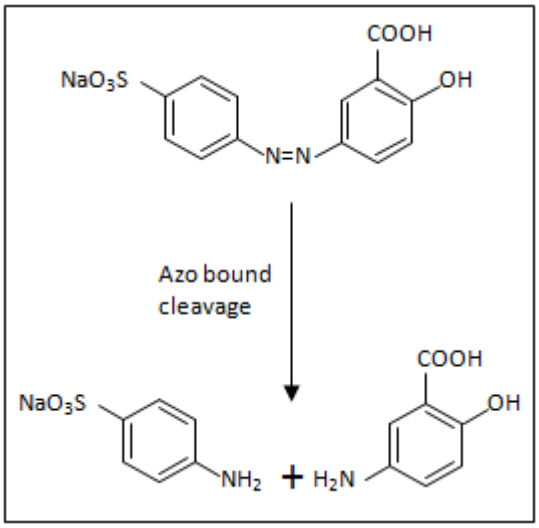

Figure 4.5. Mechanism of MY10 biodegradation with formation of the correspondent aromatic amines.

4.3.4. Carbon materials as catalysts on dye biodegradation

The extent and rates of decolourisation at the different conditions are set in Table 4.3. Except for the most recalcitrant dye, AO10, the extent of decolourisation was not affect in the presence of CM.

In the case of AO10, not biologically decolourised, the presence of CNT and CXB allowed its almost complete decolourisation, 98 %, proving the effect of redox mediation (Figure 4.6).

Table 4.3. Effect of different carbon materials (0.1 g L^{-1}) on the extent (%) and rates (d^{-1}) of dye decolourisation (1 mmol L^{-1})[a]

	MY10		RR120		AO10	
Sample	**%**	**d^{-1}**	**%**	**d^{-1}**	**%**	**d^{-1}**
No CM	83 ± 1	9.50 ± 0.49	67 ± 3	3.09 ± 0.30	0	0
AC_{H2}	85 ± 1	11.02 ± 0.68	68 ± 3	3.15 ± 0.04	46 ± 5	2.07 ± 0.24
CXA	85 ± 1	11.11 ± 0.44	73 ± 1	3.78 ± 0.19	67 ± 1	2.72 ± 0.13
CXB	85 ± 1	14.99 ± 0.18	75 ± 2	4.54 ± 0.67	98 ± 2	4.48 ± 0.74
CNT	86 ± 1	20.08 ± 1.14	75 ± 2	4.01 ± 0.28	98 ± 2	3.16 ± 0.65

[a] Controls without biomass reveal that no adsorption to carbon materials occurs (data not shown).

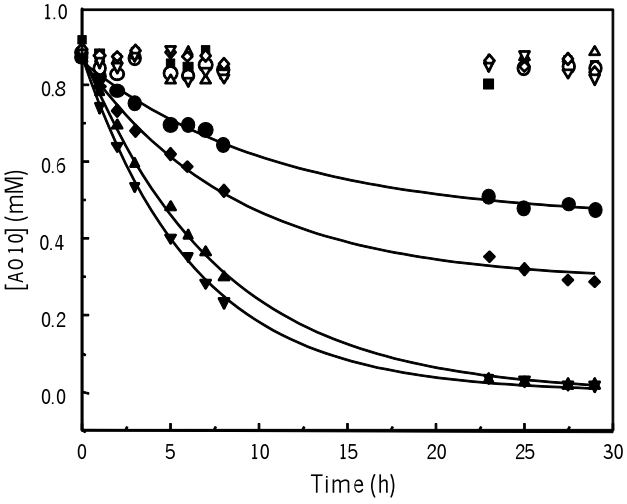

Figure 4.6. First order rate curves of AO10 biodegradation: (■) no carbon material; (●) AC_{H2}; (♦) CXA; (▲) CXB; (▼) CNT. Black symbols correspond to the biotic and white symbols to the abiotic assays.

Also, the other materials tested (AC_{H2} and CXA) lead to AO10 decolourisation, though at lower extent. Additionally, for all the three dyes, rates of biodegradation were higher in the presence of the carbon materials, with better results for CNT and CXB.

As compared with the reaction without carbon materials, rates increased 2–fold for MY10 and 1.5–fold for RR120. The better performance of the mesoporous carbon materials is explained by the easier access of the dye molecules to the surface of the catalyst. In the same way, the higher rates obtained with CXB, synthesised at lower pH, in comparison with CXA, is explained by the larger mesopores obtained in the preparation at lower pH (Table 4.4), which may allow an easier access of the dye, especially in the case of RR120. Orge *et al.* (2012), have tested different carbon xerogels as catalysts in the ozonation of Reactive Blue 5 and also observed that the catalytic activity of the carbon xerogels increases when the pH used in the preparation process decreases. In a previous work with microporous activated carbons, higher reduction rates were obtained with the thermal treated sample (sample AC_{H2}) and was related with the a high content of electron rich sites on their basal planes (electrons π), known to be active sites, and by a low concentration of electron withdrawing groups [Pereira *et al.,* 2010]. CNT are also characterised by lower oxygen-containing surface groups (Table 4.2) and high amount of delocalized π–electrons on the surface.

Other carbonaceous materials have been reported as redox mediators. As example, graphene was found as a good redox mediator for the reductive transformation of nitroaromatic compounds, increasing two orders of magnitude the abiotic (Na_2S) reduction of nitrobenzene [Fu H, 2013]. Similarly to other carbon materials such as the nanotubes, this electron transfer enhancement was attributed to the existence of delocalised π-electrons and the zigzag edges carbons. However, this high increase of the rate as cannot be directly compared with our results once biotic reactions are more complex. The effect of modified activated carbon fibres as redox mediators for the abiotic (Na_2S) reduction of nitroaromatic compounds was also studied by Amezquita-Garcia *et al.* (2013). Authors have reported that the presence of those materials is a requisite for the reduction of 4–nitrophenol and 3–chlolonitrobenzene, which was attributed to the quinone groups present in the carbon materials. The presence of carbon materials did not affect the methanogenic activity, which was maintained as compared with the control. Three cycles of fresh MY10 solution addition were carried out with the objective of

evaluating the reutilisation of carbon materials (Table 4.4). Although a decrease of the rates during the cycles was observed, an effect as redox mediator was still present.

Table 4.4. Decolourisation extent (%) and rates (d^{-1}) of MY10 (1 mmol L^{-1}) during 3 cycles of dye addition

	1st cycle		2nd cycle		3rd cycle	
Sample	**%**	**d^{-1}**	**%**	**d^{-1}**	**%**	**d^{-1}**
No CM	83 ± 1	9.50 ± 0.49	89 ± 2	9.55 ± 0.30	90 ± 1	6.44 ± 0.46
CXB	85 ± 1	14.99 ± 0.18	90 ± 1	14.20 ± 0.41	86 ± 2	9.31 ± 0.09
CNT	86 ± 1	20.08 ± 1.14	92 ± 1	16.14 ± 0.52	88 ± 1	10.81 ± 0.59

The decrease of the efficiency of the CM may be, in part, due to fact that the new cycles were performed with the materials from the previous experiment, without carbon material regeneration. Additionally, a decrease of the efficiency was also observed in the experiments without CM.

4.3.5. Textile wastewater treatment

To test the process in a real textile wastewater, biodecolourisation of two real effluents, effluent A and effluent B, was performed in the same conditions as for the single dyes. A model wastewater prepared by the mixture of the three dyes that constitute the real effluent A was also treated. Effluent A was decolourised within 24 h at the extent of 63 % and at the rate 0.59 d^{-1} (Table 4.5). The presence of CNT leads to an increase of the rate to 0.72 d^{-1}. With the other carbon materials, AC_{H2}, XA and XB, rates and degree of decolourisation were not affected. The effect of CNT was also observed with the Effluent B, which was only decolourised in the presence of CNT, although at lower extent, 32 %. Similarly with the observation for the single dyes, this result reflects the effect of dyes structure, once the two effluents only differ in the dye composition.

Table 4.5. Biodecolourisation extent (%) and rates (d^{-1}) of real and model wastewaters in the absence and presence of CNT (0.1 g L^{-1})

	No CNT		CNT	
Wastewater	**%**	**d^{-1}**	**%**	**d^{-1}**
Effluent A	63 ± 2	0.59 ± 0.07	63 ± 3	0.72 ± 0.07
Effluent B	0	0	32 ± 1	6.01 ± 0.69
Model effluent	97 ± 1	2.25 ± 0.20	97 ± 1	2.71 ± 0.32

Comparing the effluent A with the model wastewater, almost totally decolourised, 97 %, and at 4–fold higher rate, is proved that the presence of salts and other additives that composed the real effluent, affected the biological reaction. The application of CNT, though the same extent of decolourisation, lead also to an improvement of the catalytic rate. The effect of salts was investigated and the extent of decolourisation, after 24 h, was 88 % and the rate decreased 1.5 fold. However, no information about the other additives that compose the real wastewater, such as anti-foamers, detergents, dispersants, surfactants, retardants, etc., could be obtained from the textile company, which may also contribute for the lower performance of biodegradation [Zhang *et al.,* 2004]. In addition, the proportion of each dye in the real effluent was also not provided. Decolourisation of the single Procion dyes that composed the wastewaters was also done (Table 4.6). Although at different rates, all the three Procion dyes were almost totally decolourised around 90 %.

Table 4.6. Biodecolourisation extent (%) and rates (d^{-1}) of Procion dyes (1 mmol L^{-1})

Dye	**%**	**d^{-1}**
PB	83 ± 1	91.2 ± 2.4
PY	89 ± 2	8.0 ± 2.8
PR	90 ± 2	1.7 ± 0.1

4.4. CONCLUSIONS

Efficiency of microporous (AC_{H2}) and mesoporous carbons (CXA, CXB and CNT) as redox mediators on azo dye and real textile wastewater reduction was studied and compared. This is the first report on the use of CX and CNT as redox mediators for azo dye decolourisation. Results demonstrate that the presence of carbon materials increases the reduction rates. Additionally, the presence of carbon material is a requisite for biodegradation of the dye AO10. Pore sizes of the chosen carbon material play a key role on dye decolourisation and higher efficiency was obtained for the carbon materials having larger pores. In general, rates increased in the order: control < AC_{H2}< CXA < CXB < CNT. HPLC analysis confirmed the reduction of dyes with the corresponding aromatic amines formation. Results of real wastewater biological treatments demonstrate that the process can successfully be applied on textile wastewaters remediation.

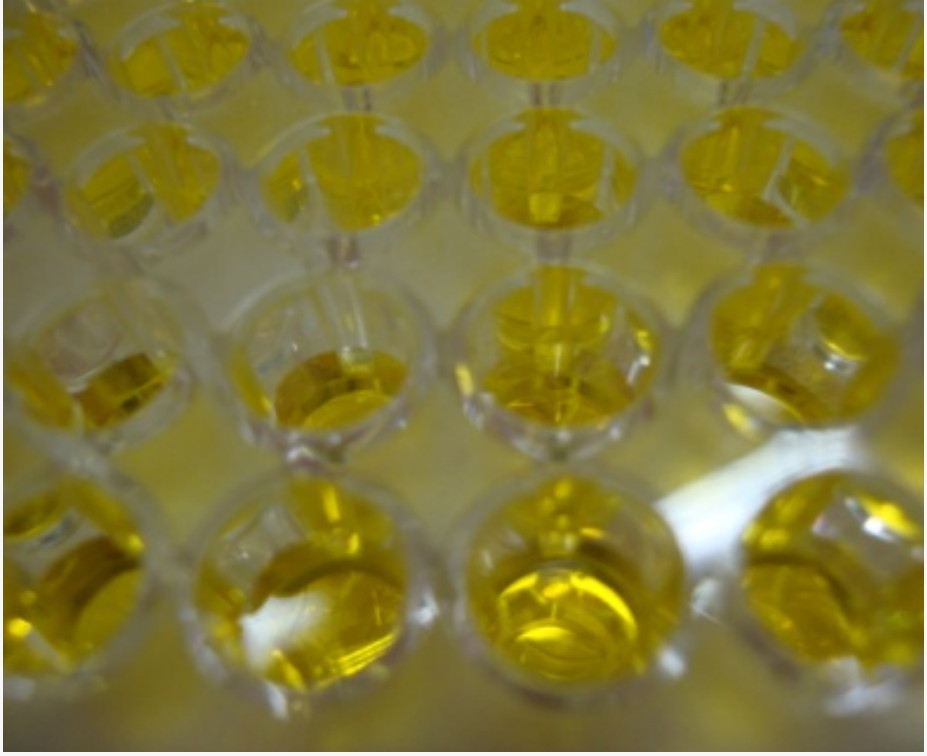

CHAPTER 5.

ANAEROBIC BIOTRANSFORMATION OF NITROANILINES ENHANCED BY THE PRESENCE OF LOW AMOUNTS OF CARBON MATERIALS

Three microporous activated carbons (AC_0, AC_{HNO3}, AC_{H2}) and three mesoporous carbons (CXA, CXB, CNT) were tested as redox mediators on the biological reduction of o-, m- and p-nitroaniline (NoA) and of a azo dye (MY1), using volatile fatty acids (VFA) as electron donor. NoA were only partially reduced in the absence of carbon materials (CM). The presence of CM lead to above 90 % reduction of NoA and up to 8–fold higher rates, with better results obtained with microporous materials. Biological reduction of MY1 lead to the formation of the correspondent aromatic amines, 5–aminosalicilic acid and m–NoA. Moreover, m–NoA was further totally reduced only in the reactions mediated by CM. The toxicity towards a methanogenic consortium degrading VFA of biologically treated NoA and MY1 solutions, decreased up to 80 and 100 %, respectively, compared to the non-treated solutions of those compounds. The electron shuttle effect of CM was proved by measuring the capacity of AC_0 to transfer the electrons accepted from the biological oxidation of VFA to Fe^{3+}, reducing it at Fe^{2+}.

CHAPTER 5.
ANAEROBIC BIOTRANSFORMATION OF NITROANILINES ENHANCED BY THE PRESENCE OF LOW AMOUNTS OF CARBON MATERIALS

5.1. INTRODUCTION

NoA are categorized as toxic and mutagenic [Chung *et al.,* 1997; Chung, 2000; Malca-Mor and Stark, 1982] and are commonly used in the industrial production of pharmaceuticals and synthetic dyes, originating contaminated wastewaters [Harter, 1985]. They are also products of anaerobic reduction of azo dyes [Donlon *et al.,* 1997; Garrigós *et al.,* 2002; Sarasa *et al.,* 1998] and explosives [Spain, 1995]. In soils, microbial degradation of herbicides also originates NoA. Some published results on biological degradation of NoA under anaerobic conditions have shown their transformation via reduction of the nitro group, forming nitroso and hydroxylamino intermediates to the corresponding amines, through a six-electron transfer mechanism donated by co-substrates [Razo-Flores *et al.,* 1997a; Spain A, 1995]. However, their biological reduction has been described as proceeding at very low rates and/or needing acclimated biomass [Khalid *et al.,* 2009; Saupe JC, 1999]. Redox mediators shuttling the electrons from a co-substrate to the target compounds to be degraded, can act as catalysts in this reduction process, increasing the corresponding biotransformation rates [Van der Zee *et al.,* 2001; Van der Zee and Cervantes, 2009]. This is very important for the efficient operation of high-rate anaerobic reactors when treating effluents containing NoA, since the electron transfer rate can limit the overall process performance (Cervantes *et al.,* 2001). Chapter 3 and 4 shows the characteristics of modified CM surface chemical structure, and the effect on their performance as catalyst [Pereira *et al.,* 2010, 2014].

In the present study, different microporous (AC_0, AC_{HNO3} and AC_{H2}) and mesoporous (CX and CNT) CM were explored as redox mediators on the anaerobic biological reduction of *o*–, *m*–and *p*–NoA (see chemical structures in Figure 5.1). Other authors have evaluated and proved the catalytic effect of CM, such as AC (Gong *et al.,* 2014) and graphene (Fu and Zhu, 2013), on chemical reduction of nitrobenzene. This is the first work on the use of diverse CM as RM for NoA biological reduction.

Once the anaerobic biological reduction of azo dyes leads to the formation of the corresponding aromatic amines, the dye MY1 was also tested, and the formation of the corresponding aromatic

amines (*m*–NoA and 5–ASA) and further biodegradation was evaluated (see chemical structures in Figure 5.1). The potential toxic effect of NoA, MY1 and of final degradation products was evaluated for a methanogenic consortium degrading VFA.

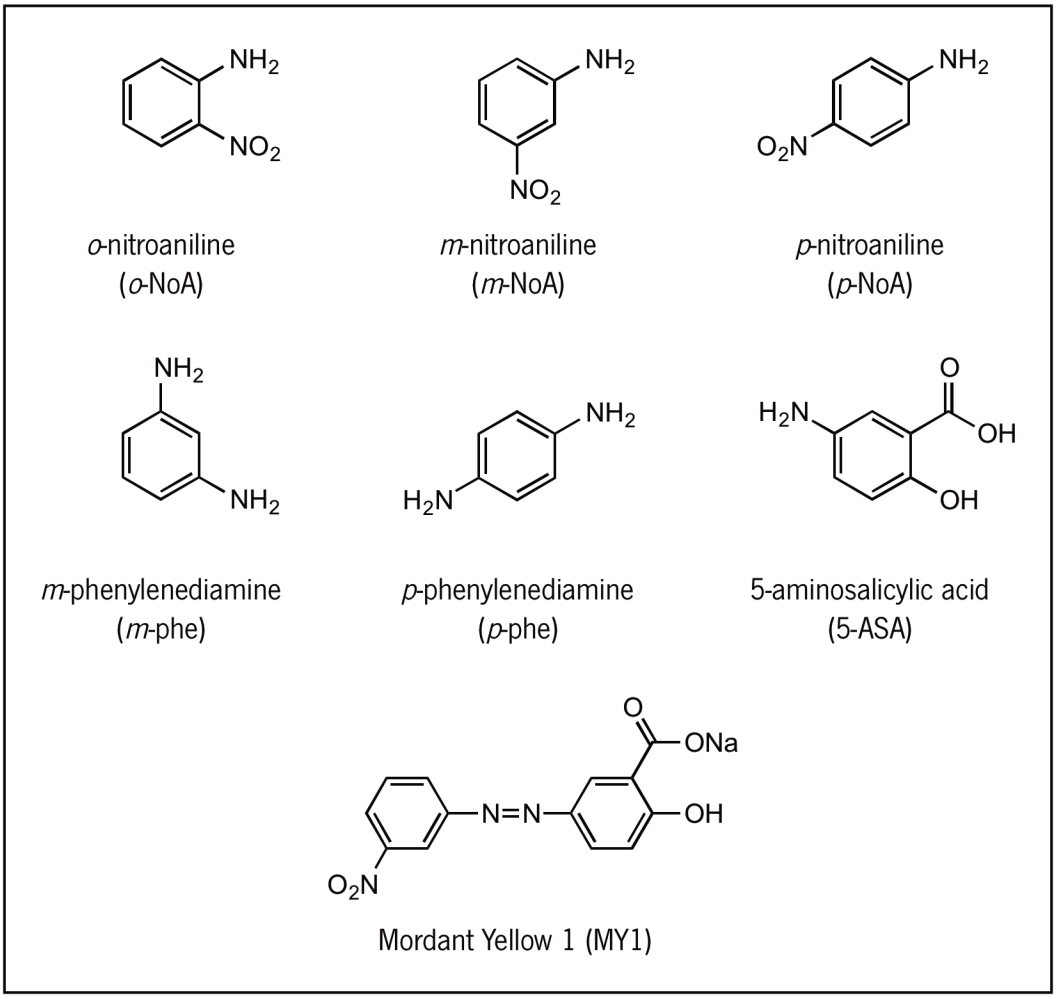

Figure 5.1. Molecular structure of the aromatic amines, *o*-, *m*- and *p*-NoA, *m*- and *p*-phe, 5-ASA and the azo dye MY10.

5.2. MATERIALS AND METHODS

5.2.1. Chemicals

o–NoA (98 %), *m*–NoA (98 %), *p*–NoA (>99 %), MY1 (50 %), 5–ASA (>99 %), *m*–phe (98 %) and *p*–phe (98 %) were purchase from Sigma and used without additional purification. The chemicals used to prepare the macronutrients solution were purchase from Sigma or Fluka at highest analytic grade purity commercially available. Acetonitrile for HPLC analysis was purchased from Panreac at HPLC analytic grade.

5.2.2. Preparation and Characterization of Carbon Materials

CM used in this study were AC_0, AC_{H2}; CXA, CXB and CNT prepared and characterized as described in Chapter 4 (section 4.2.2).

5.2.3. Biological assays

Biological reduction of NoA was conducted in 70 mL serum bottles, sealed with a butyl rubber stopper, containing 25 mL of medium. The primary electron donating substrate of the medium was composed of 2 g L^{-1} chemical oxygen demand (COD) of a NaOH-neutralised VFA mixture, containing acetate, propionate and butyrate in a COD based ratio of 1:10:10. Basal nutrients were also added: NH_4Cl (2.8 g L^{-1}), $CaCl_2$ (0.06 g L^{-1}), KH_2PO_4 (2.5 g L^{-1}), $MgSO_4 \cdot 7H_2O$ (1 g L^{-1}). Medium was buffered at a pH of 7.3 ± 0.2 with $NaHCO_3$ (2.5 g L^{-1}). Anaerobic granular sludge, collected from an anaerobic internal circulation reactor of a brewery wastewater treatment plant, was the inoculum at a concentration of (2.5 ± 0.5) g L^{-1} volatile suspended solids (VSS). NoA were added at the final concentration of 1 mmol L^{-1}. The effect of the different CM (AC_0, AC_{H2}, AC_{HNO3}, CXA, CXB, CNT) on biological reduction was tested at a concentration of 0.1 g L^{-1}. This concentration is based in the results shown in Chapter 3, where this reduced AC concentration lead to similar levels of dye

reduction rates, comparing to higher AC concentrations, for less than 10 % dye adsorption. These results are important since AC is costly and therefore the use of low amounts is an advantage for biological processes application. Furthermore, as a RM, CM are recycled from its oxidized and reduced states and thus should be effective at low concentrations. Sludge was incubated overnight at 37 °C in a rotary shaker at 120 min^{-1} rotation. After the pre-incubation period, NoA and VFAs (2 gCOD L^{-1}) were added with a syringe from the stock solution to the desired concentration. Biological reduction of the azo dye MY1, at concentration of 1 mmol L^{-1}, was performed in the same conditions, but only with the AC_0 sample. Controls without CM and without biomass were also conducted. All experiments were prepared in triplicate.

With the aim of evaluating the capacity of CM to accept electrons from the biological oxidation of VFA, similar assays were conducted, with 0.1 and 1.0 g L^{-1} of AC_0, without NoA or MY10. A set of controls excluding either biomass, or AC_0, or VFA was incorporated. To prevent the flow of electrons to methanogens, the cultures were supplemented with 20 mmol L^{-1} 2–bromoethanesulfonate (BES). After 24 h incubation, AC_0 was removed from the medium in an anaerobic chamber, and incubated with a 1 mmol L^{-1} Fe^{3+} solution. The electron transfer from AC_0 to Fe^{3+}, reducing it to Fe2+, was measured overtime by the ferrozine technique [Lovely and Phillips, 1986]. Briefly, this technique is based in the reaction of Fe^{2+} reaction with ferrozine (monosodium salt hydrate of 3-(2-pyridyl)-5,6-diphenyl-1,2,4-triazine-p,p'-disulfonic acid), forming a stable magenta complex with a maximum absorbance at 562 nm (Abs_{562}). The concentration of Fe^{2+} (C_{Fe2+}) was calculated with the calibration curve: $Abs_{562} = 8.64 * C_{Fe2+} - 0.311$ for Abs > 1 and $Abs_{562} = 10.98 * C_{Fe2+} + 0.038$ for Abs < 1.

5.2.4. Specific methanogenic activity

SMA tests were performed in serum bottles of 25 mL, containing 12.5 mL of buffer solution with 3.05 g L^{-1} sodium bicarbonate and 1 g L^{-1} of Resazurin, The vial were supplemented with 0.4 g anaerobic granular sludge which corresponds to (2.1 ± 0.2) g of VSS per litre, and the headspace was flushed with a mixture of N_2/CO_2 (80/20; v/v). The final pH was 7.2 ± 0.2. Following the addition of 0.125 mol L^{-1} Na_2S, under strict anaerobic conditions, the vials were incubated overnight at 37 °C and at 120 m^{-1} rotation. After that period, the mixture of VFA 1:10:10 (acetate, propionate

and butyrate as mass of COD) at the final concentration of 2 gCOD L^{-1}, and the solutions to be tested, were added and the vials were maintained at 37 °C and at 120 min^{-1} rotation, during the entire assay. The pressure was measured every 60 min by using a hand-held pressure transducer able of measuring a pressure variation of ± 202.6 kPa (0 to 202.6 kPa) with a minimum detectable variation of 0.5 kPa, corresponding to 0.05 mL of biogas in a 10 mL headspace. The assay was finished when the pressure remained stable. 500 μL of sample volume were collected every day using a gas-tight syringe and methane content of the biogas was measured by gas chromatography using a Chrompack Haysep Q (80–100 mesh) column (Chrompack, Les Ulis, France), with N_2 as carrier gas at 30 mL min^{-1} and a flame-ionization detector. Temperatures of the injection port, column, and flame-ionization detector were 110 °C, 35 °C and 220 °C, respectively. The values of methane production were corrected for the standard temperature and pressure conditions (STP). In order to determine the activities, the values of pressure (calibrated as an analogical signal in mV) were plotted as a function of time and the initial slopes of the methane production were calculated. SMA values were determined dividing the initial slope by the VSS content of each vial at the end of the experiment and were expressed in $mgCH_4$ $gVSS^{-1}$ day^{-1}. Background methane production due to the residual substrate was subtracted. Tests included series containing increasing concentrations of NoA (0.25 to 1 mmol L^{-1}) and MY1 (0.125 to 1 mmol L^{-1}) to evaluate their effect on the methanogenic activity. The final products of biological reduction of NoA and MY1 treated in the presence of AC_0, and the standard 5–ASA (0.2 to 4 mmol L^{-1}) were also tested. Two controls were made in the same conditions, one containing only VFAs and the other without any substrate (blank assay). All batch experiments were performed in triplicate. The effect of tested compounds was evaluated by comparing with the control containing only VFAs.

5.2.5. Analytical techniques

Reactions were monitored spectrophotometrically in a 96-well plate reader (ELISA BIO-TEK, Izasa) and by HPLC. NoA and MY1 show a yellow colour with maximum wavelengths at 410 for *o*–NoA, 350 for *m*–NoA and MY1 and 380 nm for *p*–NoA. At select intervals, samples were withdrawn (300 μL), centrifuged at 5000 rpm for 10 min to remove the biomass and/or CM and diluted to obtain less than one absorbance unit. The UV-vis spectra (200–800 nm) were recorded and NoA

concentration calculated at λ_{max}. Molar extinction coefficients were calculated at λ_{max}: $\varepsilon_{410\ nm}$= 1.345 $mM^{-1}\ cm^{-1}$ for *o*-NoA; $\varepsilon_{350\ nm}$= 0.582 $mM^{-1}\ cm^{-1}$ for *m*-NoA; $\varepsilon_{380\ nm}$= 3.104 $mM^{-1}\ cm^{-1}$ for *p*–NoA and $\varepsilon_{350\ nm}$= 0.582 $mM^{-1}\ cm^{-1}$ for MY1. First-order reduction rate constant (h^{-1}) and color removal (*CR*) were calculated according to Equations 1 and 2 (see 3.2.5. Chemical Dye Reduction).

HPLC analyses were performed in a HPLC (JASCOAS-2057 Plus) equipped with a diode array detector. A C18 reverse phase Nucleodur MNC18 column (250 x 9 x 4.0 mm, 5 μM particle size and pore of 100 Å from Machenerey-Nagel, Switzerland) was used. Mobile phase was composed of the solvents: A (ultrapure water) and B (Acetonitrile). Compounds were eluted at a flow rate of 0.5 mL min^{-1} and at room temperature, with isocratic condition containing 50 % of A and 50 % of B, during 20 min. Compounds elution was monitored at λ_{max} of compounds (410, 350 and 380 nm) and at 230 nm for reduction products (5–ASA and phenylenediamines). The retention times of NoA and products are specified in Table 5.1.

Table 5.1. HPLC retention times (min) of NoA and MY10 at initial incubation time (t0) and after 24 and 48 h biological reaction, in the presence and absence of AC_0, and of the standards *m*-phe, *p*-phe and 5-ASA (expected products of biological reduction)

	t0		After 24h		After 48h	
Compound	**No AC**	**AC_0**	**No AC**	**AC_0**	**No AC**	**AC_0**
o–NoA	12.2		5.4		N.d.	
m–NoA	10.1		5.1		N.d.	
p–NoA	8.6		4.9		N.d.	
MY1	4.6		3.8; 10.0		3.8; 10.0; 5.1	3.8; 5.1*
m–phe	5.2		N.d.		N.d.	
p–phe	5.0		N.d.		N.d.	
5–ASA	3.8		3.8		3.8	

N.d. not determined; (*) residual amount, as observed in Figure 5.5 B.

5.3. DISCUSSION

5.3.1. CM as redox mediators on NoA biological reduction

Biological reduction of structurally related NoA by granular anaerobic biomass and the effect of different CM as RM was studied and compared. During the reaction, the yellow colour decreased and, in the presence of CM, the solution turned colourless. As monitored by spectrophotometry (Figure 5.2), a decrease of the visible spectra was observed.

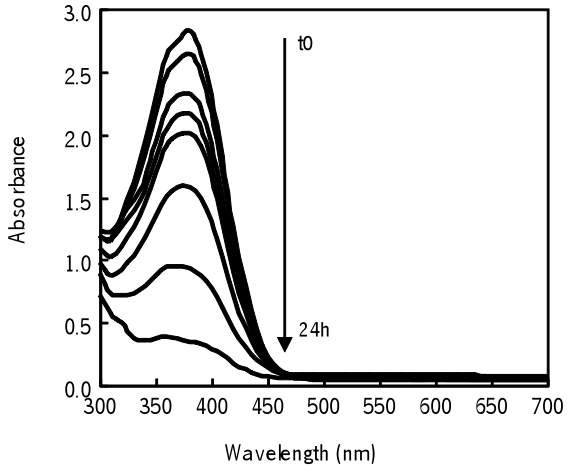

Figure 5.2. Biological reduction of *p*-NoA in the presence of AC_0 as monitored by UV-Vis spectroscopy.

In addition, the reactions were followed by HPLC, where NoA and its products are analysed individually. As observed in Figure 5.4, NoA reduction followed first-order kinetics and higher rate was obtained for the *m*–NoA: 2x higher than the obtained for *p*–NoA and 4x higher than the obtained for *o*–NoA, revealing the effect of the position of the nitro substituents in the molecule. In the absence of CM, the extent of biological reduction in the equilibrium (~24 h) was 32 %, 56 % and 52 %, for *o*–, *m*– and *p*–NoA, respectively (Table 5.2). In Table 5.2, the effect of CM on the NoA reduction rates is also shown. Almost total reduction was obtained in the presence of CM and the rates were significantly improved.

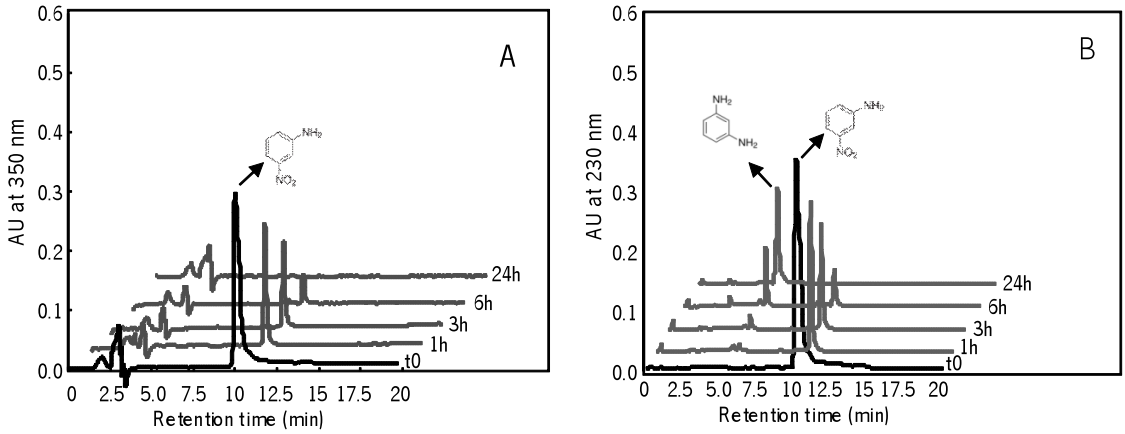

Figure 5.3. Biological reduction of *m*–NoA in the presence of AC_0 as monitored by HPLC at 350 nm (**A**) and 230 nm (**B**).

Table 5.2. Effect of different CM (0.1 g L^{-1}) on bioreduction extent (%) and rates (d^{-1}) of NoA (1 mmol L^{-1})[a]

	o–NoA		*m*–NoA		*p*–NoA	
Condition	**(%)**	**(h^{-1})**	**(%)**	**(h^{-1})**	**(%)**	**(h^{-1})**
Control	32 ± 1	0.07 ± 0.01	56 ± 4	0.26 ± 0.11	52 ± 2	0.14 ± 0.02
AC_0	97 ± 2	0.15 ± 0.02	98 ± 1	1.14 ± 0.04	89 ± 1	1.05 ± 0.01
AC_{H2}	97 ± 3	0.22 ± 0.03	97 ± 1	1.12 ± 0.01	92 ± 1	0.99 ± 0.04
AC_{HNO3}	94 ± 1	0.10 ± 0.03	95 ± 1	0.23 ± 0.01	94 ± 1	0.18 ± 0.01
XA	93 ± 2	0.10 ± 0.01	94 ± 1	0.22 ± 0.03	93 ± 1	0.14 ± 0.01
XB	91 ± 1	0.09 ± 0.01	92 ± 1	0.36 ± 0.01	91 ± 1	0.15 ± 0.01
CNT	94 ± 6	0.10 ± 0.01	91 ± 1	0.10 ± 0.01	93 ± 2	0.07 ± 0.01

[a] Controls without biomass reveal that no adsorption to CM occurs (see Figure 5.4). The values correspond to triplicate assays. The R^2 of fitting 1st-order exponential decay were all around 0.998.

Similar results were obtained for the bioreduction of *o*–, *m*– and *p*–NoA in samples of the river Elbe [Börnick *et al.*, 2001]. However, other researchers have also studied the effect of nitro group

position on different NoA reduction and, contrarily to our results, faster reduction was found for compounds carrying the nitro-group in the *o*– position [Hudlicky, 1984; McCormick *et al.*, 1976].

A decrease of the NoA peak was observed at the maximum wavelength of the NoA (Figure. 5.4 A). At 230 nm, both NoA removal and product formation could be monitored (Figure. 5.4 B), confirming the reduction of the NoA. As compared with standards, the products of NoA reduction were identified as the expected products, the correspondent phenylenediamines (Table 5.1), which is in agreement with literature (Bhushan *et al.,* 2006; Razo-Flores *et al.*, 1997b; Razo-Flores *et al.*, 1999; Saupe, 1999). According to previous literature, nitroreductases convert nitro groups either to nitroso derivatives, hydroxylamines or amines through six electron successive addition from cosubstrates to nitrocompounds. The high reactivity and instability of nitroso derivatives difficult their detection. The aromatic amines formed are usually hard to be further degraded under the anaerobic conditions, however have the possibility, in some cases, to be further degraded by aerobic processes [Van der Zee and Villaverde, 2005].

Comparing the different CM, higher reduction rates were obtained with the microporous samples, AC_0 and AC_{H2}, leading to an improvement of 3–fold, 4–fold and 8–fold higher for *o*–, *m*–, and *p*–NoA, respectively, as compared with the reaction in the absence of CM (Table 5.2). In previous results with azo dyes, better performance was achieved with the mesoporous CM, explained by the easier access of the larger molecules of the dye to the internal surface of the catalyst. NoA are smaller molecules so, the better results with the microporous materials, might be related with higher surface area of these materials instead of the size of the pores.

Similarly to the known redox mediator AQDS, the effect as redox mediator of AC has been attributed to the quinone groups on its surface [Van der Zee *et al.,* 2003]. However, in this study, comparing between the three samples of microporous AC, better results were obtained with AC_0 and AC_{H2} than with the AC_{HNO3} sample. In fact, in spite of the higher amount of quinone groups in AC_{HNO3} compared to the other samples, its effect is surpassed by the large amount of carboxylic acids and anhydrides also present in this sample, which are electron withdrawing groups.

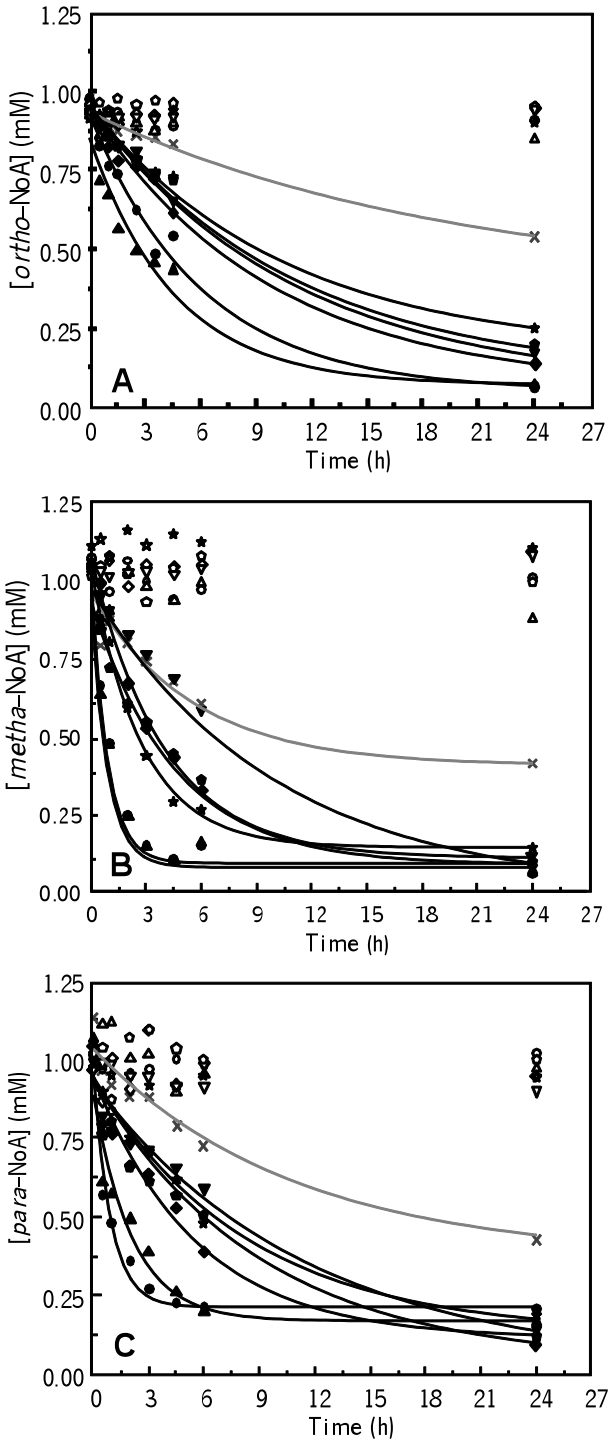

Figure 5.4. First-order rate curves of *o*–NoA (**A**), *m*–NoA (**B**) and *p*–NoA (**C**) biological reduction. (**x**) no carbon material; (●) AC_0; (▲) AC_{H2}; (♦) AC_{HNO3}; (■) CXA; (⋆) CXB and (▼) CNT. Black symbols correspond to the biotic and white symbols to the abiotic assay.

In a previous work, thermal modification of AC surface chemistry improved its capacity as redox mediator for azo dye reduction, which was related with the high content of electron rich sites on their basal planes (π–electrons), known to be active sites, and by a low concentration of electron withdrawing groups [Pereira *et al.,* 2010]. Sample AC_{H2} has the advantage of keeping some of the quinone groups without the presence of the oxygen-containing acidic groups (removed during the thermal treatment). Although AC_0 has a higher amount of oxygen containing groups than AC_{H2}, their performance as redox mediators was similar. Other characteristic of the AC materials involved, is their pH_{pzc}. Due to AC amphoteric character, when in solutions at pH below their pH_{pzc} it became positively charged and at pH above the pH_{pzc}, negatively charged. Therefore, at pH 7 AC_0 and AC_{H2} are positively charged and AC_{HNO3} negatively charged. NoA are ionisable organic compounds, they can exist either as nondissociated or dissociated species in aqueous phase, depending on the solution pH in relation to their dissociated constants (pKa). Since the pKa of *o*–, *m*– and *p*–NoA are –0.28, 2.45 and 0.98, respectively (Yang *et al.,* 2008), in solution at pH 7, deprotonation will occur generating the NoA correspondent anions. The electrostatic attraction forces between the positively charged carbons and the negatively charged NoA, will be favourable to the electron shuttling.

In opposite to our results, Amesquita-Garcia *et al.* (2013) investigating the RM effect of AC fibres, original, chemically oxidized and thermally treated, on 4–nitrophenol and 3–chloronitrobenzene chemical (Na_2S) reduction, have concluded that AC fibres chemically oxidized are better RM due to the increased number of quinone groups. Liu *et al.* (2012), have discussed about the mechanism of methanogenesis stimulation by AC in methanogenic digesters, the possibility of favouring the direct interspecies electron transfer (DIET) under anaerobic conditions between bacteria and methanogens and the role of AC surface quinone groups. Authors have demonstrated that AC could accelerate the electron transfer between *Geobacter metallireducens* and *Geobacter sulfurreducens* or *Geobacter metallireducens* and *Methanosarcina barkeri*. Studies using AQDS instead of AC put aside the potential responsibility of quinone groups and lead authors to consider, instead, the possible contribution of AC high conductivity enabling electrical connections between microorganisms. According to these authors, the investment of the cells on metabolic energy in producing conductive pili and the additional cytochromes that are required for the DIET in the absence of AC is reduced.

5.3.2. MY1 biological reduction

MY1 bioreduction was followed by UV-visible spectroscopy and by HPLC. In the first 24h, a decrease of the HPLC peak corresponding to the dye (Rt of 4.6 min) was observed with the formation of two new peaks at Rt of 3.8 and 10 min (Figure 5.5 A and B).

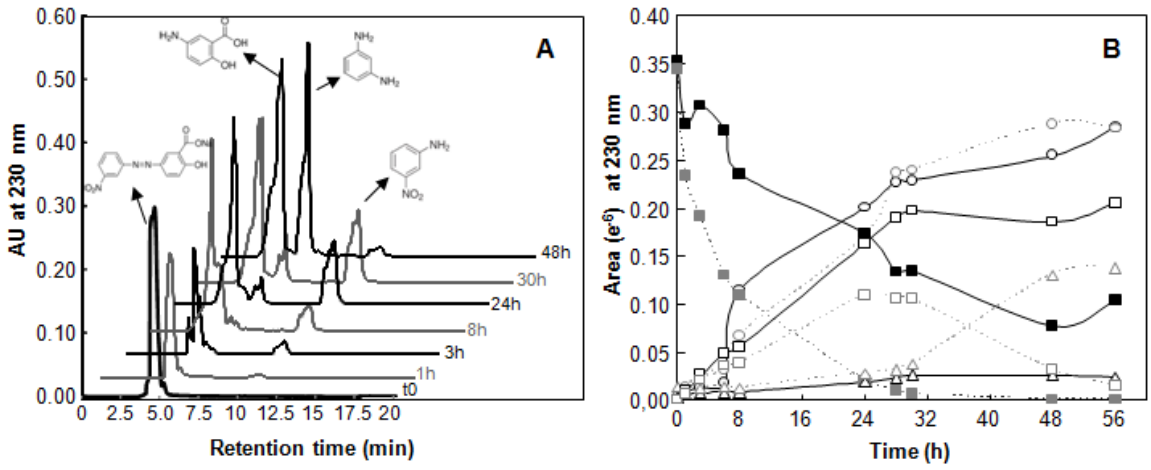

Figure 5.5. HPLC chromatograms of MY1 biological reduction at 230 nm (A) and areas of dye biological reduction, and products formed, within 48 h of reaction (B); (○) 5-ASA; (■)MY1; (Δ) *m*-Phe; (□) *m*-NoA. Black symbols correspond to the reaction in the absence of AC0 and grey to the reaction in the presence of AC_0.

As comparing with the standards, those two peaks were attributed to the correspondent aromatic amines, 5–ASA and *m*–NoA. MY1 was totally decolourised when AC_0 was present in the reaction medium, while in its absence only 70% of decolourisation was reached, and at a 3-fold higher rate: $r_{control}$ = 0.057 ± 0.015 h^{-1} and r_{ACH2} = 0.161 ± 0.013 h^{-1} (Figure 5.5 B). Moreover, in the presence of AC_0, *m*–NoA was further reduced to *m*–phenylenediamine (Rt 5.1 min), while 5–ASA was recalcitrant during the entire incubation period, 48h. Batch assays for 5–ASA biological reduction in the same conditions as for MY1, confirm its recalcitrant nature within 48h of reaction (data not shown). Donlon *et al.* (1997) have also proposed the mechanism of bioreduction of Mordant Orange 1, a similar azo dye, by a granular sludge in UASB reactors, with the formation of the correspondent aromatic amines 5–ASA and *p*–NoA. The *p*–NoA was further transformed into *p*–phenylenediamine as final product. Authors have also obtained total mineralization of 5–ASA by methanogenic

consortia in continuous reactor but only after prolong time operating, probably due to the sludge adaptation. 5–ASA degradation was also obtained only after a long period of an UASB bioreactor operation by other researchers [Razo-Flores *et al.,* 1997b; Razo-Flores *et al.,* 1999].

5.3.3. AC as electron acceptor

The electron shuttle capacity of AC_0 was evaluated by measuring the amount of Fe^{2+} formed via the AC-mediated electron transfer from VFA to Fe^{3+}. In the presence either of 0.1 or 1.0 g L^{-1} of AC_0, reduction of Fe^{3+} was observed and the total amount of Fe^{2+} was (0.20 ± 0.05) and (0.45 ± 0.06) mmol L^{-1}, respectively. In the presence of BES, similar amounts of Fe^{2+} were obtained: (0.18 ± 0.05) and (0.46 ± 0.07) mmol L^{-1}, respectively. In the controls without AC_0 or without biomass, no Fe^{3+} reduction was observed, proving the AC_0 reduction and consequent reduction of final electron acceptors (Fe^{3+}, azo dyes, NoA). In Figure 5.6, a photography of the magenta complex formed by the reaction of Fe^{2+} with ferrozine, when reduced AC_0 was incubated with Fe^{3+}, is presented.

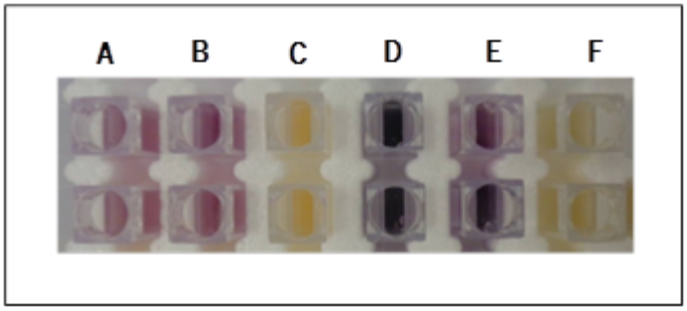

Figure 5.6. Photography of magenta complex formed from the reaction of Fe^{2+} (resulted from the reduction by AC_0) with ferrozine (duplicate experiments): (A and B) 0.1 g L^{-1} AC_0 and (D and E) 1.0 g L^{-1} AC_0, previously biologically reduced in the absence and presence of BES, respectively. C and F, are the controls with AC_0 (0.1 and 1.0 g L^{-1}, respectively) incubated in the same conditions of biotic experiments, but without biomass.

The controls present a slight yellow coloration due to the Fe^{3+} and also ferrozine colour solutions. Our results are in accordance with Van der Zee *et al.* (2003). A shift in the microbial community is not expected to have occurred, since longer times of incubation, continuous reactors or successive transfers of active cultures into fresh medium would be necessary. Our study was performed in

batch assays, operated only during 24 h, and the increase in the reduction rates was immediately observed in the presence of materials, as for example with total reduction of *m*–NoA in the first 3 h of reaction (figure B). Furthermore, in Chapter 3 the redox capacity of modified AC on chemical azo dye reduction was demonstrated, proving the electron transfer capacity of CM. Other authors have also confirmed the capacity of CM as RM of chemical reduction of nitrocompounds [Amesquita-Garcia *et al.*, 2013; Fu and Zhu, 2013; Gong *et al.,* 2014].

5.3.4. Effect of NoA and MY1 and final reduction products on the methanogenic activity

The inhibitory effects of the three NoA, the azo dye MY1 and their reduction products on the activity of acetoclastic methanogenic *Archaea* were evaluated (Table 5.6). The results revealed that the concentrations of the compounds tested in the biological assays were above their IC_{50}, which may also explain the low extent of reduction in the absence of CM. Among the NoA, similarly to the biological reduction results, the position of the nitro group had an effect on the methanogenic activity and a notorious higher toxic effect was observed for *o*–NoA.

The IC_{50} for *o*– substituted NoA was 0.23 mmol L^{-1} and for *m*– and *p*– substitutions was 0.67 mmol L^{-1} and 0.51 mmol L^{-1}, respectively. The lower reduction obtained for *o*–NoA among the NoA tested, in all the tested conditions, may also be due to its higher toxic effect on methanogenic consortium. Products of NoA biotransformation in the presence of AC_0 were also evaluated and up to 77 % of detoxification was obtained. The results obtained are in accordance with literature reporting that aromatic nitro-substituents are responsible for severe methanogenic toxicity, while correspondent aromatic amines present lower toxic effects [Donlon *et al.,* 1997; Razo-Flores *et al.,* 1997a].

The behaviour of nitroaromatics in the presence of pure cultures of sulphate-reducing bacteria, methanogenic bacteria, and *Clostridium spp.*, as well as the effect of nitroaromatics on these bacteria was investigated by Gorontzy *et al.* (1993). The nitroaromatics were transformed by all of the bacterial strains tested. While growing cells of sulphate-reducing bacteria and *Clostridium spp.* carried out nitroreduction, methanogen cells lyses occurred in the presence of nitroaromatics.

Table 5.3. Potential toxic effect of NoA, MY1 and products of their bioreduction (at concentration of 1 mmol L^{-1} and in the presence of AC_0), on acetoclastic methanogenic bacteria degrading VFA

Chemical	**Concentration** (mmol L^{-1})	**Activity** (mgCOD-CH_4gVSS^{-1} d^{-1})	**IC_{50}** (mmol L^{-1})
o–NoA	0.00 0.25 0.50 1.00	56.5 ± 3.5 25.8 ± 0.2 9.1 ± 0.5 * 0	0.23
Products of 1 mmol L^{-1} *o*–NoA bioreduction		43.7 ± 2.1	N/A
m–NoA	0.00 0.25 0.50 1.00	54.9± 3.3 43.3 ± 2.8 38.1 ± 3.7 12.6 ± 0.6 *	0.67
Products of 1 mmol L^{-1} *m*–NoA bioreduction		47.7 ± 1.2	N/A
p–NoA	0.00 0.25 0.50 1.00	45.2 ± 1.1 29.5 ± 1.6 16.9 ± 0.5 6.4 ± 0.9	0.51
Products of 1 mmol L^{-1} *p*–NoA bioreduction		34.3 ± 0.1	N/A
MY1	0.00 0.125 0.25 0.50 1.00	69.7 ± 3.5 57.0 ± 5.2 45.5 ± 3.5 24.5 ± 1.6 0	0.44
Products of 1 mmol L^{-1} MY1 bioreduction		66.6 ± 1.9	N/A
5–ASA	0.00 0.20 0.40 0.80 1.00 2.00 4.00	62.6 ± 5.1 55.1 ± 1.5 58.5 ± 2.8 51.6 ± 2.4 41.4 ± 0.5 16.5 ± 0.5 0	2.0

N/A not applicable; *methanogenic activity calculated after one day of lag phase.

The azo dye MY1 also presents toxic effect to the consortium, being the IC_{50} of 0.44 mmol L^{-1}, but a solution containing 1.0 mmol L^{-1} of this dye was almost total detoxified after the biological process

with AC_0 as catalyst. On the other hand, according to our results and based on previous published work by Razo-Flores *et al.* (1997a), the recalcitrant nature of 5–ASA seems to not be related with its toxic effect (IC_{50} of 2 mmol L^{-1}).

5.4. CONCLUSIONS

The efficiency of microporous (AC_0, and AC_{HNO3}, AC_{H2}) and mesoporous carbon materials (CXA, CXB and CNT) as RM on isomeric NoA reduction was evaluated. Rates were dependent on the nitro group position, increasing in the order *meta* > *para* > *ortho*. The presence of CM increased significantly both the extent and the rates of compounds bioreduction. The surface area of CM had greater effect than the pore sizes, with better results obtained for AC_0 and AC_{H2}. The pH_{pzc} of the materials is also an important factor on reduction reactions, and at pH 7 the electrostatic attraction between the positively charged carbons AC_0 and AC_{H2}, and the NoA anions favoured the electron transfer. The effect of AC_0 on azo dye MY1 was also observed with a 2–fold rate increase as compared with the biological reaction without mediator.

Additionally, the correspondent NoA formed was further reduced in the presence of the catalyst. The capacity of CM to act as redox mediators, explaining the higher bioreduction rates, was proved by measuring the abiotic transfer of electrons from biological oxidation of VFA to AC_0 and from reduced AC_0 to Fe^{3+}. The high extent of compounds reduction in the presence of CM even when present at toxic levels to the methanogenic consortium, and the detoxification obtained with the mediated treatment, up to 80 % for NoA and 100 % for MY1, demonstrates the effectiveness of the process and their promising application in continuous high rate bioreactors.

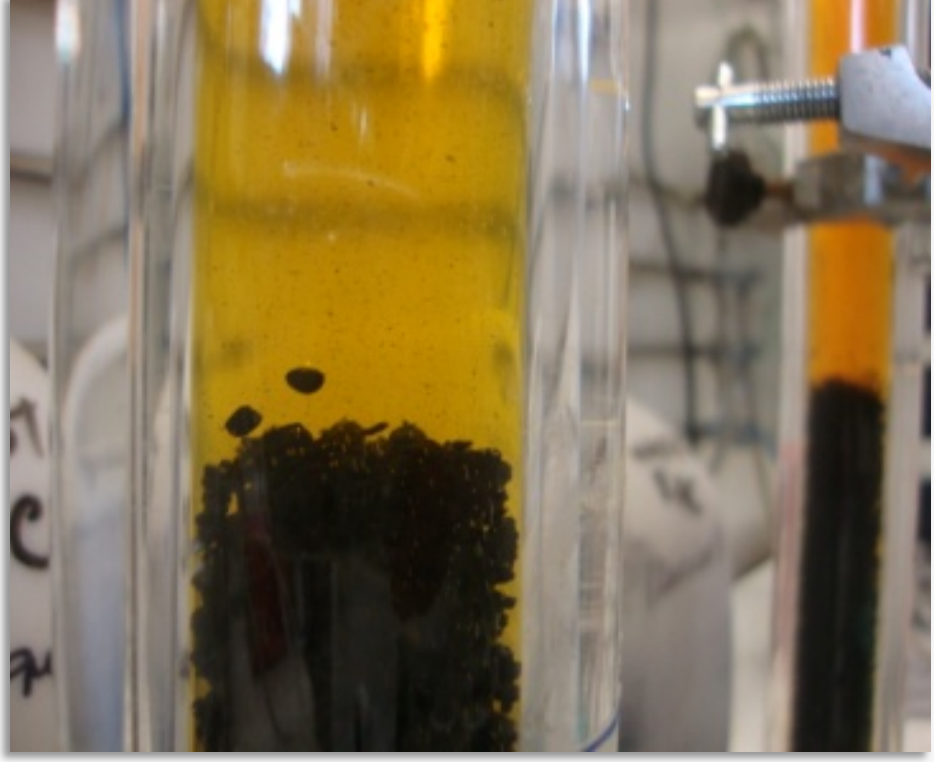

CHAPTER 6.

AZO DYE REDUCTION IN UASB REACTOR AMENDED WITH CARBON MATERIALS

Carbon Materials (CM) were investigated as redox mediators on the anaerobic biological reduction of the azo dye acid orange 10 (AO10), in a laboratory scale UASB reactor. The effect of different CM (microporous AC and mesoporous CNT), size of CM, concentration of CM, and the hydraulic retention time (HRT) was investigated. Biological reduction of AO10 was 98 % with both CM and at a diameter less than 0.25 mm, a concentration of 0.12 g per g of volatile solids and a HRT of 10 h. In the same conditions, above 90 % of colour removal and 80 % of chemical oxygen demand (COD) removal was achieved in mediated bioreactors operating with a HRT of 5 h. In the reactor control, although similar COD removal was obtained, AO10 decolourisation was only circa 20 %, evidencing the ability of CM to significantly accelerate the reduction reactions in continuous reactors. AO10 reduction to the correspondent aromatic amines was proved by HPLC. The presence of AC in the UASB reactor had no effect in the diversity of the microbial community when compared to the reactor control (without AC).

CHAPTER 6.
AZO DYE REDUCTION IN UASB BIOREACTORS AMENDED WITH CARBON MATERIALS

6.1. INTRODUCTION

Textile industry has grown economically worldwide leading to a high production of wastewater with considerable amounts of non fixed dyes lost during the dyeing or printing process. Among the strong colour, dyed wastewater is characterized by high pH, high COD content and low biodegradability [Wu *et al.*, 2007]. Several physical-chemical methods can be used to remove dyes from wastewater. However, these methods are not as efficient as expected. Furthermore, the high cost for expensive equipment or energy requirement are limiting factors [Yahiaoui *et al.*, 2013]. The most promising alternatives for textile wastewater treatment are biological methods. The UASB reactor system developed by Lettinga and co-workers (1890) has been successfully used to treat a variety of biodegradable industrial wastewaters. Compared with other advanced anaerobic systems (e.g. anaerobic filter and fluidized bed reactors), UASB process is able to retain a high concentration of biomass with high specific activity and thereby can achieve good COD removal efficiency at high organic loading rates [Van der Berg *et al.*, 1983]. Due to electron transfer limitations in dye anaerobic reduction reactions, longer HRT are required in UASB reactors, however, the use of RM can accelerate the rate of azo dye reduction [van der Zee, 2001]. In Chapters 3 and 4, it was demonstrated different CM acting as RM on anaerobic dye reduction and the reduction rates of several dyes increased compared with assays in the absence of CM. The purpose of the present work was to evaluate the performance of CM as RM on the biological reduction of azo dye (AO10) in a continuous UASB reactor. In order to optimize the process, different parameters were studied: type of CM (either AC or CNT); concentration of CM (0.06 to 0.12 g of CM per g of VS); size of CM (0.25 to 0.6 mm) and HRT (5 to 20 h). Additionally, molecular biology techniques were used to provide detailed description of the microbial community present in the UASB reactors.

6.2. EXPERIMENTAL

6.2.1. Carbon materials and chemicals

Carbon materials tested were the commercial AC NORIT ROX0.8 (pellets of 0.8 mm diameter and 5 mm length) and a commercial CNT (Nanocyl 3100) with an average diameter of 9.5 nm, an average length of 1.5 mm with carbon purity higher than 95 %. The characteristics of those materials were previously described in Chapter 4. In order to prepare AC with different size ($0.3 < d < 0.6$ or $d < 0.25$ mm), it was crushed and sieved. Acid Orange 10 (AO10, dye content 90 %) was purchased from Sigma and used without additional purification. The chemicals used to prepare the nutrients and substrate solutions were purchase from Sigma or Fluka at highest analytic grade purity commercially available. The solvent acetonitrile (ACN) and ammonium acetate for HPLC analysis were purchased from Acros and Panreac, respectively.

6.2.2. UASB reactor operation

Three lab scale UASB reactors, made of acrylic glass and 400 mL of work volume (L= 98 cm; d= 2 cm) were maintained at (37 ± 2) °C (Figure 6.1). One contained AC (RAC), other CM (RCNT) and a third serving as control, without CM (R0).

The reactors were seeded with 10 g L^{-1} of VS of anaerobic sludge obtained from a full-scale UASB reactor treating brewery wastes (Central de Cervejas, Portugal). The reactors were feed with synthetic wastewater containing 0.50 mmol L^{-1} of AO10 and nutrients (0.23 g L^{-1} ZnCl; 0.29 g L^{-1} $CuSO_4.5H_2O$; 0.29 g L^{-1} $(NH_4)_6Mo_7O_{24}.4H_2O$; 0.26 g L^{-1} $CoCl_2.6H_2O$; 0.16 g L^{-1} $MnSO_4.H_2O$; 90.41 g L^{-1} $MgSO_4.7H_2O$; 6.74 g L^{-1} $CaCl_2.2H_2O$; 14.53 g L^{-1} $FeCl_3.6H_2O$; 190.90 g L^{-1} NH_4Cl; 33.40 g L^{-1} $Na_2PO_4.2H_2O$; 28.50 g L^{-1} $K_2HPO_4.3H_2O$; 8.50 g L^{-1} KH_2PO_4. A mixture of 2 g L^{-1} of VFAs at 1:10:10 COD ratio of acetate, propionate and butyrate, was added as the primary electron donor. This solution was refrigerated at 4 °C and feed to the reactor with a peristaltic pump. The reactors recycle was made by a second peristaltic pump with a constant flow rate of 100 mL min^{-1}.

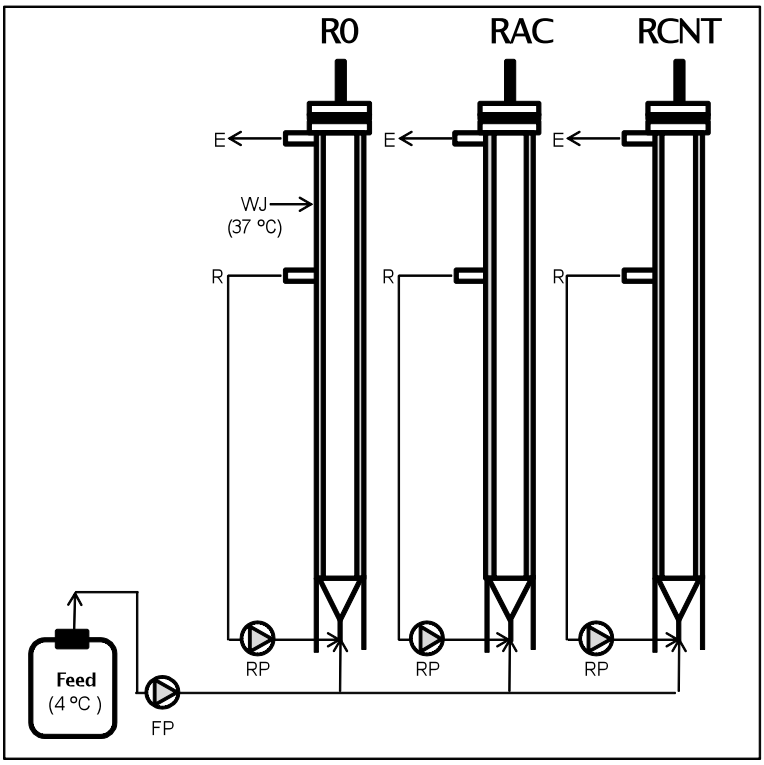

Figure 6.1. Schematic representation of the UASB reactors. E (effluent out); R (recyclic out); RP (recycling pump); FP (feeding pump); WJ (water jacket).

The bioreactors were operated for 89 days in six different phases as resumed in Table 6.1, testing different combinations of CM concentrations; CM size and HRT. R0 and RAC were operated from phase I to VI and RCNT was operated in phases V and VI.

Table 6.1. Experimental conditions for the different phases of the UASB bioreactors operation

Operation phases	I	II	III	IV	V	VI
Days (d)	1 - 9	10 - 36	37 - 61	62 - 67	68 – 67	78 - 89
HRT (h)	10	10	20	10	10	5
CM type	AC				AC; CNT	
CM concentration (g CM per g VS)	0.06	0.12				
CM size (mm)	0.3 < d < 0.6				d < 0.25	

6.2.3. Analysis

Samples were withdrawn for the bioreactors every 24 h, centrifuged and diluted up to an absorbance of less than 1, by using a freshly solution of ascorbic acid (200 mg L^{-1}), to prevent aromatic amines oxidation. AO10 decolourisation was monitored via absorbance measurements at the dye wavelength of maximum absorbance (480 nm), in a 96-well plate reader (ELISA BIO-TEK, Izasa). The molar extinction coefficient of the dye (ε_{480nm}=24.56 mmol L^{-1} cm^{-1}) was used to convert the concentration. The COD was determined using a commercial kit (Hach Lange, Düsseldorf, Germany). Dye reduction was confirmed in an Ultra HPLC (Shimadzu Nexera XZ) equipped with a diode array detector (SPD-M20A), autosampler (SIL-30AC), degassing (DGU-20A5R) and LC -30AD, a RP-18 endcapped Purospher Star column (250 mm x 4 mm, 5 µm particle size, from MERK, Germany). Mobile phase was composed of two solvents: 10 mmol L^{-1} ammonium acetate solution and ACN. Compounds were eluted at room temperature and at a flow rate of 0.8 mL min^{-1}, with an increase from 0 % to 95 % of ACN over 25 min and followed by an isocratic gradient during 10 min. Samples were monitored at 480 nm, for dye, and at 230 nm, for aromatic amines identification. VS were determined according to standard methods (APHA, 1998). VFA consumption was determined by HPLC (Jasco, Japan) equipped with a UV detector (210 nm) and a Chrompack column (6.5 x 30 mm^2) at 60 °C. Sulphuric acid (0.01 N) was used as mobile phase, at a flow rate of 0.6 mL min^{-1}.

6.2.4. Microbial analysis

Biomass samples were collected from R0 and RAC during phase V of reactor operation, frozen and stored until DNA extraction. In order to estimate the microbial diversity, DNA was extracted using FastDNA Spin kit for soil (MP Biomedicals, USA) and 16S rRNA genes were amplified prior to DGGE analysis by using the primer sets U968-f/L1401-r and A109(T)-f/515-r for bacterial and archaeal groups, respectively, as described elsewhere [Sousa *et al.,* 2007]. The composition of microbial communities was determined by sequencing variable regions (V3 and V4) of the 16S rRNA gene. Amplification, 16S rRNA gene library preparation, sequencing via an Illumina MiSeq and taxonomic classification were performed by Macrogen (Macrogen Inc., Republic of Korea).

6.3. RESULTS

6.3.1. Reduction of AO10 in the UASB reactor

Percentage of decolourisation of AO10 in RAC and R0 reactors, at different phases of operation is presented in Table 6.2 and Figure 6.2 A. In phase I, at an HRT of 10 h and 0.06 g of granular AC per g of VS, the colour removal was 28 % and 22 % in RAC and R0 respectively.

Table 6.2. Average of decolourisation (%) and COD removal (%) obtained at each phase in UASB reactors operation

	Operation Phases	I	II	III	IV	V	VI
R0	Decolourisation (%)	22 ± 4	18 ± 5	52 ± 4	28 ± 3	23 ± 5	16 ± 4
	COD removal (%)	68 ± 10	71 ± 7	86 ± 2	82 ± 3	79 ± 5	80 ± 3
RAC	Decolourisation (%)	28 ± 6	60 ± 3	73 ± 3	63 ± 3	98 ± 1	93 ± 2
	COD removal (%)	79 ± 6	79 ± 6	85 ± 1	85 ± 1	84 ± 2	81 ± 3
RCNT	Decolourisation (%)	N/A	N/A	N/A	N/A	98 ± 1	97 ± 3
	COD removal (%)					85 ± 1	81 ± 3

N/A not applicable.

Once colour removal was similar in both reactors, concentration of granular AC was duplicated, phase II. Consequently, AO10 decolourisation in RAC increased to (60 ± 3) %, while in the control reactor decolourisation was kept at approximately 20 % during all the reactor operation time. During phase III of reactor operation the increase of HRT to 20 h led to an increase of AO10 decolourisation in both reactors, although higher at mediated reactor: 80 % in RAC and 50 % in R0. The increase of AO10 decolourisation, from (18 ± 5) % to (52 ± 4) %, in the reactor control at higher HRT is in accordance with studies from Muda *et al.* (2011) who reported that colour removal increased with a longer contact time between biomass and dye.

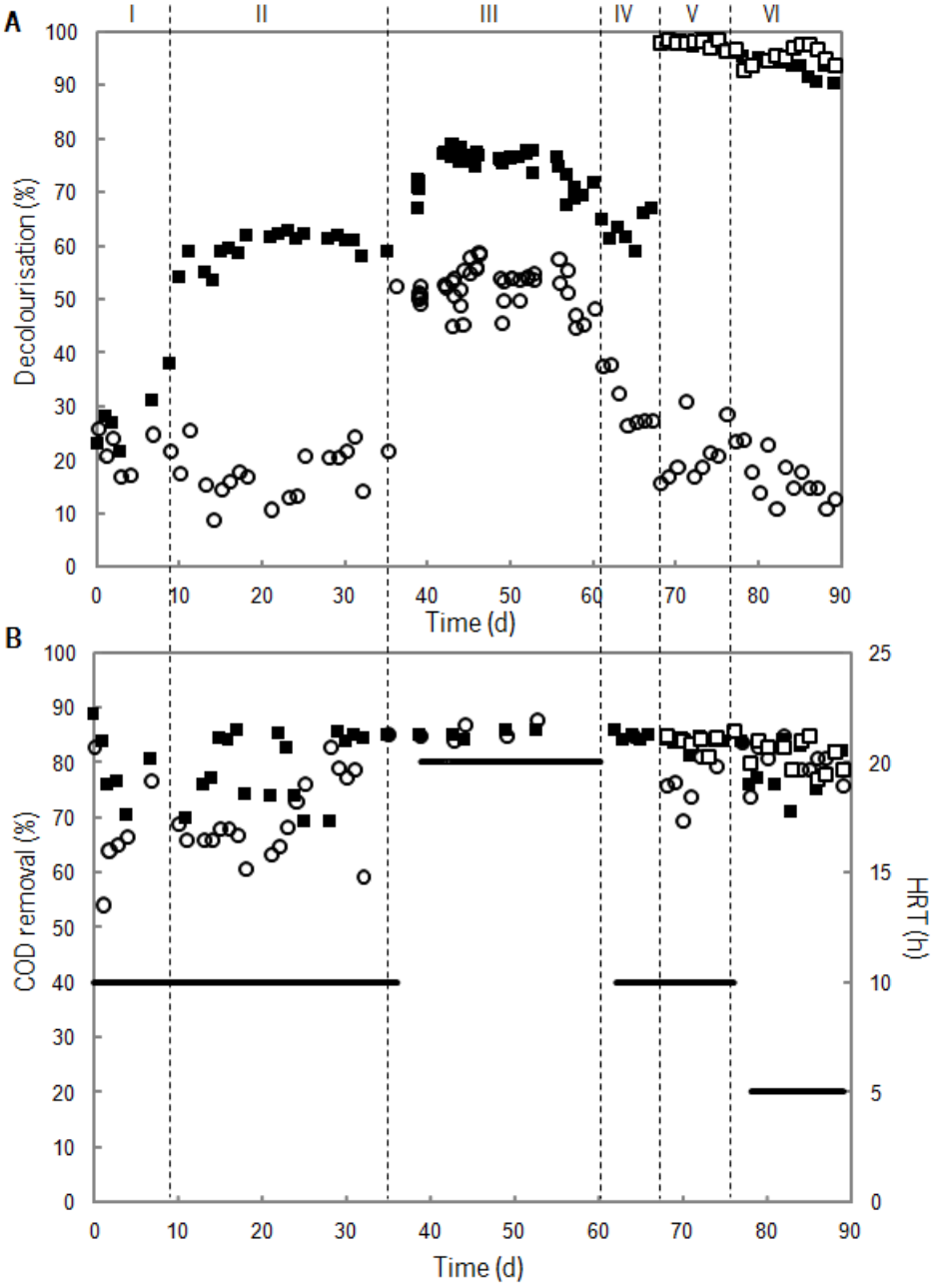

Figure 6.2. Percentage of AO10 decolourisation (A), COD removal and HRT (B) during the experiment for reactor R0 (○), reactor RAC (■) and reactor RCNT (□).

Other studies also reported an increased efficiency colour removal with an increased HRT [Isik and Sponza, 2004; Kapdan *et al.,* 2005; van der Zer *et al.,* 2005]. This is related with the slow process in the absence of RM [Van der zee and Cervantes, 2009]. In phase IV, the conditions of phase II were retaken and, consequently, the percentage of AO10 decolourisation decreased to values

previously obtained in phase II. This result suggest that the higher decolourisation obtained in R0 at HRT of 20 h was due to the higher HRT rather than biomass adaptation to the dye. Furthermore, the results clearly show that AC is needed to accelerate colour removal. In phase V of reactor operation, granular AC ($0.3 < d < 0.6$ mm) was substituted by powder AC ($d < 0.25$ mm) with the aim of evaluating the effect of increasing the AC surface area available. Under those conditions, the percentage of AO10 decolourisation in R0 increased from (63 ± 3) % to (98 ± 2) %, and was maintained constant during the bioreactor operation. Despite the lower density of powder AC, as compared with granular AC, this material was not washed out and could easily be retained inside the reactor RAC, assuring the high reduction rate of AO10 during the bioreactor operation.

The percentage of decolourisation in RCNT was the highest observed in all bioreactors, being complete during phase V, at an HRT of 10 h. During phase VI, the HRT was diminished to 5 h and the value was maintained in nearly 100 % decolourisation in reactor RCNT and 93 % in reactor RAC. The high efficiency of the proposed system, applying CM to accelerate the process of treatment has a great economic importance as time of treatment is reduced.

Decolourisation of AO10 was previously studied in batch (Chapter 4) and, similarly to the results here obtained in continuous system, the presence of CM was a pre-requisite for the biological decolourisation of AO10. Among the CM tested in batch assays (Chapter 4), better results were also obtained with CNT: around 70 % within 5 h and 98 % within 24 h. Though the larger surface area of AC, the high colour removal with CNT was attributed to the larger pores of this material and therefore, the later can better allow the access for the dye molecules.

Good COD removal efficiencies were obtained in all phases of the three reactors: around 70 % in R0 and 80 % in RAC, at phases I and II, and above 80 % in the following phases for all reactors (Figure 6.2 B). The similar COD removal is explained by the fact that dyes contributed for COD only at very little percentage (0.33 gCOD L^{-1}) and also, they are converted to the corresponding aromatic amines, rather than mineralization. So most of the COD decrease is due to VFA (witch contribute with 2 g L^{-1} of COD) consumption which was confirmed by HPLC (data not shown), indicating that the activity of microorganisms is similar and that higher colour removal in the presence of CM is due to the electron shuttle capacity of CM. For aromatic amine degradation, a combined process is necessary, as stated in Chapter 2. However, the increase of rates and, consequently, the decrease of time necessary for this first process, will decrease the time of complete process.

The pH in the reactors was constant over the entire reactors operation (7.4 ± 0.2), even without the utilization of any buffered solution, indicating a good stability of anaerobic reactors conditions.

6.3.2. Products of AO10 decolourisation in the UASB reactor

Samples taken from the influent and effluent of both reactors were analysed by HPLC aiming the identification of reduction products resulted from AO10 decolourisation (Figure 6.3).

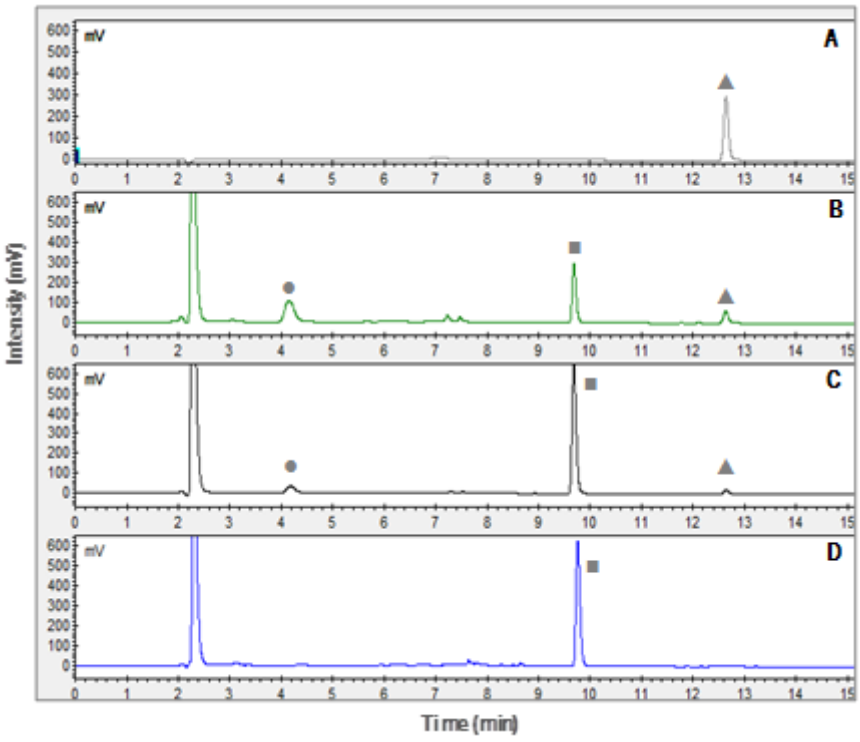

Figure 6.3. HPLC results from reactor RAC and R0 phase IV. (A) Chromatogram for 0.5 mmol L^{-1} of aniline at 230 nm; (b) Sample from RAC in phase IV at 230 nm; (c) Sample from R0 in phase IV at 230 nm; (D) Feed sample at 480 nm; (■) AO10 at Rt= 9.6 min; (▲) Aniline at Rt=12.6 min; (●) Aromatic product at Rt=4.3 min.

In the feed sample, analysed at 480 nm (Figure 6.3, chromatogram d), a peak corresponding to AO10 was detected at 9.6 min of retention time. In phases V and VI, in the effluent samples of RAC, the intensity of this peak decreased, confirming the high colour removal (around 98 %). On the other

hand, the 20 % of colour removal in R0 obtained by spectrophotometry was confirmed in the HPLC results (Figure 6.3, chromatogram c). Furthermore, two new peaks were detected at 4.3 and 12.6 min of retention time in the effluent samples collected from RAC (Figure 6.3, chromatogram b), which correspond to 8-amino-7-hydroxynaphthalene-1,3-disodiumsulfonate and aniline, respectively. Additionally, the results shown for RAC were representative of the chromatograms obtained for RCNT (*data not shown*). These results confirm that decolourisation occurred due to the reduction of the dye instead of an adsorption process onto CM.

6.3.3. Microbial Communities in UASB reactor treating AO10

Bacterial communities present in R0 and RAC are diverse as determined by 16S rRNA amplicons and the total community 16S rRNA genes sequencing. No major differences between the microbial communities developed in R0 and RAC were detected (Figure 6.4).

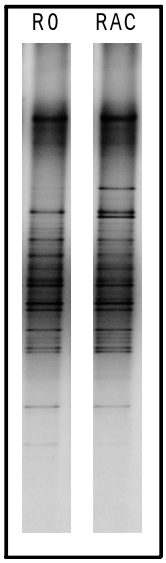

Figure 6.4. DGGE profile of Bacteria in UASB reactor samples.

According to our results, AC did not cause a shift on the composition of microbial communities, suggesting that colour removal in RAC was not due to the activity of different groups of

microorganisms but mainly to the presence of AC. Most abundant microorganisms identified, belong to genera *Synthrophobacter*, *Nitrospira*, *Geobacter*, *Pseudomonas* and *Synthrophomonas*, among others, and also to unknown bacteria, representing over 30 % of the total sequences obtained from both reactors (Figure 6.5).

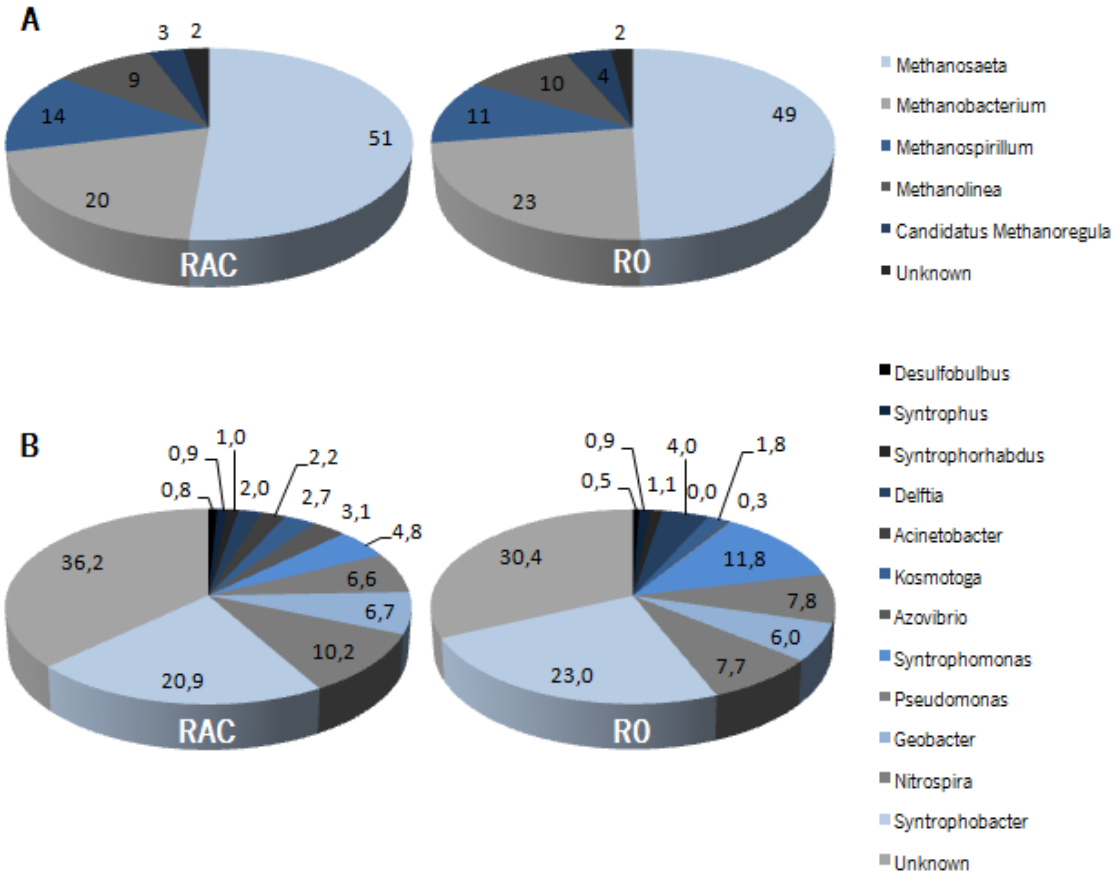

Figure 6.5. Distribution of 16S rRNA genes sequences among *Archaea* (A) and *Bacteria* (B) genera.

Geobacter and *Pseudomonas* species were present in R0 and RAC reactors, representing about 7 % of the total bacterial sequences obtained. Microorganisms belonging to these genera are reported as involved in azo dyes reduction [Khehra *et al.,* 2005; Lui *et al.,* 2013] and might have an important role on decolourisation in the bioreactors.

The high microbial diversity detected in both reactors is dependent on the electron and carbon donors, *i.e.* VFA. Several bacterial groups for example, *Synthrophobacter* and *Syntrophomonas* (23 % and 13 % respectively, in R0; 21 % and 5 % in reactor RAC) are well known syntrophic VFAs oxidizers [Zhang *et al.,* 2005; Lueders *et al.,* 2004], contributing for VFAs conversion to methane together with acetoclastic and hydrogenotrophic methanogens. These archaeal microorganisms were also identified in this study, being the acetate consumer, *Methanosaeta*, the most abundant methanogen (with 50 % of total archaeal sequences assigned). Diversity of hydrogenotrophic methanogens was higher with half of the archaeal sequences being assigned to *Methanobacterium* (23 % and 20 % for R0 and RAC respectively), *Methanospirillum* (11 % and 14 % for R0 and RAC respectively), *Methanolinea* (10 % and 9 % for R0 and RAC respectively) and *Methanoregula* (4 % and 3 % for R0 and RAC, respectively) genera.

6.4. CONCLUSIONS

Decolourisation of AO10 in a continuous process was significantly improved in the presence of low amounts of CM. Circa 97 % of colour and 85 % of COD removal were obtained in the UASB reactor amended with 0.12 g of CNT per g of VS with an HRT of 5h. The size of CM was an important factor influencing decolourisation rate and extent, and better results were achieved with powder CM (diameter below 0.25 mm). In R0, without CM, colour removal was circa 20% in all phases, except at high HRT (20 h) which reached 52 %, showing that decolourisation reactions are slow and need very high HRT in the absence of RM, such as CM. Relatively to microbial community analyses, no significant differences were observed between reactor R0 and RAC. The presence of AC did not significantly affect the microbial diversity and composition which suggest that the higher colour removal observed was mainly due to the effect of AC as RM, shuttling electron from the biological oxidation of VFA to the azo dye, accelerating it biotransformation to the correspondent aromatic amines. The results achieved of high process efficiency using very low concentration of CM, has also great significance in terms of costs. In addition, compared with soluble RM, insoluble materials, like CM, have the advantage of being retained inside the reactor, without the need for continuous feeding of RM. Furthermore, the characteristics of these materials allow for its reutilization, which contributes greatly for an efficacy and economic attractive process for dyed wastewaters treatment.

CHAPTER 7.

GENERAL CONCLUSIONS AND FUTURE PERSPECTIVES

In this chapter the general conclusions of the work developed in this thesis are presented. Furthermore, some suggestions for future research are also given.

CHAPTER 7.
GENERAL CONCLUSIONS AND FUTURE PERSPECTIVES

The efficiency of different carbon based materials as being an efficient RM in bioreduction of several azo dyes and aromatic amines was proved. CM were also tested with a real textile wastewater improving both the extent and the catalytic rate.

The effect of surface chemistry and porosity was evaluated. Modifying the surface chemistry of AC by thermal treatments, producing materials with low amount of oxygen containing groups and high basicity, was favourable in chemical and biological azo dye reduction. Bioreduction rates were also found to be highly affected by pore sizes of the materials. For bigger molecules, such as the azo dyes, the mesoporous materials (CNT and CX) presented better performance as compared with microporous materials (AC), explained by the easier access of the larger molecules of the dye to the internal surface of the catalyst. On the other hand, for NoA, smaller molecules, microporous AC_{H2} was the most efficient mediator, explained by the higher surface area of these materials instead of the size of the pores. Additionally, the position and nature of substituent groups in dye molecule have interference in reduction rates. In the case of azo dyes, the lower electron density around the azo bond caused by substituent groups as –OH and $–NH_2$, $–SO_3Na$ and COOH, present in MY10 and DR71 dyes, facilitate reduction of the azo bound. Contrarily, the –NH group in RR2 hinders the azo bound reduction. Moreover, the triazyl group in RR2 influenced negatively the decolourisation rate, which can be explain by the reducing equivalents required for the reductive dechlorination of the reactive group, which may compete with the azo chromophore. In the case of NoA, rates were dependent on the nitro group position in NoA structure studied, increasing in the order *meta* > *para* > *ortho*. Furthermore, in the presence of AC_{H2}, the m-NoA resulted from the biological reduction of MY1 was further bioreduced.

AC and CNT were proved as efficient RM in continuous UASB reactors, as well, demonstrating the applicability of the process. Powder CM were retained within the sludge during the entire operation time and total AO10 bioreduction was obtained with a short HRT of 5 h and 1.2 g L^{-1} of CNT, while without CM only 20 % was achieved.

Results obtained within this work gave a better insight into the important role of using CM as RM for the anaerobic degradation of aromatic compounds. The improved reduction rates make the process attractive for the application on wastewaters remediation, specially the textile ones.

In sequence of the developed work, future studies should be carried out in high rate bioreactor systems in detoxification of other aromatic xenobitic compounds (for example diphenylamines) and also real textile and other industrial wastewaters in order to evaluate the feasibility of the developed technology in the market. Among dyes, some care should be taken to the presence of others several compounds present in real wastewaters, such as anti-foamers, detergents, dispersants, surfactants, retardants, that could affect the performance of bioreactors.

Combination processes, either pre- or post-treatment to the anaerobic process developed, aiming at a higher and, preferentially, total xenobiotic mineralisation. In this way, the identification of the main reaction products and obtain toxicological data of initial model compounds and of final products should be taken into account, for complete understanding of reduction pathway of xenobiotics compounds mineralisation.

It would also be interesting to develop and test other materials such as the combination of CM with nanomagnetic nanoparticles and the combination of different CM.

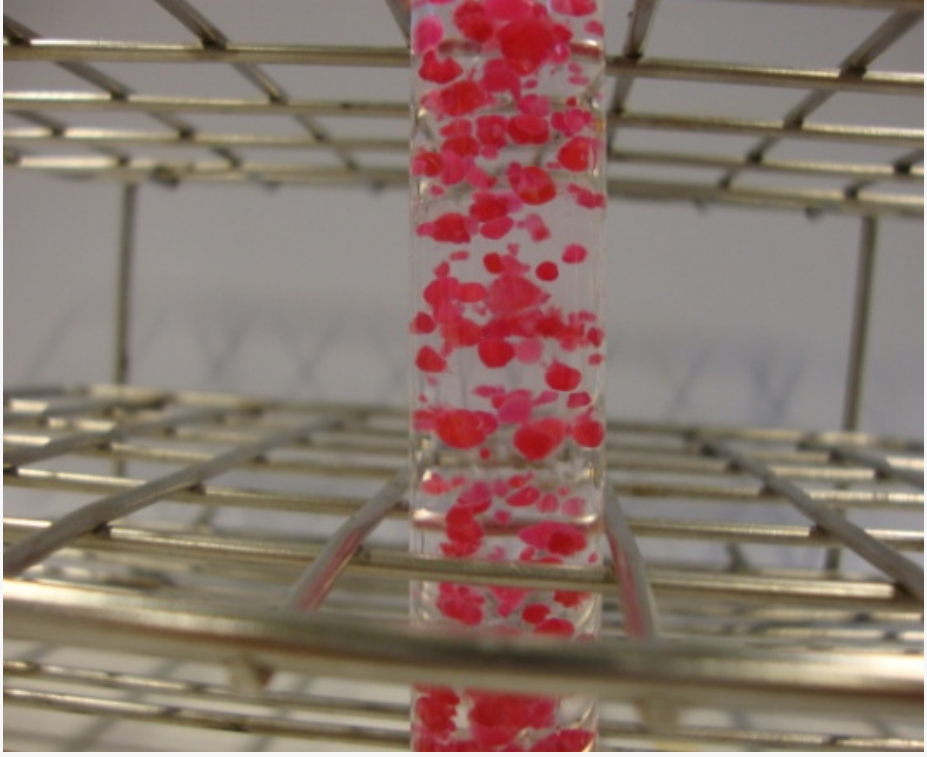

REFERENCES

REFERENCES

Al-Yang K, Wu W, Jing Q, Zhu A (2008). Aqueous Adsorption of Aniline, Phenol, and their Substitutes by Multi-Walled Carbon Nanotubes. Environmental Science and Technology 42, 7931–7936.

Al-Degs MAM, Khraisheh SJ, Allen MN (2000). Effect of carbon surface chemistry on the removal of reactive dyes from textile effluent, Water Research 34, 927-935.

Al-Degs YS, El-Barghouthi MI, El-Sheikh AH, Walker GM (2008). Effect of solution pH, ionic strength, and temperature on adsorption behaviour of reactive dyes on activated carbon. Dyes and Pigments 77, 16–23.

Amezquita-Garcia HJ, Razo-Flores E, Cervantes FJ, Rangel-Mendez JR (2013). Activated carbon fibers as redox mediators for the increased reduction of nitroaromatics. Carbon 55, 276–84.

Anson JG and MacKinnon G (1984). Novel *Pseudomonas* plasmid involved in aniline degradation. Applied and Environmental Microbiology 48, 868–869.

APHA, AWWA & WPCF. Standard Methods for the Examination of Water and Wastewater (17th Edition). American Public Health Association, Washington, D.C. 1998.

Baird R, Camona L, Jenkins RL (1977). Behavior of benzidine and other aromatic amines in aerobic wastewater treatment. Water Pollution Control Federation 49, 1609–1615.

Bansal RC, Donnet JB, Stoeckli F, Active Carbon. Marcel Decker, New York, 1988.

Beydilli MI, Pavlostathis SG and Tincher WC (2000). Decolorization and toxicity screening of selected reactive azo dyes under methanogenic conditions. Water Environment Research 72(6), 698–705.

Bhushan B, Halas A, Hawari J (2006). Effect of iron(III), humic acids and anthraquinone-2,6-disulfonate on biodegradation of cyclic nitramines by *Clostridium sp*. EDB2. Journal of Applied Microbiology 100, 555–563.

Börnick H, Eppinger P, Grischek T, Worch E (2001). Simulation of Biological Degradation of Aromatic Amines in River Bed Sediments. Water Research 35(3), 619–624.

Brás R, Gomes A, Ferra MIA, Pinheiro HM, Gonçalves IC, (2005). Monoazo and diazo dye decolourisation studies in a methanogenic UASB reactor, Journal of Biotechnology 115, 57–66.

Carliell CM, Barclay SJ, Naidoo N, Buckley CA, Mullholland DA and Senior E (1995). Microbial decolourisation of a reactive azo dye under anaerobic conditions. Water SA 21, 61–69.

Carliell CM, Barclay SJ, Shaw C, Wheatley AD and Buckley CA (1998). The effect of salts used in textile dyeing on microbial decolourisation of a reactive azo dye. Environmental Technology 19, 1133–1137.

Cervantes FJ, Enríquez JE, Galindo-Petatán E, Arvayo H, Razo-Flores E, Field, JA (2007). Biogenic sulphide plays a major role on the riboflavin-mediated decolourisation of azo dyes under sulphate-reducing conditions. Chemosphere 68, 1082–1089.

Cervantes FJ, van der Zee FP, Lettinga G, Field JA (2001). Enhanced decolourisation of acid orange 7 in a continuous UASB reactor with quinines as redox mediators. Water Science and Technology 44, 123–128.

Chang JS, Chou C, Lin YC, Lin PJ, Ho JY and Hu TL (2001). Kinetic characteristics of bacterial azo–dye decolorization by *Pseudomonas luteola*. Water Research 35(12), 2841–2850.

Charpentier JC (2003). Market demands versus technological development: the future of chemical engineering. International Journal of Chemical Reactor Engineering 1, article A14.

Chen H (2006). Recent advances in azo dye degrading enzyme research. Current Protein and Peptide Science 7(2), 101–111.

Chen KC, Wu JY, Liou DJ and Hwang SCJ (2003). Decolorization of the textile dyes by newly isolated bacterial strains. Journal of Biotechnology 101(1), 57–68.

Chen RJ, Zhang Y, Wang D, Dai H (2001). Noncovalent sidewall functionalization of single-walled carbon nanotube for protein immobilization. Journal of American Chemistry Society 123, 3838–3039.

Chung K-T, Kirkovsky L, Kirkovsky A, Purcel WP (1997). Review of mutagenicity of monocyclic aromatic amines: quantitative structure–activity relationships. Mutation Research 387, 1–16.

Chung K-T (2000). Mutagenicity and Carcinogenicity of Aromatic Amines Metabolically Produced from Azo Dyes. Environmental Carcinogenesis and Health 18, 51–74

Chung KT, Stevens SEJ, Cerniglia CE, (1992). Remediation of dyes in textile effluent: *a*critical review on current treatment technologies with a proposed alternative. Critical Reviews in Microbiology, 18175–197.

Cooper P (1993). Removing colour from dyehouse waste waters - a critical review of technology available. Journal of Society of Dyers Colourists 109, 97–100.

Cooper C and Burch R (1999). Mesoporous materials for water treatment processes. Water Research 33, 3689–3694.

Davis VM and Bailey JEJ (1993). Chemical reduction of FD and C yellow No. 5 to determine combined benzidine. Journal of Chromatography 635, 160–164.

Di ZC, Ding J, Peng XJ, Li YH, Luan ZK, Liang J (2006). Chromium adsorption by aligned carbon nanotubes supported ceria nanoparticles. Chemosphere 62, 861-865.

Dojilido R and Best GA (1993). Chemistry of waters and water pollution. Ellis Horwood, New York.

Donlon B, Razo-Flores E, Luijten M, Swarts H, Lettinga G, Field J (1997). Detoxification and partial mineralization of the azo dye mordant orange 1 in a continuous upflow anaerobic sludge-blanket reactor. Applied Microbiology and Biotechnology 47, 83–90.

Easton JR (1995). The dye maker's view, in Colour in dyehouse effluent, Cooper P, Editor, Society of Dyers and Colourists, Bradford, England, p. 9–21.

Eitan A, Jian K, Dukes D, Andrews R and Schadler LS (2003). Surface Modification of Multiwalled Carbon Nanotubes: Toward the Tailoring of the Interface in Polymer Composites. Chemistry of Materials 15, 3198–3201.

El-Moneim MRA (2010). Biological Function of Xenobiotics through Protein Binding and Transportation in Living Cells. International Journal of Agricultural Research 5, 562–575.

Eltaief K, Hana G, Youssef T, Hassib B, Moktar H, (2008). Aerobic decolourization of the indigo dye-containing textile wastewater using continuous combined bioreactors, Journal of Hazardous Materials 52 (2), 683–689.

Esteve-Nunez A, Caballero A, Ramos JL (2001). Biological degradation of 2,4,6-trinitrotoluene. Microbiology and Molecular Biology Reviews 65, 335–352.

Faria PCC, Orfão JJM, Pereira MFR, (2005). Mineralisation of coloured aqueous solutions byozonation in the presence of activated carbon. Water Research 39, 1461–1470.

Faria PCC, Orfão JJM, Figueiredo JL, Pereira MFR (2008). Adsorption of aromatic compounds from the biodegradation of azo dyes on activated carbon, Applyed Surface Science 254, 3497–3503.

Fetzner S (1998). Bacterial dehalogenation. Applied Microbiology Biotechnology 50, 633–657.

Field JA, Stams AJM, Kato M and Schraa G (1995). Enhanced biodegradation of aromatic pollutants in cocultures of anaerobic and aerobic bacterial consortia. Anton van Leeuwenhoek Int. J. G. 67, 47–77.

Figueiredo JL, Pereira MFR, Freitas MMA, Orfão JJM (1999). Modification of the surface chemistry of activated carbons. Carbon 37, 1379–1389

Figueiredo JL, Pereira MFR , Freitas MMA, Orfão JJM (2007). Characterization of active sites on carbon catalysts. Industrial Engineering Chemistry Research 46 4110–4115.

Figueiredo JL (2013) Functionalization of porous carbons for catalytic applications. Journal of Materials Chemistry A 1, 9351–9364.

.Fu H and Zhu D. (2013). Graphene Oxide-Facilitated Reduction of Nitrobenzene in Sulfide-Containing Aqueous Solutions. Environmental Science and Technology 47, 4204–4210.

Garrigós MC, Reche F, Marín ML, Jiménez A (2002). Determination of aromatic amines formed from azo colorants in toy products. Journal of Chromatography A 976, 309–317.

Ghosh DK, Ghosh S, Sadhukhan P, Mandal A and Chaudhuri J (1993). Purification of two azoreductases from *Escherichia coli* K12. Indian Journal of Experimental Biology 31, 951–954.

Ghosh DK, Mandal A and Chaudhuri J (1992). Purification and partial characterization of two azoreductases from *Shigella dysenteriae* type 1. FEMS Microbiology Letters 98, 229–234.

Gingell R and Walker R (1971). Mechanism of azo reduction by *Streptococcus faecalis* II. The role of soluble flavins. Xenobiotica 1, 231–239.

Gonçalves AG, Figueiredo JL, Órfão JJM, Pereira MFR (2010). Functionalization of textiles with multi-walled carbon nanotubes by a novel dyeing-like process. Carbon 48, 4369–4381.

Gong W, Liu X, Tao L, Xue W, Fu W, Cheng D (2014). Reduction of nitrobenzene with sulfides catalyzed by the black carbons from crop-residue ashes. Environmental Science and Pollution Research 21, 6162–6169.

Gorontzy T, Kuver J, Blotevog K-H (1993). Microbial transformation of nitroaromatic compounds under anaerobic conditions . Journal of General Microbiology 139, 1331–1336.

Gorontzy T, Kuver J, Blotevog K-H (1993). Microbial transformation of nitroaromatic compounds under anaerobic conditions. Journal of General Microbiology 139, 1331-1336.

Grén I (2012). Microbial transformation of xenobiotics. Chemik 66 (8), 835–842.

Guaratini CCI and Zanoni MVB (2000). Corantes Têxteis. Química Nova 23, 71–78.

Harris PJF, Liu Z and Suenaga K (2008). Imaging the atomic structure of activated carbon. Journal of Physics: Condensed Matter 20, 362201.

Harter DR (1985). The use and importance of nitroaromatic chemicals in the chemical industry, In: Rickert DE, editor. Toxic of Nitroaromatic Compounds; Chemical Industry Institute of Toxicology Series, Chemosphere, Washington, DC; p. 1–14.

Heider J, Fuchs G (1997). Anaerobic metabolism of aromatic compounds. European Journal of Biochemistry 243, 577–59.

Houk, VS (1992). The genotoxicity of industrial wastes and effluents - a Review. Mutation Research 77, 91–138.

Hsueh C-C, Chen B-Y, Yen C-Y (2009). Understanding effects of chemical structure on azo dye decolorization characteristics by *Aeromonas hydrophila*. Journal of Hazardous Materials 167 ,995–1001.

Hu T-L (2001) Kinetics of azoreductase and assessment of toxicity of metabolic products from azo dyes by *Pseudomonas luteola* , Water Science and Technology 43 (2) 261–269.

Hudlicky M (1984). Reductions in organic chemistry; Halsted Press, New York.

Huser BA, Wuhrmann K, Zehnder AJB (1982). *Methanothrix soehngenii gen. nov. sp. nov., a new* acetotrophic non-hydrogenoxidizing methanogen bacterium. Archives of . Microbiology (132), 1–9

Hwang HM, Hodson RE and Lee RF (1987). Degradation of aniline and chloroaniline by sunlight and microbes in estuarine water. Water Research 21, 309–316.

Iijima S, Helical microtubules of graphitic carbon (1991). Nature 354, 56-58.

Ingamells W (1993). Colour for textiles A user's handbook. Society of Dyers and Colourist, West Yorkshire.

Işık M and Sponza DT (2006). The fate and inhibition effect of Direct Red 28 in an anaerobic mixed culture. Journal of International Environmental Application & Science 1(1–2), 1–26.

Isık M and Sponza DT (2004). A batch kinetic study on decolorization and inhibition of reactive black and direct brown 2 in an anaerobic mixed culture. Chemosphere 55 119–128.

Job N, Théry A, Pirard R, Marien J, Kocon L, Rouzaud J-N, Béguin F, Pirard J-P (2005). Carbon aerogels, cryogels and xerogels: Influence of the drying method on the textural properties of porous carbon materials. Carbon 43, 2481–2494.

Jothimani P, Kalaichelvan G, Bhaskaran, Selvaseelan (2003). Anaerobic biodegradation of aromatic amines. Indian Journal of Experimental Biology 41, 1046–1067.

Kabbashi NA, Atieh MA, Al-Mamun A, Mirghami ME, Alam MD, Yahya N (2009). Kinetic adsorption of application of carbon nanotubes for Pb(II) removal from aqueous solution. Journal of Environmental Sciences (China) 21, 539–544.

Kalyani DC, Telke AA, Dhanve RS and Jadhav JP (2009). Ecofriendly biodegradation and detoxification of Reactive Red 2 textile dye by newly isolated *Pseudomonas sp*. SUK1. Journal of Hazardous Materials 163, 735–742.

Kalyuzhnyi S, Sklyar V, Mosolova T, Kucherenko I, Russkova J and Degtyaryova N (2000). Methanogenic biodegradation of aromatic amines. Water Science and Technology 42, 363–370.

Kandelbauer A and Guebitz GM (2005). Bioremediation for the Decolorization of Textile Dyes — A Review. Environmental Chemistry 26, 269–288.

Kang KY, Hong SJ, Lee BI, Lee JS (2008). Enhance electrochemical capacitance of nitrogen-doped carbon-gels synthesized by microwave-assisted polymerization of resoursinol and formaldehyde. Electrochemistry Communications 10, 1105-1108

Kang S, Pinault M, Pfefferle LD and Elimelech M (2007). Single-walled carbon nanotubes exhibit strong antimicrobial activity. Langmuir 23 (17), 8670-8673.

Kapdan I K and Alparslan S (2005) Application of anaerobic–aerobic sequential treatment system to real textile wastewater for color and COD removal. Enzyme and Microbial Technology (36), 273–279.

Kapdan IK and Kargi F (2002).Biological decolourisation of textile dyestuff containing wastewater by Coriolus versicolor in a rotating biological contactor. Enzyme and Microbial Technology 30 195–199.

Khalid A, Arshad M, Crowleyc DE (2009). Biodegradation potential of pure and mixed bacterial cultures for removal of 4-nitroaniline from textile dye wastewater. Water Research 43, 1110–1116.

Khehra MS, Saini SN, Sharma DK, Chadha DS, Chimni SS (2005). Decolorization of various azo dyes by bacterial consortia, Dyes Pigments (67)55–61.

Kulla HG, Klausener F, Meyer U, Luedeke B and Leisinger T (1983). Evolution of new bacterial enzyme activities during adaptation to azo dyes. Archives of Microbiology 135, 1–7.

Kumar M and Ando Y (2007). Carbon Nanotubes from Camphor: An Environment-Friendly Nanotechnology. Journal of Physic 61, 643–646.

Kumar P, Prasad B, Mishra IM, Chand S (2008). Treatment of composite wastewater of a cotton textile mill by thermolysis and coagulation. Journal Hazardous Materials 151, 770–779.

Kuo, C-Y, Wu C-H, Wu J-Y (2008). Adsorption of direct dyes from aqueous solutions by carbon nanotubes: Determination of equilibrium, kinetics and thermodynamics parameters. Journal of Colloid and Interface Science 327, 308–315.

Laszlo JA (2000). Regeneration of azo–dye–saturated cellulosic anion exchange resin by *Burholderia cepacia* anaerobic dye reduction. Environmental Science and Technology 34, 164–172.

Lee DH, Behera SK, Kim JW, Park HS (2009). Methane production potential of leachate generated from Korean food waste recycling facilities: a lab–scale study. Waste Management 29(2), 876–882.

Lettinga G, Vanvelsen AFM, Hobina SM, Zee W and Klapswik A (1980). Use of the Upflow sludge blanket (USB) reactor concept for biological wastewater treatment, especially for anaerobic treatment. Biotechnology and Bioengineering 22, 699–734.

Li Y-H, Wang S, Luan Z, Ding J, Xu C, Wu D (2003). Adsorption of cadmium (II) from aqueous solution by surface oxidized carbon nanotubes. Carbon 41, 1057–1062.

Li Q, Mahendra S, Lyon DY, Brunet L, Liga MV, Li D and Alvarez PJJ (2008). Antimicrobial nanomaterials for water disinfection and microbial control: Potential applications and implications. Water Research 42 (18), 4591–4602.

Li XZ and Zhao YG (1999). Advanced treatment of dyeing wastewater for reuse. Water Science and Technology 39, 249–255.

Li Y-H, Wang S, Zhang X, Wei J, Xu C, Luan Z, Wu D (2003b). Adsorption of fluoride from water by aligned carbon nanotubes. Materials Research Bulletin 38, 469–476.

Liu F, Rotaru A-E, Shrestha PM, Malvankar NS, Nevin KP, Lovley DR (2012). Promoting direct interspecies electron transfer with activated carbon. Energy & Environmental Science 5, 8982–8989.

Liu F, Rotaru A-E, Shrestha PM, Malvankar NS, Nevin KP, Lovley DR (2012). Promoting direct interspecies electron transfer with activated carbon. Energy & Environmental Science 5, 8982-8989.

Liu G, Zhou J, Chen C, Wang J, Jin R, Hong L (2013). Decolorization of azo dyes by Geobacter metallireducens, Applyied Microbiololgy Biotechnology (97), 7935–7942,

Liu G, Zhou J, Wang J, Wang X, Jin R and Lu H (2011). Decolorization of azo dyes by *Shewanella oneidensis* MR–1 in the presence of humic acids. Applied Microbiology and Biotechnology 91(2), 417–424.

Liu Y and Tay JH (2004). State of the art of biogranulation technology from wastewater treatment. Biotechnology Advances 22, 533–563.

Liu Y-T, Zhao W, Huang ZY, Gao YF, Xie X-M, Wang X-H and Ye X-Y (2006). Noncovalent surface modification of carbon nanotubes for solubility in organic solvents. Carbon 44, 1581–1616.

Loidl M, Hinteregger C, Ditzelmuller G, Ferschl A and Streichsbier F (1990). Degradation of aniline and monochlorinated anilines by soil–born *Pseudomonas acidovorans* strains. Archives of Microbiology 155, 56–61.

Long RQ and Yang RT (2001). Carbon nanotubes as superior sorbent for dioxin removal. Journal of the American Chemical Society 123, 2058–2059.

Lourenço ND, Novais JM and Pinheiro HM (2000). Reactive textile dye colour removal in a sequencing batch reactor. Water Science and Technology 42 (5–6), 321–328.

Lovely D and Phillips EJP (1986). Availability of ferric iron for microbial reduction in bottom sediments of the freshwater tidal Potomac River. Applied and Environmental Microbiology 52, 751–757.

Lovley DR, Coates JD, Blunt Harris EL, Phillips EJP and Woodward JC (1996). Humic substances as electron acceptors for microbial respiration. Nature 382, 445–448.

Lu C and Chiu H (2008). Chemical modification of multiwalled carbon nanotubes for sorption of Zn2+ from aqueous solution. Chemical Engineering Journal 139, 462.

Lu CS, Chung YL, Chang KF (2005). Adsorption of trihalomethanes from water with carbontubes, Water Research 39, 1183-1189.

Lu X , Yang B , Chen J, Su R (2009).Treatment of wastewater containing azo dye reactive brilliant red X3B using sequential ozonation and upflow biological aerated filter process. Journal Hazard Materials 161, 241–251.

Luangdilok W and Panswad T (2000). Effect of chemical structures of reactive dyes on color removal by an anaerobic–aerobic process. Water Science and Technology 42, 377–382.

Lueders T, Pommerenke B, and Friedrich MW (2004). Stable-Isotope Probing of Microorganisms Thriving at Thermodynamic Limits: Syntrophic Propionate Oxidation in Flooded Soil. Applied and Environmental Microbiology (70), 5778–5786.

Lufrano F, Staiti P, Calvo EG, Juárez-Pérez E, Menéndez JA, Arenillas A (2011). Carbon Xerogela and Manganese Oxide Capacitive Materials for Advanced Supercapacitors. International Journal of Electrochemistry and Science 6, 596–612

Malca-Mor L, Stark AA (1982). Mutagenicity and Toxicity of Carcinogenic and Other Hydrazine Derivatives: Correlation Between Toxic Potency in Animals and Toxic Potency in *Salmonella typhimurium* TA1538. Applied and Environmental Microbiology 44(4), 801–808.

Malik PK (2004). Dye removal from wastewater using activated carbon developed from sawdust: adsorption equilibrium and kinetics, Journal Hazardous Materials B 113, 81–88.

McCormick NG, Feeherry FF, Levinson HS (1976). Microbial transformation of 2,4,6-trinitrotoluene and other nitroaromatic compounds. Applied and Environmental Microbiology 31, 949–958.

Meenal K, Ambalal C (2007). Microbial remediation of nitro-aromatic compounds: An overview Journal of Environmental Management 85, 496–512.

Mendes S, Pereira L, Batista C, Martins LO (2011). Molecular determinansts of azo reduction activity in the satrain *Pseudomonas putida* MET94. Applied Microbiology and Biotechnology 92, 393–405.

Menéndez JA, Phillips J, Xia B, Radovic LR (1996). On the Modification and Characterization of Chemical Surface Properties of Activated Carbon: In the Search of Carbons with Stable Basic Properties. Langmuir 12, 4404–4410.

Mezohegyi G, Gonçalves F, Órfão JJM, Fabregat A, Fortuny A, Font J, Bengoa C, Stuber F (2010). Tailored activated carbons as catalysts in biodegradation of textile azo dyes. Applied Catalysis B: Environmental 94, 179–185.

Mogensen AS, Dolfing J, Haagensen F, Ahring BK (2003). Potential for Anaerobic Conversion of Xenobiotics. Advances in Biochemical Engineering/Biotechnology Biomethanation 82, 69–134.

Moliner R, Suelves I, Lazaro MJ, Moreno O (2005). Thermocatalytic decomposition of methane over activated carbons: influence of textural properties and surface chemistry. International Journal of Hydrogen Energy 30, 293–300.

Moreno-Castilla C (2004), Adsorption of organic molecules from aqueous solutions on carbon materials. Carbon 42, 83–94.

Morones JR, Elechiguerra JL, Camacho A, Holt K, Kouri JB, Ramírez JT and Yacaman MJ (2005). The bactericidal effect of silver nanoparticles. Nanotechnology, 16 (10), 2346–2353.

Mostafavi ST, Mehrnia MR and Rashidi AM (2009). Preparation of nanofilter from carbon nanotubes for application in virus removal from water. Desalination 238, 1-3, 271–282.

Moteleb MA, Suidan MT, Kim J, Davel JL, Adrian NR (2001). Anaerobic degradation of 2,4,6 trinitrotoluene in granular activated carbon fluidized bed and batch reactors. Water Science and Technology 43, 67–75.

Muda K, Aris A, Salim MR, Ibrahim Z, van Loosdrecht MCM, Ahmad A, Nawahwi MZ (2011). The effect of hydraulic retention time on granular sludge biomass in treating textile wastewater. Water Research 45, 4711-4721.

Muñiz J, Marbán G, Fuertes AB (2000). Low temperature selective catalytic reduction of NO over modified activated carbon fibres. Applied Catalysis B: Environmental 27, 27–36.

Nam S and Tratnyek PG (2000). Reduction of azo dyes with zero–valent iron. Water Research 34, 1837–1845.

Nepal D, Balasubramanian S, Simonian A L and Davis VA (2008). Strong antimicrobial coatings: Single-walled carbon nanotubes armored with biopolymers. Nano Letters 8 (7), 1896–1901.

Nieto-Delgado C and Rangel-Mendez JR (2011) Production of activated carbon from organic by-products from the alcoholic beverage industry: Surface area and hardness optimization by using the response surface methodology. Industrial Crops and Products 34, 1528–1537.

Nigam P, Banat IM, Singh D, Marchant R (1996). Microbial process for the decolorization of textile effluent containing azo, diazo and reactive dyes. Process Biochemistry 31 (5), 435–442.

O'Neill C, Hawkes FR, Hawkes DL, Lourenco ND, Pinheiro HM, Deleé W (1999). Colour in textile effluents–sources, measurement, discharge consents and simulation: a review. Journal of Chemical Technology and Biotechnology 74, 1009–1018.

Ong YT, Abdul LA, Hussein S Z and Soon HT (2010). Reviwe on carbon nanotubes in an environmental protection and green engineering perspectives. Brazilian Journal of Chemical Engineering 2, 227–242.

Orge CA, Sousa JPS, Gonçalves F, Freire C, Órfão JJM and Pereira MFR (2009). Development of novel mesoporous carbon materials for the catalytic ozonation of organic pollutants. Catalysis Letters 132, 1–9.

Orge CA, Órfão JJM, Pereira MFR (2012). Carbon xerogels and ceria-carbon xerogel materials as catalysts in the ozonation of organic pollutants. Applied Catalysis B: Environmental 126, 22–28.

Özen AS, Aviyente PDV (2007). Effect of cooperative hydrogen bonding in azo–hydrazone tautomerism of azo dye. Journal of Physical Chemistry A 111, 13506–13514.

Ozer C and Kevser Demiroz (2010). Biodegradation of Azo Dyes in Anaerobic–Aerobic Sequencing Batch Reactors. The Handbook of Environmental Chemistry 9, 59–72.

Pandey A, Poonam S and Leela L (2007). Bacterial decolorization and degradation of azo dyes. International Biodeterioration and Biodegradation 59, 73–84.

Panswad T, Iamsamer K and Anotai J (2001). Decolorisation of azo–reactive dye by polyphosphate and glycogen–accumulating organisms in an anaerobic–aerobic sequencing batch reactor. Bioresource Technology 76, 151–159.

Pearce CI, Lloyd JR and Guthrie JT (2003). The removal of colour from textile wastewater using whole bacterial cells: a r–eview. Dyes and Pigments 58, 179–196.

Pekala RW (1989). Organic Aerogels From the Polycondensation of Resorcinol with Formaldehyde. Journal of Mateials Science 24, 3221–3231.

Peng X, Li Y, Luan Z, Di Z, Wang H, Tian B, Jia Z (2003). Adsorption of 1,2-dichlorobenzene from water to carbon nanotubes. Chemical Physics Letters 376, 154–158.

Peng X, Luan Z, Ding J, Di Z, Li Y, Tian B (2005). Ceria nanoparticles supporte on carbon nanotubes for the removal of arsenate from water, Materials Letters 59, 399–403.

Pereira L and Alves MM (2012). Dyes–Environmental Impact and Remediation. Chapter 4 in Malik A ,Grohmann E (eds.) Environmental Protection Strategies for Sustainable Development, Springer, Dordrecht, 111–162.

Pereira L, Coelho AV, Viegas CA, Dos Santos MMC, Robalo MP, Martins LO (2009). On the mechanism of biotransformation of the anthraquinonic dye acid blue 62 by laccases, Journal of Biotechnology 139, 68–77.

Pereira L, Pereira R, Pereira MFR, van der Zee FP, Cervantes FJ, Alves MM (2010) Thermal modification of activated carbon surface chemistry improves its capacity as redox mediator for azo dye reduction. Journal of Hazardous Materials 183, 931–939.

Pereira MFR, Orfão JJM, Figueiredo JL (1999). Oxidative dehydrogenation of ethylbenzene on activated carbon catalysts. I. Influence of surface chemical groups, Applied Catalyse A: General 184, 153-160.

Pereira MFR, Soares SF, Órfão JJM and Figueiredo JL (2003). A desorption of dyes on activated carbons: influence of surface chemical groups. Carbon 41, 811–821.

Pereira RA, Pereira MFR, Alves MM, Pereira L (2014). Carbon based materials as novel redox mediators for dye wastewater biodegradation. Applied Catalysis B: Environmental 144, 713–720.

Pinheiro HM, Touraud E, Thomas O (2004). Aromatic amines from azo dye reduction: status review with emphasis on direct UV spectrophotometric detection in textile industry wastewaters. Dyes and Pigments 61, 121–139.

Puvaneswari N, Mutthukrishnam J, Gunasekaran P(2006). Toxicity assessment and microbial degradation of azo dyes. Indian journal of Experimental Biology 44, 618–629.

Qiang T, Luo M, Bu Q, Wang X (2012). Adsorption of an acid dye on hyper branched aminated collagen fibers. Journal Chemistry Engineering 197, 343–349.

Rajaguru P, Kalaiselvi K, Palanivel M and Subburam V (2000). Biodegradation of azo dyes in a sequential anaerobic–aerobic system. Applied Microbiology and Biotechnology 54, 268–273.

Ramalho PA, Scholze H, Cardoso MH, Ramalho MT, Oliveira-Campos AM (2002). Improved conditions for the aerobic reductive decolourisation of azo dyes by Candida zeylanoide. Enzyme and Microbial Technology 31, 848–854.

Ramalho PA, Cardoso MH, Cavaco-Paulo A, Ramalho MT (2004). Characterization of azo reduction activity in a novel ascomycete yeast strain. Applied and Environment Microbiology 70 (4), 2279–2288.

Razo Flores E, Luijten M, Donlon BA, Lettinga G and Field JA (1997). Complete biodegradation of the azo dye azodisalicylate under anaerobic conditions. Environmental Science Technology 31, 2098–2103.

Razo-Flores E, Donlon B, Lettinga G, Field JA (1997a). Biotransformation and biodegradation of N-substituted aromatics in methanogenic granular sludge. FEMS Microbiology Reviews 20, 525–538.

Razo-Flores E, Luijten M, Donlon BA, Lettinga G, Field JA (1997b). Complete Biodegradation of the Azo Dye Azodisalicylate under Anaerobic Conditions. Environmental Science and Technology 31(7), 2098–2103.

Razo–Flores E, Lettinga G, Field JA (1999). Biotransformation and biodegradation of selected nitroaromatics under anaerobic conditions. Biotechnology Progress 15, 358–65.

Rieger PG, Meier HM, Gerle M, Vogt U, Groth T and Knackmuss HJ (2002). Xenobiotics in the environment: present and future strategies to obviate the problem of biological persistence, Journal Biotechnology 94, 101–123.

Robinson T, McMullan G, Marchant R, Nigam P (2001). Remediation of dyes in textile effluent on current treatment technologies with a proposed alternative, Bioresource Technology 77, 247–255.

Rodríguez-Reinoso F (1998). The role of carbon materials in heterogeneous catalysis. Carbon 36, 159–175.

Rodriguez-Reinoso F, Martin-Martinez JM, Prado-Burguete C, McEnaney B (1987). A standard adsorption isotherm for the characterization of activated carbons, Journal Physical Chemistry 91, 515–516.

Russ R, Rau J and Stolz A (2000). The function of cytoplasmic flavin reductases in the reduction of azo dyes by bacteria. Applied and Environmental Microbiology 66, 1429–1434.

Sandhaya S, Padmavathy S, Swaminathan K, Subrahmanyam YV, Kaul, Microaerophilic SN (2005). Aerobic sequential batch reactor for treatment of azo dyes containing simulated wastewater. Process Biochemistry 40, 885–890.

Sani RK and Banerjee UC (1999). Decolorization of triphenylmethane dyes and textile and dye–stuff effluent by *Kurthia sp*. Enzyme and Microbial Technology 24, 433–437.

Santos AB, Cervantes FJ, Yaya-Beas RE, Van Lier JB (2003). Effect of redox mediator, AQDS, on the decolourisation of a reactive azo dye containing triazine group in a thermophilic anaerobic EGSB reactor, Enzyme Microbiol Technology 33, 942–951.

Santos AB, Bisschops IAE, Cervantes FJ, Van Lier JB (2004). Effect of different redox mediators during thermophilic azo dye reduction by anaerobic granular sludge and comparative study between mesophilic (30°C) and thermophilic (55°C) treatments for decolourisation of textile wastewaters. Chemosphere 55, 1149–1157.

Sarasa J, Roche MP, Ormad MP, Gimeno E, Puig A, Ovelleiro JL (1998). Treatment of a wastewater resulting from dyes manufacturing with ozone and chemical coagulation. Water Research 32, 2721 –2727.

Saratale RG, Saratale GD, Chang JS and Govindwar SP (2011). Bacterial decolorization and degradation of azo dyes: a review. Journal of the Taiwan Institute of Chemical Engineers 42(1) 138–157.

Saupe A (1999). High-Rate Biodegaradtion of 3- and 4-Nitroaniline. Chemosphere 13(39), 2325–2346.

Sen S and Demirer GN (2003). Anaerobic treatment of real textile wastewater with a fluidized bed reactor, Water Research 37, 1868–1878

Shahryari Z, Goharrizi AS and Azadi M (2010). Experimental study of methylene blue adsorption from aqueous solutions onto carbon nanotubes. International Journal of Water Resources and Environmental Engineering 2, 16–28.

Shaul GM, Holdsworth TJ, Dempsey CR, Dostal KA (1991). Fate of water-soluble azo dyes in the activated-sludge process. Chemosphere 22, 107–119.

Shen Z, Wang W, Jia J, Ye J, Feng X, Peng A (2001). Degradation of dye solution by an activated carbon fibre electrode electrolysis system. Journal Hazardous Materials B 84, 107–116.

Sinha S, Chattopadhyay P, Pan I, Chatterjee S, Chanda P (2009). Microbial transformation of xenobiotics for environmental bioremediation. African Journal of Biotechnology 8, 6016–6027.

Sousa DZ, Pereira MA, Smidt H, Stams AJ, Alves MM (2007) Molecular assessment of complex microbial communities degrading long chain fatty acids in methanogenic bioreactors. FEMS Microbiol Ecol (60),252–265. doi:10.1111/j.1574-6941.2007.00291.x

Spain JC (1995). Biodegradation of Nitroaromatic Compounds. Annual Reviews in Microbiology 49, 523–555.

Sponza DT and Işık M (2002). Ultimate azo dye degradation in anaerobic/aerobic sequential processes. Water Science Technology 45(12), 271–278.

Sponza DT and Işık M (2004). Decolorization and inhibition kinetic of Direct Black 38 azo dye with granulated anaerobic sludge. Enzyme and Microbial Technology 34(2), 147–158.

Sponza DT and Işık M (2005). Reactor performances and fate of aromatic amines through decolorization of Direct Black 38 dye under anaerobic/aerobic sequentials. Process Biochemistry 40(1), 35–44.

Sridevi V, Lakshmi MVVC, Swamy AVN, Rao MN (2011). Implementation of response surface methodology for phenol degradation using *Pseudomonas putida* . Journal Bioremediation Biodegradation 2, 121.

Stoeckli HF, Ballerini L, De Bernardini S (1989). On the evolution of micropore widths and areas in the course of activation, Carbon 27, 501-502.

Stolz A, (2001). Basic and applied aspects in the microbial degradation of azo dyes. Applied Microbiology and Biotechnology 56, 69-80.

Stolz A, Nortemann B, Knackmuss HJ (1992). Bacterial metabolism of 5–aminosalicylic acid: Initial ring cleavage. Biochemical Journal 282, 675–680.

Tan NCG, Prenafeta-Bolduâ FX, Opsteeg JL, Lettinga G, Field JA (1999). Biodegradation of azo dyes in coculture of anaerobic granular sludge with aerobic aromatic amine degrading enrichment cocultures, Applied Microbiology and Biotechnology 51, 865–871.

Tan NCG, Van Leeuwen A, Van Voorthuizen EM, Slenders P, Prenafeta-Boldu F, Temmink H, Lettinga G, Field JA (2005). Fate and biodegradability of sulfonated aromatic amines. Biodegradation 16, 527–537.

Tessonnier JP, Rosenthal D, Hansen TW, Hess C, Schuste ME, Blume R, Girgsdies F, Pfänder, N, Timpe O, Su DS, Schlögl R (2009). Analysis of the structure and chemical properties of some commercial carbon nanostructures. Carbon 47(7), 1779–1798.

Thakur I (2008). Xenobiotics: Pollutants and their degradation-methane, benzene, pesticides, bioabsorption of metals.

Thess A, Lee R, Nikolaev P, Dai H, Petit P, Robert J, Xu C, Smalley R (1996) Crystalline ropes of metallic carbon nanotubes . Science 27, 483–487.

Tsang DCW, Hu J, Liu MY, Zhang W, Lai KCK and Lo IMC (2007). Activated Carbon Produced from Waste Wood Pallets: Adsorption of Three Classes of Dyes. Water Air and Soil Pollution 184, 141–155.

van der Berg L, Kennedy KJ, Dairy Waste Treatment with Anaerobic Stationary Fixed Film Reactors Water Sci Technol (15),359–368.

van der Zee FP, Lettinga G and Field JA (2000). The role of (auto)catalysis in the mechanism of an anaerobic azo reduction. Water Science and Technology 42, 301–308.

van der Zee FP, Bouwman RHM, Strik DPBTB, Lettinga G and Field JA (2001). Application of redox mediators to accelerate the transformation of reactive azo dyes in anaerobic bioreactors. Biotechnology and Bioengineering 75, 691–701.

van der Zee FP, Lettinga G, Field JA (2001). Azo dye decolourisation by anaerobic granular sludge, Chemosphere 44, 1169–1176.

van der Zee FP (2002). Anaerobic azo dyes reduction. Doctoral thesis, Wageningen University Wageningen, Netherlands, 1–31.

van der Zee FP, Bisschops IA, Lettinga G, Field JA (2003). Activated carbon as an electron acceptor and redox mediator during the anaerobic biotransformation of azo dyes. Environmental Science and Technology 37, 402–408.

van der Zee FP, Bisschops IAE, Blanchard VGR, Bouwman HM, Lettinga G, Field JA (2003b).The contribution of biotic and abiotic processes during azo dye reduction in anaerobic sludge Water Research 37, 3098-3109.

van der Zee FP, Villaverde S (2005). Combined anaerobic-aerobic treatment of azo dyes- A short review of bioreactors studies. Water Research 39, 1425–1440

van der Zee FP and Cervantes FJ (2009). Impact and application of electron shuttles on the redox (bio)transformation of contaminants: a review. Biotechnology Advances 27, 256–277.

Werner D, Higgins CP and Luthy RG (2005). The sequestration of PCBs in Lake Hartwell sedimentwith activated carbon. Water Research 3, 2105–2113.

Wijetunga S, Xiufen L, Wenquan R, Chen J (2008).Evaluation of the efficacy of upflow anaerobic sludge blanket reactor in removal of colour and reduction of COD in real textile wastewater, Bioresource Technology 99, 3692–3699.

Willmott NJ (1997). The Use of Bacteria–Polymer Composites for the Removal of Colour from Reactive Dye Effluents. PhD thesis, University of Leeds, UK.

Wu C-H (2007). Studies of the equilibrium and thermodynamics of the adsorption of Cu^{2+} onto as produced and modified carbon nanotubes. Journal of Colloid and Interface Science 311, 338–346.

Wu C-H (2007b) Adsorption of reactive dye onto carbon nanotubes: Equilibrium, kinetics and thermodynamics. Journal of Hazardous Materials 144, 93–100.

Wu HF, Wang SH, Kong HL, Liu TT, Xia MF (2007) Performance of combined process of anoxic baffled reactor-biological contact oxidation treating printing and dyeing wastewater. Bioresourse Technology 98 (2007) 1501–1504

Wu Z, Joo H, Lee K (2005). Kinetics and thermodynamics of the organic dye adsorption on the mesoporous hybrid xerogel. Chemical Engineering Journal 112, 227–236.

Xie, XL, Mai YW and Zhou XP (2005). Dispersion and alignment of carbon nanotubes in polymer matrix: A review. Materials Science and Engineering R: Reports, 49, n° 4.

Yahiaoui I, Aissani-Benissad F, Fourcbe F, Amrane A (2013). *Journal of Environmental Progress and Sustainable Energy* 33,160–169

Yamamoto T, Sugimoto T, Suzuki SR, Tamon H (2002). Preparation and characterization of carbon cryogel microspheres, Carbon 40 (8), 1345–1351.

Yang K, Wu W, Jing Q, Zhu A (2008). Aqueous Adsorption of Aniline, Phenol, and their Substitutes by Multi-Walled Carbon Nanotubes. Environmental Science and Technology 42, 7931–7936.

Yang Q, Li C, Li H, Li Y, Yu N (2009). Degradation of synthetic reactive azo dyes and treatment of textile wastewater by a fungi consortium reactor. Biochemical Engineering Journal 43 (3), 225–230.

Yau Y, Xu F, Chen M, Xu Z and Zhu Z (2010). Adsorption behavior of methylene bue on carbon nanotubes. Bioresource Technology 101, 3040–3046.

Yoo ES, Libra J and Wiesmann U (2000). Reduction of azo dyes by Desulfovibrio desulfuricans. Water Science and Technology 41, 15–22.

Zanto EJ, Al-Muhtaseb SA, Ritter JA (2002). Sol-Gel derived carbon aerogels and xerogels: design of experiments approach to materials synthesis. Industry and Engennering Chemistry Research 41, 3151–3162.

Zhang F, Yediler A, Liang X, Kettrup A, (2004). Effects of dye additives on the ozonation process and oxidation by-products: a comparative study using hydrolyzed C.I.Reactive Red 120. Dyes and Pigments 60, 1–7.

Zhang SY, Wang QF, Xie SG , (2012).Molecular characterization of phenanthrene-degrading methanogenic communities in leachate-contaminated aquifer sediment, International Journal Environmental Science Technology (9)705–712.

Zhu ZH, Radovic LR and Lu GQ (2000). Effects of acid treatments of carbon on NO and NO2 reductionby carbon-supported copper catalysts. Carbon 38, 451– 464.

Zimmerman JR, Ghosh U, Millward RN, Bridges TS and Luthy RG (2004). Addition of carbon sorbents to reduce PCB and PAH bioavailability in marine sediments: Physicochemical tests. Bioresource Technology 38, 5458–5464.

Zimmermann T, Kulla H and Leisinger T (1982). Purification and properties of orange II azoreductase from *Pseudomonas* KF46. Experientia 38, 1380.